Sebastian Hendrix, BSc

The role of HDL-S1P axis in inflammation and endothelial dysfunction at the feto-placental endothelium

MASTER'S THESIS

to achieve the university degree of

Master of Science

Master's degree program: Biochemistry and Molecular Biomedicine

submitted to

Graz University of Technology

Supervisor

Assoc. Prof., PhD, Christian Wadsack
Medical University of Graz
Department of Obstetrics and Gynecology

Graz, September 2018

AFFIDAVIT

I declare that I have authored this thesis independently, that I have not used other than the declared sources/resources, and that I have explicitly indicated all material which has been quoted either literally or by content from the sources used. The text document uploaded to TUGRAZonline is identical to the present master‘s thesis.

Date	Signature

Acknowledgements

First of all I would like to thank Assoc. Prof., PhD, Christian Wadsack for the opportunity to do my master thesis in his research group and for his guidance and support throughout the whole project. I learned a lot about how scientific research is done, how to approach a specific scientific issue and how it is to work in a scientific environment.

My biggest gratitude goes to Ilaria Del Gaudio because without her this project would not have been possible. She was always there if I needed anything although she was busy enough with her own project. She always took time to discuss any problems thereby spending the one or other “troubleshooting session” with me and she really helped me a great deal to plan, realize and finish this project. So I want to say thank you at this point I really appreciate your support and help.

I am very grateful that I could do my master thesis in the perinatal research laboratory especially because I met some really nice people here and it is difficult to imagine to find another lab where the working environment is as great as in this lab. Everybody was always helpful no matter what I needed and we always a lot of fun which made working sometimes a lot easier. In that matter I want to thank Denise who “hired” me in the first place therefore introducing me to the lab and for always being helpful throughout my whole project. I specially want to thank Jassi and Susi for teaching me cell culture and the basic research techniques I needed for my master thesis. Furthermore, I want to thank Michi for his support and all the fruitful scientific discussions as well as for the less fruitful but nevertheless often very amusing discussions we had. Unfortunately, there is not enough space to mention everybody by name but nevertheless I want say thanks to everyone else in the lab so: Thank you.

I want to thank Dr. Franz Radner from the Karl-Franzens University Graz for his help and input regarding the radioactive tracer assay for measuring SPT activity.

And last but not least I want to thank my parents who always supported me emotionally and financially throughout my whole studies. Without them it would not have been possible or would have been a whole lot harder to get to this point. Thank you for everything you did for me.

Zusammenfassung

Präeklampsie ist eine Schwangerschaftskomplikation die durch eine gestörte Implantation der Plazenta charakterisiert ist. Daraus resultiert, dass sich das plazentare Gefäßsystem nicht so umbauen und erweitern kann wie dies während der Schwangerschaft notwendig wäre. Dies führt in weitere folge unter anderem zur Entzündung des Gefäßsystems, zu endothelialer Dysfunktion und zu Hypertonie. Dies zeigt, dass das Endothelium in dieser Schwangerschaftskomplikation eine wesentliche Rolle spielt. Sphingosin-1-Phosphat (S1P) ist ein bioaktives Phospholipid, welches, wenn es im Blutkreislauf zirkuliert, hauptsächlich mit high-density Lipoproteinen (HDL) assoziiert ist und dafür bekannt ist, positive Auswirkungen auf das Endothelium zu haben. Das Ziel dieser Studie ist es daher, die Rolle von neonatalen HDL-S1P Komplexen in Bezug auf Entzündung und Dysfunktion des feto-plazentaren Endotheliums aufzuklären. Darüber hinaus wird untersucht, ob präeklamptische Bedingungen den intrazellulären S1P Metabolismus in Endothelzellen in einer negativen Art und Weise beeinflussen.

Um präeklamptische Bedingungen zu simulieren, wurden Endothelzellen aus plazentaren Aorten (HPAECs) mit Tumornekrosefaktor Alpha (TNF-α; 10 ng / ml) oder Angiotensin II (AngII; 0,5 und 1 µM) behandelt. Quantitative real time PCR (qPCR) Experimente zeigten, dass die Behandlung von HPAECs mit TNF-α zu einer Steigerung der mRNA Expression von vascular adhesion molecule 1 (VCAM1), intracellular adhesion molecule 1 (ICAM1), Interleukin 8 (IL-8) und monocyte chemoattractant protein 1 (MCP1) führte, welche durch das Zugeben von neonatalem HDL (nHDL; 800 µg/ml) und S1P (1 µM) wieder reduziert werden konnte. Zusätzlich konnte mittels Western Blot gezeigt werden, dass sich die, durch TNF-α gesteigerte Aktivität des Transkriptionsfaktors nuclear factor kappa B (NF-kB) in der Gegenwart von nHDL und S1P wieder reduzierte. Interessanterweise demonstrierten weitere Western Blot und fluorescence activtated cell sorting (FACS) Experimente, dass die Zugabe von nHDL und S1P weder zu einer Reduktion der intrazellulären Proteinmenge von VCAM1-, ICAM1-, IL-8- oder MCP1 noch zu einer reduzierten Expression der Adhäsionsmoleküle VCAM1, ICAM1 und E-Selectin an der Zelloberfläche führten. Mithilfe eines Dichlorodihydrofluorescein diacetate (DCFDA) Fluoreszenzassays wurde die intrazelluläre Bildung von reaktiven Sauerstoffspezies (ROS) in HAPECs gemessen, welche durch die Administration von AngII induziert wurde. Es konnte gezeigt werden, dass durch nHDL die Menge an gebildeten ROS stark reduziert wird wohingegen S1P eine geringere und statistisch nicht signifikante Reduktion der ROS bewirkte. Um die Auswirkungen von präeklamptischen Bedingungen auf den S1P Metabolismus zu untersuchen, wurde die Serin Palmitoyl Transferase (SPT) Aktivität in einem Experiment mit radioaktiven Tracern untersucht. Dabei zeigte sich, dass die Behandlung von HAPECs mit TNF-α zu einer zweifach erhöhten Aktivität von SPT führte, während AngII keine Auswirkungen

auf die Aktivität zeigte. Zusätzlich konnte in qPCR Experimente demonstriert werden, dass TNF-α die Expression der Sphingosin Kinase 1 (SPHK1) in HPAECs um das 3,5 fache erhöhte, wohingegen die Expression der Sphingosin Phosphatase 1 (SPP1) unverändert blieb. Interessanterweise zeigten Untersuchungen in präeklamptischem Gewebe, dass die SPP1-Expression um das 3,8-fache erhöht war wohingegen die SPHK1-Expression leicht, aber nicht statistisch signifikant herunterreguliert war.

Zusammenfassend konnte gezeigt werden, dass nHDL und S1P entzündungshemmende und antioxidative Eigenschaften aufweisen, die das feto-plazentare Endothel schützen. Obwohl nHDL insbesondere in Bezug auf die Prävention von oxidativem Stress wesentlich effizienter ist, ist es sehr wahrscheinlich, dass ein Teil des bei nHDL beobachteten Effekts dem mit nHDL assoziiertem S1P zuzuschreiben ist. Zusätzlich zeigte sich in dieser Studie, dass der S1P-Metabolismus unter präeklamptischen Bedingungen in einer Weise beeinträchtigt ist, die zu reduzierten Mengen an verfügbaren S1P führt wodurch der Verlauf von Präeklampsie möglicherweise verschlechtert wird.

Abstract

Improper placentation and the resulting failure of the endothelium to show normal pregnancy adaption is associated with the manifestation of preeclampsia (PE). Hallmark features of PE are vascular inflammation, endothelial dysfunction and hypertension highlighting the important role of the endothelium in PE. The bioactive sphingolipid sphingosine 1-phosphate (S1P) which is mainly associated with high-density lipoproteins (HDL) in the circulation, is known to positively influence endothelial integrity. The goal of this study is to elucidate the role of neonatal HDL-S1P complexes in vascular inflammation and endothelial dysfunction at the feto-placental endothelium. Furthermore, this study investigates whether preeclamptic conditions alter the intracellular S1P homeostasis in endothelial cells possibly leading to adverse outcomes.

Human placental aortic endothelial cells (HPAECs) were treated with tumor necrosis factor alpha (TNF-α; 10 ng/ml) or Angiotensin II (AngII; 0.5 and 1 µM) to mimic preeclamptic conditions. The presence of nHDL (800 µg/ml) and S1P (1µM) downregulated the TNF-α induced mRNA expression of vascular adhesion molecule 1 (VCAM1), intracellular adhesion molecule 1 (ICAM1), interleukin 8 (IL-8) and monocyte chemoattractant protein 1 (MCP1) as shown by quantitative real time PCR (qPCR). Accordingly, nuclear factor kappa B (NF-κB) activation was significantly decreased in the presence of nHDL and S1P as demonstrated by Western blotting. Interestingly, Western blot and fluorescence activated cell sorting (FACS) experiments could not show any changes in VCAM1, ICAM1, IL-8 or MCP1 protein levels or in the cell surface expression of the adhesion molecules VCAM1, ICAM1 and E-Selectin. Measurement of reactive oxygen species (ROS) by a Dichlorodihydrofluorescein diacetate (DCFDA) fluorescence assay showed that nHDL was highly effective in reducing ROS production in AngII treated HAPECs whereas S1P showed a smaller and statistically not significant reduction of ROS. Serine palmitoyl transferase (SPT) activity was increased 2-fold upon TNF-α treatment whereas AngII had no effect as demonstrated by a radioactive tracer experiment. QPCR experiments revealed that sphingosine kinase 1 (SPHK1) expression was increased 3.5 fold and sphingosine phosphatase 1 (SPP1) expression remained unchanged in TNF-α treated HAPECs. In preeclamptic tissue SPP1 expression was increased 3.8 fold whereas SPHK1 expression was slightly but not statistically significant downregulated.

In conclusion we could show that nHDL and S1P show anti-inflammatory and anti-oxidative properties that protect the feto-placental endothelium. Although nHDL is more efficient especially in reducing oxidative stress it is likely that nHDL associated S1P is partially responsible for the observed effects. Additionally, this study revealed that S1P metabolism is impaired under preeclamptic conditions in a way that interferes with the protective properties of S1P possibly contributing to adverse outcomes in preeclampsia.

Contents

Abbreviations

ABCA1	ATP binding cassette transporter A1
AJ	Adherens junction
AngII	Angiotensin II
AP1	Activator Protein 1
Apo	Apolipoproteins
ApoA-1	Apolipoprotein A1
Aβ	Amyloid-β peptide
BCA	Bicinchoninic acid assay
cAMP	Cyclic adenosine monophosphate
CE	Cholesteryl esters
CETP	Cholesterol ester transfer protein
COX1	Cyclooxygenase-1
Cq	Quantification cycle
CRP	C-reactive protein
DCFDA	2',7'–dichlorofluorescindiacetate
Depp	Decidual protein induced by progesterone
DLL4	Delta-like 4
EBM	Endothelial basal medium
EC	Endothelial cell
EDHF	Endothelium derived hyperpolarizing factor
EDTA	Ethylenediaminetetraacetic acid
eNOS	Endothelial nitric oxide synthase
ET-1	Endothelin-1
FACS	Fluorescence activated cell sorting
FC	Free cholesterol
GPCR	G-protein coupled receptor
H_2B	Dihydrobiopterine
H_4B	Tetrahydrobiopterine
HBSS	Hank's Balanced Salt Solution
HDL	High density lipoproteins
HPAEC	Human placental aortic endothelial cells
HPRT1	Hypoxanthine phosphoribosyltransferase1
HSA	Human serum albumin
ICAM1	Intercellular adhesion molecule 1

IL-8	Interleukine 8
IP_3	Inositol 3,4,5-triphsophate
LCAT	Lecithin-cholesterol acyl transferase
LDL	Low density lipoproteins
LPP	lipid phosphate phosphatases
MCP1	Monocyte chemoattractant protein 1
MLC	Myosin light chain
MLCK	Myosin light chain kinase
MLCP	Myosin light chain phosphatase
NF-κB	Nuclear factor kappa B
nHDL	Neonatal high density lipoprotein-S1P complex
NO	Nitric oxide
NOX	NADPH oxidase
PAF	Platelet activating factor
PBS	Phosphate buffered saline
PE	Preeclampsia
PGI_2	Prostaglandin I_2
PHB2	Prohibitin 2
PI3K	Phosphatidylinositide 3-kinase
PLC	Phospholipase C
PPIA	Peptidylprolyl isomerase A
PSMB6	Proteasome subunit beta 6
qPCR	Quantitative real-time PCR
RhoK	Rho kinase
S1P	Sphingosine-1-phosphate
S1PR	Sphingosine-1-phosphate receptor
SMC	Smooth muscle cells
SPHK	Sphingosine Kinase
SPNS2	Spinster homologue 2
SPP	Sphingosine Phosphatase
SPT	Serine palmitoyl transferase
SR BI	Scavenger receptor class B type I
TAG	Triacylglycerol
TBP	TATA-box binding protein
TBS	Tris-buffered saline
TJ	Tight junction

TLC	Thin layer chromatography
TXA2	Thromboxane A2
VCAM1	Vascular cell adhesion molecule 1
VLDL	Very low density lipoproteins

1 INTRODUCTION

1.1 The Placenta

The placenta is a tissue with a limited life span that develops during pregnancy and represents the interface between maternal and fetal circulation. The main purpose of the placenta is to transport nutrients and gases between the mother and the fetus as well as transportation of waste products back from the fetus to the mother for excretion. In doing so the placenta takes on a major role in the proper development and growth of the fetus [1].

1.1.1 Placental structure

The placenta is composed of tissue derived from the fetus. The so called chorionic plate is faced to the fetus whereas the basal plate is on the maternal side and in contact with the

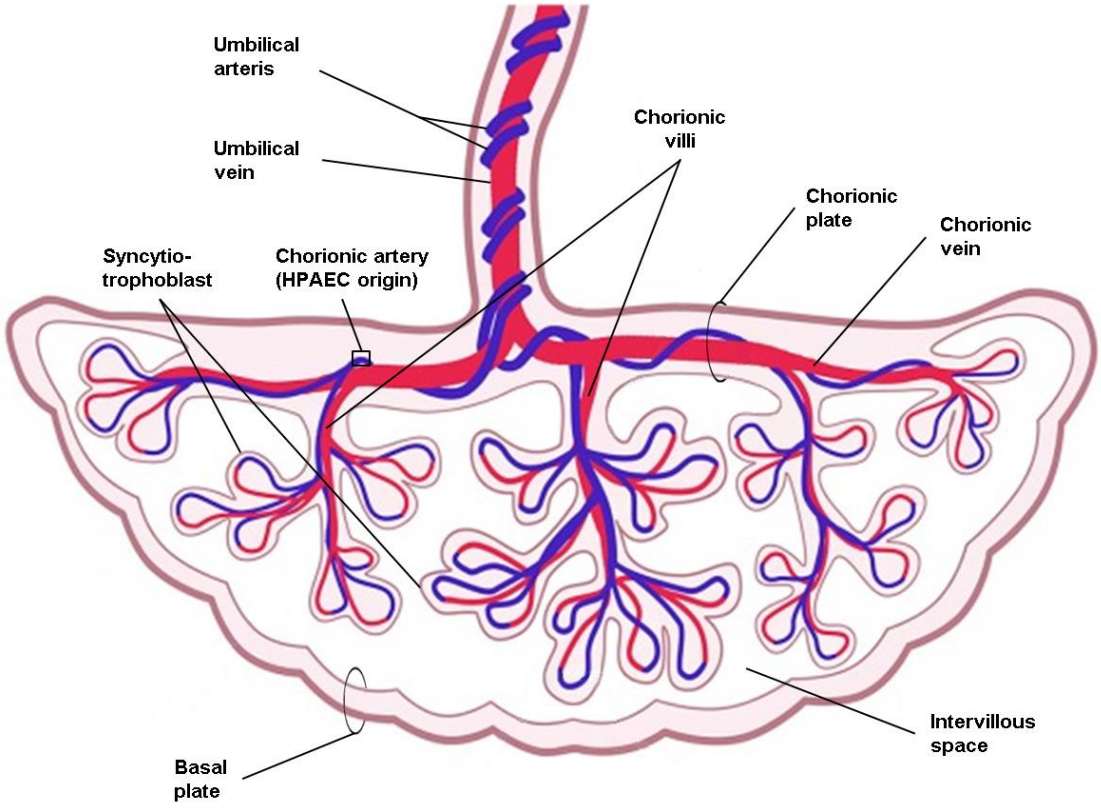

Figure 1: Schematic representation of term placental structure. The placenta consists of tissue derived from the fetus. The part that faces the fetus is termed chorionic plate whereas the basal plate faces the mother and is in contact with the uterine wall. Between these parts, the intervillous space is located which is bathed in maternal blood. The intervillous space harbours the chorionic villi where nutrient and waste product exchange between mother and fetus occurs. Chorionic villi are lined with a syncytiotrophoblast that separates the maternal and fetal circulation. Fetal blood circulates from the umbilical arteries through the chorionic arteries into the villi and back to the fetus via chorionic veins and the umbilical vein. HAPECs used in this study were isolated from the chorionic plate. HAPEC: human placental aortic endothelial cell. Modified illustration from Gaccioli et al [3] www.frontiersin.org /articles/10.3389/ fphys.2016.00040/full [Accessed 01.08.2018]

uterine wall. Between these parts the intervillous space is located which harbors the chorionic villi which are the central structure of the placenta [2]. Villi are tree-like entities that contain an extensive network of densely packed fetal blood vessels. These villous structures are lined with the so called syncytiotrophoblast which is a multinucleated syncytium that is in direct contact with the maternal blood [2]. The syncytiotrophoblast forms a continuous lining that strictly separates the maternal and the fetal circulation [4]. The intervillous space around the villi is bathed in maternal blood which enters through spiral arteries in order to enable nutrient and waste product exchange between mother and fetus through the villous trees. The maternal blood leaves the intervillous space through endometrial veins to re-enter maternal circulation. Nutrient poor fetal blood enters the placenta through two umbilical cord arteries which branch into chorionic arteries. These chorionic arteries in turn are connected to the blood vessel network within the villi. Nutrients from the maternal blood pass through the syncytiotrophoblast and the endothelium of the villous blood vessels into the fetal blood. Blood enriched with nutrients then circulates back into the fetus through chorionic veins which drain into a single umbilical cord vein [5] (Figure 1)

1.1.2 Preeclampsia

PE is currently one of the leading pregnancy complications. It is estimated that around 2 to 8 % of pregnancies worldwide are complicated by PE [6]. This syndrome is characterized by the development of hypertension, proteinuria, vascular dysfunction, chronic immune system activation, renal dysfunction and intrauterine growth restriction. Unfortunately, the etiology for PE is currently insufficiently understood and treatment is restricted to managing the resulting symptoms mentioned above [7]. There is a close relationship between PE and the placenta as placental invasion and remodeling of the spiral arteries is impaired [8]. This leads to an insufficient blood supply to the placenta and causes insufficient oxygenation [9]. Furthermore, the delivery of the placenta terminates the clinical symptoms of PE [7].

This improper placentation leads to systemic inflammation and endothelial dysfunction which are major and closely interconnected hallmarks of PE. During the progression of PE, levels of circulating anti-angiogenic factors, vasoconstrictors, placental debris, reactive oxygen species (ROS) and pro-inflammatory cytokines are increasingly elevated. The inflammatory response and endothelial dysfunction substantially drive the development of other cardinal symptoms of PE like hypertension and proteinuria [9]. From what is known about PE it becomes evident that the endothelium plays an important role in the pathophysiology of PE. That is because many of the circulating factors mentioned above originate from the endothelium and the functionality of the endothelium is increasingly impaired during the progression of PE.

1.2 Functions of the healthy endothelium

The endothelium is formed by endothelial cells (EC) and represents a cellular monolayer that lines the inner walls of all blood and lymphatic vessels in the human body [10]. Because of its location the endothelium forms the interface between the circulating blood and its constituents and the surrounding tissue [11]. First just considered a simple and inert physical barrier that hinders free passage of blood into the tissue, it now has become clear that the endothelium is a highly dynamic organ which fulfills several important functions [10]. The most important functions at rest include a) acting as a semi-permeable barrier, b) modulation of the vascular tone, c) maintaining blood fluidity and d) controlling the formation of new blood vessels (angiogenesis) [10]. Furthermore, vascular ECs are not homogeneous as initially anticipated but there is a considerable morphological and functional heterogeneity observable depending on their tissue of origin, whether they are located in large vessels or capillaries [12] or if they line veins or arteries [13].

1.2.1 The barrier function of the endothelium

A main function of the endothelium is to maintain the exchange of molecules between blood and tissue. To maintain this barrier, endothelial cells are linked to each other by cell junction proteins which prevent uncontrolled paracellular molecule transport. These junctions are formed by transmembrane proteins that are attached to cytoskeletal structures in the cells [14]. Hence, by cytoskeletal rearrangements endothelial cells can alter the restrictiveness of their barrier. The junctional proteins of adjacent cells bind each other to establish a seal that prevents paracellular molecule transport. There are two main classes of junctions termed adherens and tight junctions [14]. Adherens junctions (AJ) are the most common junctions present in the endothelium and prevent the crossing of molecules larger than ~ 3 nm [15]. The main constituent of AJs are cadherins, with VE-cadherin being the most important one [14]. Tight junctions (TJ) are much more restrictive and only allow transportation of molecules smaller than ~ 1 nm. Occludin, claudines and JAM-A are the main components of TJs. These junctions are not as widespread as AJs and are mainly located at sites where transportation is very restrictive like the blood-brain or the blood-retinal barrier [15].

Transcellular permeability of endothelial cells is another aspect that further influences the barrier function of the endothelium. This form of transportation is mainly receptor mediated and therefore tightly controlled and selective [16]. Transcytosis is the main mechanism driving transcellular permeability. This process can be divided in three major steps: I) endocytosis of macromolecules at the luminal membrane of ECs, II) transcytosis of the formed vesicle through the endothelial cytoplasm and III) exocytosis of the macromolecules on the apical site of ECs [15].

1.2.2 Regulation of vascular tone

ECs play an important role in regulating the vascular tone by releasing vasodilators or vasoconstrictors upon physical or hormonal stimulation, which then affect vascular smooth muscle cells (SMC) [17]. Prominent vasodilating agents released by the endothelium are prostaglandin I_2 (PGI_2) and nitric oxide (NO), whose synthesis and mode of action are described in more detail below (section 1.3.1 and section 1.4.2 respectively). Endothelium derived vasoconstrictors worth mentioning are endothelin-1 (ET-1) and thromboxane A_2 (TXA_2). ET-1 binds to ET_A receptors on SMCs which leads to an increase of intracellular Ca^{++}. Elevated levels of cytoplasmic Ca^{++} concentrations cause contraction of actin filaments and thereby vasoconstriction. ET-1 production is negatively regulated by NO and PGI_2 [18]. In a similar mode of action as ET-1, TXA_2 binds to the thromboxane-prostanoid receptor on SMCs and thereby causes Ca^{++} release from internal storages [18].

1.2.3 Maintenance of blood fluidity

In a resting state, ECs are essential players in maintaining proper blood fluidity by preventing adhesion, activation and aggregation of platelets and by regulating the coagulation cascade. This is mainly ensured by the production of NO and PGI_2 which cause increased cyclic adenosine monophosphate (cAMP) synthesis in platelets thereby preventing their adhesion and aggregation [14]. ECs also express thrombomodulin on their cell surface which binds thrombin and renders it from a pro-coagulant that converts fibrinogen to fibrin to an anti-coagulant that activates protein C [19]. Protein C interferes with the clotting cascade by inactivating factor VIIIa and Va [14]. Additionally, EC surfaces are rich in sulphated glycosaminoglycans which bind and activate anti-thrombin, the predominant inhibitor of thrombin and factor Xa [10]. ECs also synthesize tissue factor pathway inhibitor (TFPI) which block the activation of coagulation via the tissue factor - factor VIIa complex [20]. On the other hand if the endothelium gets activated, it switches from an anti-coagulant to a pro-coagulant state. Upon activation, ECs release von Willebrand factor (vWF) which promotes adhesion of platelets to the vascular wall as well as platelet aggregation. Furthermore it stabilizes the enzymatic activity of factor VIII [20]. Activated ECs release platelet activating factor that further facilitates the binding of platelets to ECs. Upon resolution of the insult on the blood vessel the formed clot has to be removed by fibrinolysis. ECs also support this process by releasing tissue plasminogen activator which in turn converts plasminogen to plasmin which then catalyzes the proteolysis of fibrin to resolve the clot [21].

1.2.4 Angiogenesis

Angiogenesis is the process of forming new blood vessels starting from already existing ones. Angiogenesis is an important physiological process in embryonic development, placentation, menstruation and wound healing. Angiogenesis is a tightly controlled process because uncontrolled angiogenesis contributes to pathologies like tumor growth and metastasis, arthritis and blindness [22]. Angiogenesis is induced by proangiogenic growth factors with the most important one being vascular endothelial growth factor (VEGF) which is rapidly released by tissue cells suffering from hypoxic conditions. Binding of VEGF to the VEGFR2 causes ECs to abandon their quiescent state and to start proliferation and migration towards the angiogenic cue [23]. The first step in angiogenesis is the local degradation of the extracellular matrix (ECM) of existing vessel to liberate the ECs. The proteolytic degradation of the ECM is executed by matrix metalloproteinases [24]. VEGF mediates the transient disassembly of AJs and TJs and dilation of the nascent vessel. This process increases the permeability of the vessel and allows plasma proteins to extravasate and to form an ECM that supports the migration of ECs [24]. The EC that is exposed to the highest VEGF concentration becomes the so called tip cell that leads the vessel formation. Tip cells form filopodia, which help to guide the direction of vessel formation towards the origin of the angiogenic cue [24] . ECs neighboring the tip cell become stalk cells whose task is to divide and elongate the stalk and to form a new lumen. In order to ensure controlled vessel formation there is only one tip cell per sprouting vessel. This is ensured via Notch signaling. Binding of VEGF to the VEGFR2 upregulates delta-like 4 (DLL4) expression in the designated tip cell. DLL4 binds to the Notch receptor on neighboring cells which leads to the downregulation of VEGFR2 making the cell less responsive to VEGF thereby preventing differentiation into another tip cell [23]. Fusion with a neighboring sprout or an already existing vessel terminates angiogenesis. Finally, the newly formed microvasculature is stabilized by the formation of a new basement membrane and the attachment of pericytes or SMCs [25].

1.2.5 The feto-placental endothelium

Naturally, the functions described above for the endothelium is also applicable for the feto-placental endothelium. However, the feto-placental endothelium shows higher cellular proliferation rates (especially in the villous structures) than the endothelium of other organs which is needed to meet the increasing nutritional demands of the growing fetus during pregnancy [12]. The feto-placental endothelium is part of a barrier that, together with the syncytiotrophoblast, separates the maternal and fetal circulation and regulates gas and nutrient exchange between mother and fetus. Because of this delicate position at the interface of two circulations, the feto-placental endothelium is fairly restrictive [26]. As the placenta lacks

innervation the regulation of the vascular tone is solely dependent on locally produced vasoreactive agents like NO, PGI_2, ET-1 and TXA_2, most of which are synthesized in the endothelium [27]. Another unique feature of the feto-placental endothelium is that oxygenated and nutrient rich blood is transported through veins whereas de-oxygenated and nutrient poor blood is transported through arteries [8].

Our laboratory established a protocol to isolate human placental aortic endothelial cells from arteries located at the chorionic plate (Figure 1). HAPECs present a polygonal shape and when grown to confluency they show the classical cobblestone morphology (Figure 2).Furthermore they strongly express genes like connexin40, hey-2, aldehyde dehydrogenase ADH1 and decidual protein induced by progesterone (Depp) which are specific for arterial ECs. HPAECs exhibit a low trans-differentiation potential towards osteoblasts and adipocytes which confirms their fully differentiated endothelial phenotype [13].

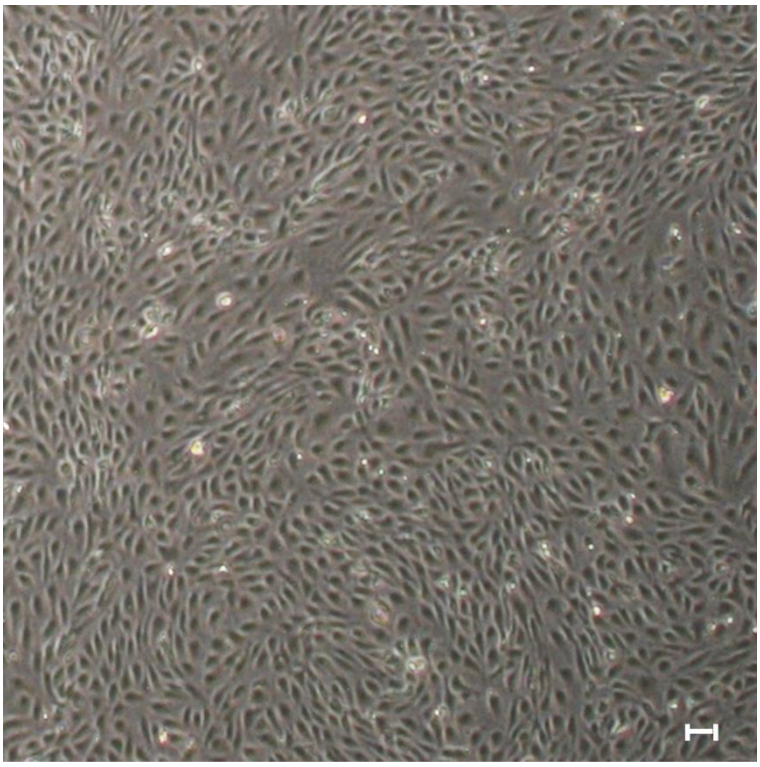

Figure 2: Morphology of human placental aortic endothelial cells. HAPECs are polygonal shaped cells that grow in loose arrangements and show the typical cobblestone pattern when grown to confluency. Scale bar = 50 µm

1.3 The endothelium and inflammation

Under normal physiological conditions the endothelium maintains an anti-inflammatory and anti-thrombotic state by exerting the tasks described above in section 1.2. If this state is disturbed by mechanic, chemical or immunologic influences which trigger inflammation, the endothelium becomes activated meaning the properties of the endothelium are changing. Hence the endothelium is not only a target of inflammatory stimuli but is also actively involved in the regulation of the inflammatory process.

Activation of the endothelium leads to three main processes: a) increased blood flow by dilating the vessels; b) increased vascular leakage and c) increased recruitment of leukocytes. Endothelial activation during acute inflammation is initiated by a fast (within minutes), stimulatory response that is independent of gene expression [28]. This first response is mediated by binding of ligands (e.g. histamine or thrombin) to G-protein coupled receptors (GPCR) [19]. Upon this fast stimulatory response a slower (within hours) but more sustained response that depends on gene expression follows which is triggered by cytokines like TNF-α and IL-1 [28]. This cytokines mediate the inflammatory response of endothelial cells mainly via the transcription factors NF-κB and activator protein 1 (AP1) [19].

1.3.1 Blood flow regulation

Initial increase in blood flow is mediated via GPCRs that activate phospholipase Cβ (PLC). PLC in turn converts membrane bound phosphatidylinositol 4,5-bisphosphate to inositol 3,4,5-triphsophate (IP_3) which causes a rise in intracellular Ca^{++} levels. Ca^{++} then activates phospholipase A_2 which cleaves phosphatidylcholine into arachidonic acid and lysophosphatidylcholine [19]. Arachidonic acid is then converted to PGI_2 via cyclooxygenase-1 (COX_1) and prostacyclin synthase [29]. PGI_2 is a potent vasodilator that leads to relaxation of SMCs which widens the blood vessel leading to increased blood flow at the site of inflammation [19]. This is mediated through G protein coupled prostacyclin receptors expressed on SMCs. Receptor binding leads to adenylate cyclase activation and thereby increased cAMP levels. CAMP increases protein kinase A activity which leads to the dephosphorylation of myosin light chain (MLC) causing SMC relaxation [18]. Additionally, Ca^{++} interacts with calmodulin and this complex activates endothelial nitric oxide synthase (eNOS), which produces the vasodilating agent NO [29]. Later on in the inflammatory response cytokines like IL-1 and TNF-α additionally induce COX_2. COX_2 catalyzes the same reaction as COX_1 in PGI_2 synthesis but at a much higher rate [19] (Figure 3). Increased blood flow is necessary to increase the number of immune cells present at the site of inflammation.

1.3.2 Changes in vascular permeability

Apart from increasing intracellular Ca^{++} concentration ligand binding to GPCRs activates RHO signaling pathway. The βγ subunit of heterotrimeric G-proteins enables the exchange of GDP to GTP on RHO because it activates the RHO guanine exchange factor [19]. RHO in turn activates a RHO dependent kinase which then phosphorylates myosin light chain phosphatase (MLCP) thereby deactivating it. Inhibition of MLCP prevents dephosphorylation of myosin light chain (MLC). At the same time Ca^{++} - calmodulin complexes activate myosin light chain kinase (MLCK) that phosphorylates MLC [30]. This mechanism leads to a net increase in MLC phosphorylation. Phosphorylated MLC is essential for the contraction of actin filaments which are associated with tight and adherens junction proteins. This contraction thereby leads to the opening of the junctions and consequently vascular leakage [15] (Figure 3). TNF-α and IL-1 further contribute to vascular leakage by causing rearrangement of endothelial actin and

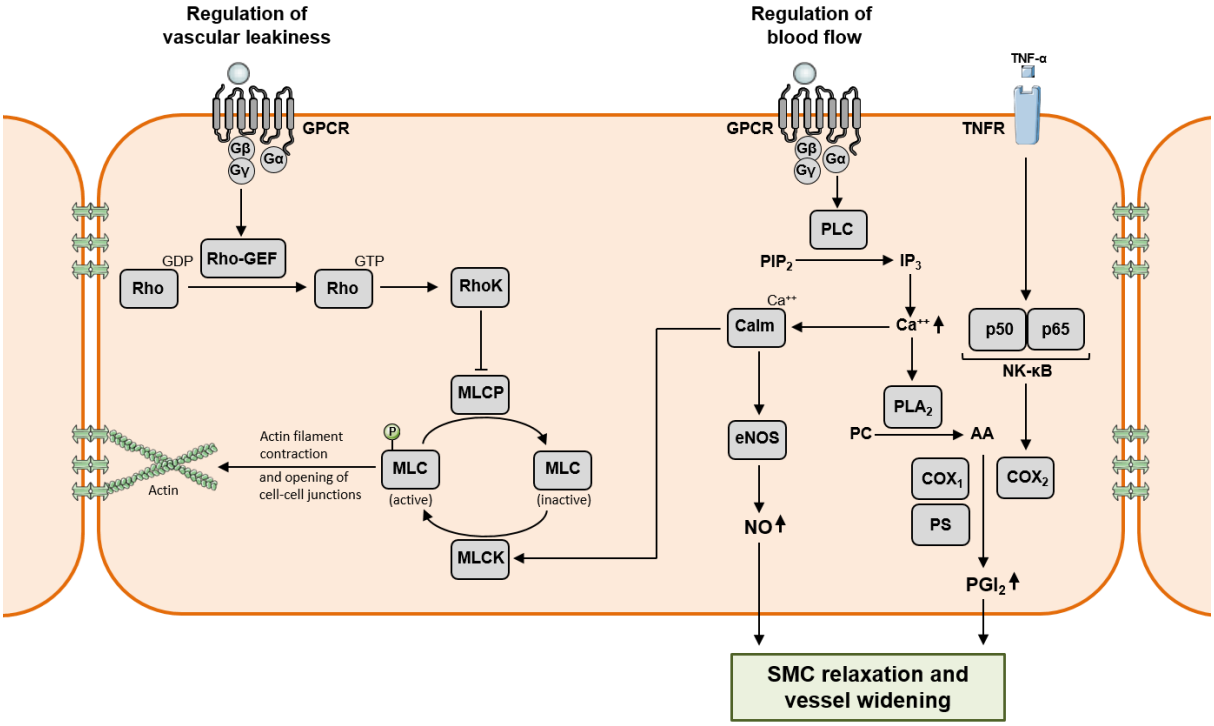

Figure 3: Regulation of vascular permeability and blood flow in endothelial cells during inflammation. Vascular leakiness is regulated via the Rho pathway. Upon activation of GPCR the Gβγ subunit activates Rho-GEF. Rho-GEF mediates the exchange of GDP for GTP on Rho which in turn activates RohK. RhoK inactivates MLCP whereas the activity of MLCK is increased by Ca^{++}-Calm complexes. This leads to a net increase in MLC phosphorylation which in turn causes actin filament contraction and opening of the attached cell-cell junctions to increase vascular leakiness. The increase in blood flow during inflammation is initially mediated by GPCRs. Ligand binding to GPCRs causes the activation of PLC via the Gα subunit. PLC catalyses the formation of IP_3 which in turn increases intracellular Ca^{++} levels. Ca^{++} activates PLA_2 and leads to the formation of AA. AA is converted to PGI_2 by COX_1 and PS. At the same time Ca^{++} associates with Calm and the Ca-Calm complex activates eNOS to stimulate NO production. Later on during the inflammatory response TNF-α mediates the upregulation of COX_2 expression via NF-κB. COX_2 further boosts the formation of PGI_2. PGI_2 and NO cause relaxation of SMC which leads to vessel widening and helps to increase the number of immune cells present at the site of inflammation. GPCR: G-Protein coupled receptor; Rho-GEF: Rho guanosine exchange factor; GDP: Guanosine diphosphate; GTP: Guanosine triphosphate; RohK: Roh kinase; MLC: Myosin light chain; MLCP: Myosin light chain phosphatase; MLCK; Myosin light chain kinase; PLC: Phospholipase C; PIP_2: phosphatidylinositol 4,5-bisphosphate; IP_3: inositol 3,4,5-triphsophate; Calm: Calmodulin; PLA_2: phospholipase A_2; PC: Phosphatidylcholine; AA: Arachidonic acid; $COX_{1/2}$: Cyclooxygenase 1/2; PS: Prostacyclin synthase; NO: nitric oxide; PGI_2: prostaglandin I_2.

tubulin cytoskeleton structures mainly via NF-κB dependent pathways. Leakage of plasma proteins into the tissue provides a matrix that helps immune cells to attach, survive and migrate [19]. Furthermore, leukocyte migration into the tissue is facilitated by the formation of intercellular gaps in the endothelial lining.

1.3.3 Recruitment of leukocytes

The increased activation of MLC caused by elevated Ca^{++} concentrations and MLCP inactivation also impacts leukocyte recruitment to the site of inflammation. Phosphorylated MLC triggers the fusion of Weibel-Palade bodies (WPB) with the plasma membrane of ECs. Weibel-Palade bodies are endothelium specific vesicles that harbor proteins essential for leukocyte interaction [19]. The fusion leads to the presentation of P-Selectin on the surface of endothelial cells. P-Selectin enables the interaction with selectin ligands present on leukocytes (Figure 4). This initial interactions are weak and cause the leukocytes to roll along the endothelial lining of blood vessels [31]. Furthermore, as a byproduct of arachidonic acid synthesis, platelet activating factor (PAF) is produced which supports leukocyte adhesion by integrin activation and cell regulation [19]. Leukocyte recruitment becomes way more effective as soon as the endothelium is further activated by cytokines like TNF-α or IL-1. This cytokines initiate the expression of IL-8, a chemoattractant for neutrophils, and the surface expression of E-selectin which has the same function as P-Selectin. As mentioned before cytokine mediated endothelial activation is more sustained and evolves over time. With somewhat delayed kinetics compared to E-Selectin the expression of VCAM1 and ICAM1 is upregulated in endothelial cells. ICAM1 and VCAM1 enable a tighter adhesion of leukocytes to the endothelial layer [31]. This goes along with increased expression of chemokines like MCP1 which further drives leukocyte recruitment and additionally leads to a switch from a neutrophil dominated immune response to a monocyte dominated one [19] (Figure 4). Once recruited to the endothelium leukocytes migrate into the tissue through the gaps between adjacent ECs. This process of transmigration is additionally facilitated by platelet-endothelial cell adhesion molecule 1 and CD99 [31].

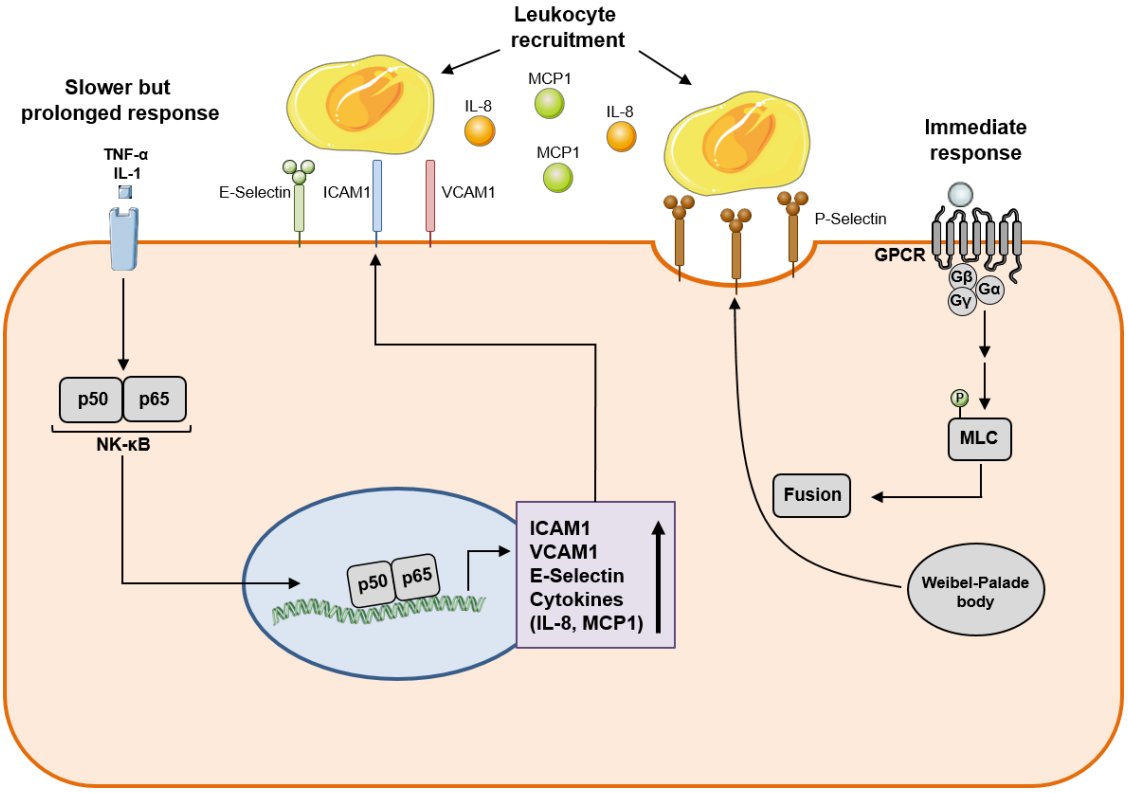

Figure 4: Regulation of leukocyte recruitment during inflammation. Initial activation of GPCRs by mediators like histamine or thrombin leads to a net increase in activated phosphorylated MLC. Activated MLC triggers the fusion of WPB with the cell membrane thereby releasing stored P-Selectin molecules. P-Selectin mediates the first weak interactions between the endothelium and leukocytes during inflammation. With progressing inflammation cytokines like TNF-α and IL-1 are released. Upon their interaction with ECs through their respective receptors the NF-κB pathway is activated. NF-κB controls and increases the expression of adhesion molecules like ICAM1, VCAM1 or E-Selectin and of cytokines like IL-8 and MCP1. Expression of this adhesion molecules enables a tighter interaction of ECs and leukocytes making the recruitment process more effective. The released chemokines navigate the chemotactic movement of leukocytes towards the site of inflammation. GPCR: G-Protein coupled receptor; MLC: Myosin light chain; ICAM1: Intercellular adhesion molecule 1; VCAM1: Vascular cell-adhesion molecule 1; MCP1: monocyte chemoattractant protein1; IL-8: Interleukin 8; WPB: Weibel-Palade body; TNF-α: Tumor necrosis factor alpha; IL-1: Interleukin 1.

1.4 Endothelial dysfunction

Endothelial dysfunction is a complex condition and there are several mechanism that lead to its manifestation. It is associated with multiple diseases including hypertension, inflammatory diseases, atherosclerosis, preeclampsia and cancer metastasis [32]. In general, endothelial dysfunction is associated with an impaired balance between vasorelaxation and vasoconstriction. This is caused by an increased concentration of vasoconstrictors and a decreased concentration of vasodilators. Additionally, the sensitivity of ECs to vasoconstrictors increases whereas the reactivity of vascular smooth muscle cells to vasodilators is reduced [32]. This goes along with activation of the endothelium corroborated by a switch to a more pro-inflammatory and pro-coagulatory state [33].

1.4.1 Oxidative stress and endothelial dysfunction

The underlying mechanisms of endothelial dysfunction is based on elevated oxidative stress. Oxidative stress is caused by an increased production of reactive oxygen species (ROS) like $O_2^{\bullet -}$, hydrogen peroxide (H_2O_2), the hydroxyl radical ($\bullet OH$) and $ONOO^-$. Under normal physiological conditions ROS are involved in cell metabolism and cell signaling but when their production is deregulated they become cytotoxic because of their high reactivity with cellular constituents like DNA, RNA, proteins and lipids [34]. The main contributor for ROS in the vascular system is NADPH oxidase (NOX), which is an enzyme that specifically produces $O_2^{\bullet -}$ by reducing O_2 using NADPH as an electron donor [32] (Figure 5). NOX activity in endothelial cells is elevated upon AngII stimulation via the angiotensin 1 receptor. This creates a link between hypertension, increased oxidative stress and resulting endothelial dysfunction. This context was demonstrated in rats, which were infused with AngII and then displayed increased NOX activity and impaired endothelial function [35]. Apart from NOX, other sources of ROS are the respiratory chain of the mitochondria, xanthine oxidase and - as described in more detail below - uncoupled eNOS [36].

1.4.2 Role of nitric oxide in endothelial dysfunction

A central role in endothelial dysfunction can be attributed to NO, whose bioavailability is strongly reduced in endothelial dysfunction. NO is a vasodilating molecule, which is produced in the endothelium and dilates vessels by increasing the production of cyclic guanosine monophosphate through stimulation of soluble guanylyl cyclase in smooth muscle cells [37]. NO is synthesized by nitric oxide synthase (NOS) and there are three known isoforms of NOS: neuronal NOS, inducible NOS and endothelial NOS (eNOS). Unsurprisingly, eNOS is the dominating isoform in the endothelium. eNOS catalyzes the formation of NO where L-arginine serves as a substrate and is oxidized into NO and L-citrulline [34] (Figure 5B). The formation

of NO depends on the presence of tetrahydrobiopterine (H_4B) as a cofactor. As outlined in section 1.4.1, endothelial dysfunction goes along with increased production of $O_2^{\bullet-}$, which can react with NO to form peroxynitrite. This process leads to the aforementioned reduction of NO bioavailability and in addition, peroxynitrite oxidizes H_4B to dihydrobiopterin (H_2B) thereby depleting NOS of its cofactor [38]. Under normal conditions NOS is a homodimeric enzyme but in the absence of B_4H the homodimer dissociates. Monomeric NOS or, as it is called,

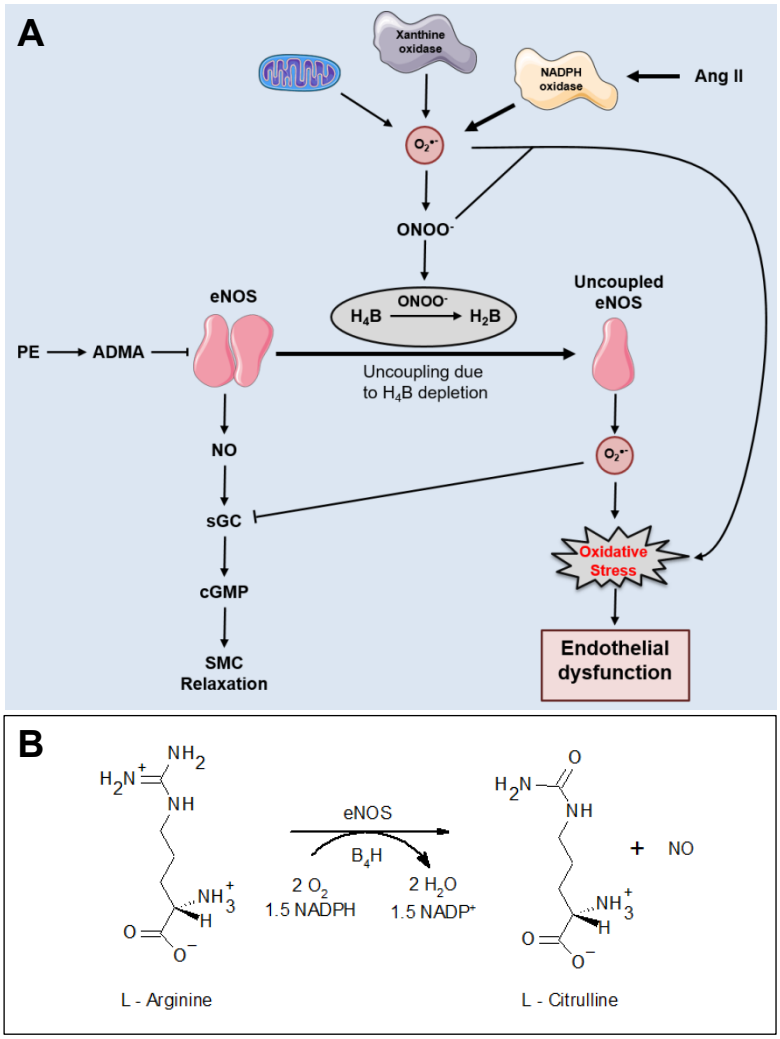

Figure 5: Sources and role of reactive oxygen species in endothelial dysfunction. **(A)** The mitochondria, xanthine oxidase and NADPH oxidase are primary sources of $O_2^{\bullet-}$ with NADPH oxidase being the dominant one in ECs. $O_2^{\bullet-}$ reacts with NO to form $ONOO^-$ which oxidizes H_4B to H_2B thereby depleting eNOS of its cofactor. This leads to eNOS uncoupling and causes eNOS to switch from producing vasculoprotective NO to produce $O_2^{\bullet-}$ which further drives oxidative stress and endothelial dysfunction. Additionally, ADMA levels which is an inhibitor of eNOS are increased by oxidative stress and in preeclampsia. When not uncoupled by oxidative stress, eNOS produces NO which induces sGC in SMCs causing cGMP levels to rise ultimately leading to vascular relaxation.**(B)** Functional eNOS catalyzes the oxidation of L-arginine to produce NO and L-Citrulline. H_4B serves as a cofactor in this reaction. AngII: Angiotensin II; PE: Preeclampsia; ADMA: Asymmetric dimethylarginine; H_4B: Tetrahydrobiopterin; H_2B: Dihydrobiopterin; NO; Nitric oxide; sGC: Soluble guanylate cyclase; cGMP: Cyclic guanosine monophosphate; SMC: Smooth muscle cell.

uncoupled NOS switches from synthesizing NO to the production of $O2^{\bullet-}$ [34]. Apart from directly influencing eNOS functionality, oxidative stress raises the levels of asymmetric dimethylarginine (ADMA), which is a competitive inhibitor of eNOS. ADMA levels increase because oxidative stress lowers the activity of the ADMA degrading enzyme dimethylarginine dimethylaminohydrolase, and/or increases the activity of the ADMA producing enzyme arginine methyltransferase [36]. Interestingly, ADMA levels are also increased in women suffering from preeclampsia compared to normotensive pregnant women [39] (Figure 5A). This mechanisms generate a vicious cycle where NO levels are constantly decreasing whereas the concentration of $O_2^{\bullet-}$ and other ROS is continuously increasing thereby further boosting endothelial dysfunction.

1.4.3 Endothelial dysfunction and inflammation

As mentioned before, endothelial dysfunction causes ECs to switch to a pro-inflammatory state. Inflammatory responses of the vasculature during endothelial dysfunction are to a large extent induced by ROS. This is because ROS interfere with intercellular signaling pathways like NF-κB and AP1 which are central in inducing inflammation [40]. Apart from driving inflammation on a transcriptional level, ROS increase vascular permeability which facilitates the infiltration of immune cells [40]. Furthermore, it was shown that NO depletion enhances leukocyte rolling and adhesion *in vivo*. Interestingly, although *in vitro* experiments showed that NO depletion increased the expression of the adhesion molecules P-Selectin and E-Selectin, increased leukocyte adhesion could not be observed *in vitro*, indicating that there is still a missing link that remains to be elucidated [41]. On the other hand, inflammation can also be the cause for endothelial dysfunction in the first place. This is mainly caused by infiltrating mononuclear cells which produce ROS via NADPH oxidase as a part of their defense system against invading pathogens. Under normal inflammatory conditions this defense system would not lead to endothelial dysfunction but a prolonged, pathogenic inflammatory stimulus (like it is the case in preeclampsia) or inappropriate and/or unspecific activation of this defense system is able to cause endothelial dysfunction [40]. Additionally, inflammation impacts the NO metabolism in ECs. For instance, it has been demonstrated that C-reactive protein (CRP) [42] and TNF-α [43], both potent mediators of inflammation, negatively impact the transcription of eNOS. From this observations it becomes evident that inflammation and endothelial dysfunction are closely interconnected and that endothelial dysfunction can be the cause and/or the result of inflammation.

1.5 Neonatal high density lipoprotein

Human serum lipoproteins are soluble complexes composed of proteins (apolipoproteins) and lipids. They are mainly synthesized in the liver and intestine and fulfill the needs to transport hydrophobic lipids through the aqueous environment of the blood [44]. Mature lipoproteins are composed of a core of neutral lipids like triacylglycerol (TAG) and cholesteryl esters (CE) which is surrounded by a surface layer of phospholipids, apolipoproteins (Apo) and free cholesterol (FC). There are four main classes of lipoproteins which are distinguished based on their densities [44]. These classes are termed chylomicrons, very low density lipoproteins (VLDL), low density lipoproteins (LDL) and high density lipoproteins (HDL). Apart from their density, these particles also differ in lipid and protein composition and are not rigid entities but are constantly remodeled, dependent on the metabolic demands, by lipid transfer, enzymatic reactions, and protein exchange while they are circulating.

1.5.1 Formation of HDL particles

The formation of HDL particles starts predominantly in the liver where apolipoprotein A1 (ApoA-1) accepts lipids (mainly FC and phospholipids) mainly from the circulation to form a discoidal shaped pre-β HDL particle. This transport of lipids from peripheral cells to circulating HDL is facilitated by ATP binding cassette transporter A1 (ABCA1) [45]. FC acquired from cells accumulates at the surface of HDL particles and needs to be esterified by lecithin-cholesterol acyl transferase (LCAT). The highly hydrophobic CEs then move to the core of the HDL particle which causes the formation of a mature spherical HDL_3 particle. Spherical HDL_3 further accumulates FC from the circulation which is continuously esterified by LCAT. This FC transfer leads to the formation of lager HDL_2 particles and is mainly dependent on ABCG1, scavenger receptor class B type 1 (SR-BI) and passive diffusion. [45]. HDL also interacts with LDL and VLDL particles by a cholesterol ester transfer protein (CETP) mediated process, which enables HDL to acquire triglycerides from LDL or VDL in exchange for CE [46].

1.5.2 Composition of neonatal HDL

HDL is the smallest lipoprotein particle and the main protein constituent of HDL is ApoA-1 which accounts for up to 70 % of the total protein load together with ApoA-2 (20 %) [47]. Other protein constituents are ApoA-4, ApoC, ApoD, ApoE and ApoM and enzymes like CETP and LCAT. In addition to this lipid metabolism related proteins, HDL particles carry many other proteins and enzymes that are involved in processes like hemostasis, inflammatory and immune response, vitamin transport, energy balance or heme and iron metabolism [48,49]. Apart from the lipids mentioned above, HDL particles carry a multiplicity of other lipid species like sphingomyelin, ceramide, phosphatidylcholine [50] or S1P [51]. Recently, even the

presence of microRNAs on HDL particles was reported [52]. The composition of HDL is dynamic and changes spatial-temporally while HDL is circulating and eventually becomes dysfunctional during some diseases which adds even more complexity [48].

The lipoprotein profile and composition of HDL is different between offspring and adults. In the fetal circulation the lipoprotein concentrations are in general lower than in adults and HDL is the major lipoprotein class whereas in adults LDL is the dominating lipoprotein class [53]. Hence, a greater portion of cholesterol is carried by HDL in the newborn compared to adults. In adults the LDL-C/HDL-C ration is ~ 2 whereas this ratio is only 0.5 – 1 in the fetus [49]. Because of the lower lipoprotein concentration, levels of total cholesterol, triglycerides and phospholipids in the fetal circulation are only one third to one half of the concentration in adults [53]. Apart from differences in total levels and relative distribution of lipoproteins there are also differences with respect to the composition. Although ApoA-1, ApoA-2, ApoC-3, and ApoD are associated with fetal HDL, their concentrations are considerably lower than on adult HDL [49,54,55]. ApoF and ApoL are found on adult HDL but not on fetal HDL [55]. The only apolipoprotein which is overrepresented in fetal HDL is ApoE, indicating enhanced cholesterol transport properties [54]. When looking at other proteins than apolipoproteins, it is interesting to mention that fetal HDL is enriched in proteins associated with coagulation and transport. Furthermore, paroxonase 1 content was considerably lower on fetal HDL which implies a reduced anti-oxidative capacity compared to adult HDL [55].

1.5.3 Function of HDL

Lipoproteins are key players in the lipid metabolism of the human body and the main function of HDL in lipid metabolism is the reverse transport of FC form peripheral cells to the liver for processing. HDL particles and hepatocytes interact via the SR-BI receptors in order to unload FC and CE from HDL to the liver. This process yields smaller HDL particles depleted of cholesterol which are released back into circulation. After delivery to the liver, cholesterol can be eliminated by secreting it into the bile either directly or by first converting cholesterol into bile acids [45]. Hence, HDL protects the cardiovascular system as removal of excess cholesterol reduces the risk for formation of atherosclerotic lesions and helps improving outcomes for already existing lesions [51]. It is worth to mention that in the fetus transport of cholesterol back to the liver for excretion is very limited as bile acid production is poorly established and most of the cholesterol provided is needed to cover the demands of the growing fetus. Therefore, in the fetus HDL rather supports the delivery of cholesterol to peripheral cells and compensates for the low amounts of LDL in the circulation rather than transporting cholesterol back to the liver [49]. This is further supported by the high ApoE levels on fetal HDL as ApoE increases the transport capacity of lipoproteins by interacting with the

LDL receptor on peripheral cells [47]. Apart from reverse cholesterol transport HDL particles exert other biological functions, which lead to anti-inflammatory, anti-oxidative and anti-apoptotic effects and further increase the protective effect of HDL on the cardiovascular system [51]. Although it is quite clear that these effects are caused by HDL, the molecular basis of these effects is less well understood. As mentioned above HDL particles show a very diverse composition and each of the components present could theoretically be responsible for this protective effects of HDL. This diversity as well as the huge compositional variation of HDL between individuals are the reasons why it is so difficult to map the diverse function of HDL to specific constituents [51]. Nevertheless, much effort is made to clarify this issue. For example, among the lipid species present on HDL, S1P has recently drawn a lot of attention as it seems to mediate several of the biological effects exerted by HDL.

1.6 Sphingosine 1-phosphate

Sphingolipids are important and omnipresent constituents of the mammalian cell membrane. Apart from being a mere building block for cell membranes, sphingolipids also act as signaling molecule and exert important regulatory tasks in many cellular processes critical for health and disease. Among the sphingolipids, S1P is one of the most interesting bioactive lipids. S1P is an amphoteric, zwitterionic molecule consisting of a hydrophobic hydrocarbon tail and a hydrophilic amino-phosphate head group [56] (Figure 6**Fehler! Verweisquelle konnte nicht gefunden werden.**). Because of its amphiphilic properties S1P is usually associated with the cell membrane but is also sufficiently soluble to move between different membrane compartments. However, in order to cross membranes active transportation is necessary [57]. When first described in 1970, S1P was thought to be just an intermediate product in the degradation of sphingosine with no biological funcion [58]. It took another two decades before the role of S1P as a signaling molecule became evident for the first time [59]. Since then it became clear that S1P is involved in a multiplicity of biological processes like cell growth [59], apoptosis [60], calcium signaling [61], cell migration [62], differentiation, survival [63] and

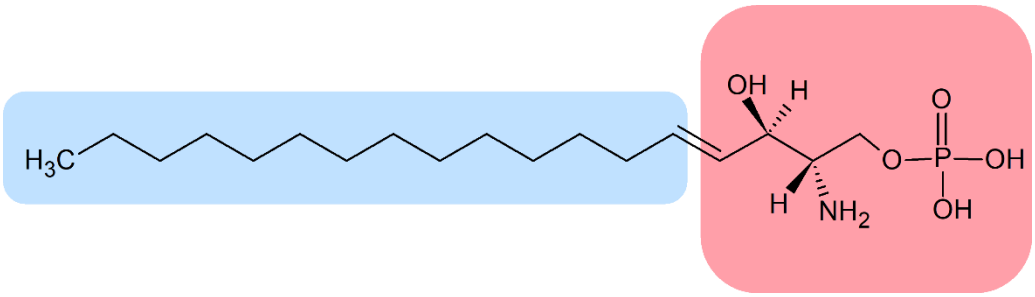

Figure 6: Structural formula of S1P. The hydrophobic hydrocarbon tail is highlighted in blue whereas the hydrophilic amino-phosphate head is highlighted in red showing the amphiphilic character of S1P.

cytoskeletal organization [64]. Because of its considerable impact on cellular processes it is not surprising that S1P activity also plays a role in various pathophysiological conditions and diseases for example inflammation [65] atherosclerosis [66], asthma [67], diabetes and obesity [68], multiple sclerosis [69] and cancer [70]. In mammals S1P concentrations are the highest in blood (~ 1 µM) followed by lymph (~ 100 nM) whereas S1P amounts are low in the interstitial fluid of tissues. In the blood S1P is provided primarily by erythrocytes [71] and to a lesser extent by ECs [72]. Many of the conditions just mentioned do affect the vascular system and it is also know of S1P that it markedly impacts the vasculature. S1P affects the maturation of vessels, angiogenesis and permeability of the vasculature as well as vascular tone by influencing ECs and vascular SMCs [73].

1.6.1 Sphingolipid metabolism

De novo synthesis of sphingolipids starts with serine and palmitoyl CoA which are condensed by serine palmitoyl transferase (SPT) to produce dehydrosphinganine [74]. SPT is a membrane bound heterodimeric protein formed by the subunits SPTLC1 and SPTLC2. SPT requires pyridoxal 5'-phosphate as a cofactor in order to exert its catalytic function [75]. This first reaction is the rate limiting step in the synthesis process of sphingolipids. Dehydrosphinganine is quickly reduced to dihydrosphingosine by ketosphinganine reductase in an NADPH dependent reaction [76]. In the next step dihydrosphingosine is N-acetylated to dihydrocermide which is then further desaturated by dihydroceramide desaturase to form ceramide, an important key molecule in the sphingolipid metabolism [76]. The *de novo* synthesis beginning with serine to produce ceramide takes place in the endoplasmic reticulum [74]. Additionally, ceramide can be synthesized by the hydrolysis of sphingomyelin catalyzed by sphingomyelinase which is a quicker and more convenient method. Technically speaking S1P is a breakdown product of ceramide. Ceramide can be reversibly de-acetylated by a ceramidase to form sphingosine [74]. The reverse reaction back to ceramide is catalyzed by ceramide synthease [76]. Sphingosine is then finally phosphorylated by SPHK1 and 2 to produce S1P. SPHK1 is localized in the cytosol and moves to the plasma membrane upon activation. SPHK1 can also be transported to the extracellular space to increase S1P levels in vicinity of secreting cells. SPHK2 on the other hand is mainly located in the nucleus and cannot be secreted [77]. The reaction performed by SPHK is reversible and the dephosphorylation of S1P back to sphingosine is exerted by SPP [78]. SPP is localized at the endoplasmic reticulum and there are two known isoforms (SPP1 and SPP2). SPPs are differently expressed in various tissues where SPP1 dominates in placenta and kidney whereas SPP2 is mostly found in the heart and kidney. Besides SPP1 and 2 there are other enzymes which are capable of dephosphorylating S1P. These enzymes are called lipid phosphate phosphatases (LPP) and there are 3 known isoforms termed LPP1, LPP2 and LPP3 [79]. These LPPs are mainly located

at the plasma membrane with their active site facing the extracellular space meaning they are dephosphorylating extracellular S1P rather than S1P synthesized within the cells [79]. Unlike SPPs, which have a rather high substrate specificity limited to S1P and dihydrosphingosine, LPPs are capable of dephosphorylating a broader spectrum of phosphorylated lipids including S1P, lysophosphatidic acid, phosphatidic acid and ceramide-1-phosphate. Among LPPs LPP2 is most effective in degrading S1P [79]. Besides the reversible degradation of S1P there is another irreversible degradation pathway which is executed by S1P lyase. S1P lyase cleaves the C2-C3 bond of S1P to yield hexadecenal and phosphoetanolamine (Figure 7). Like SPT this enzyme is a pyridoxal 5'-phosphate dependant enzyme and it is ubiquitously expressed in mammalian tissues [76].

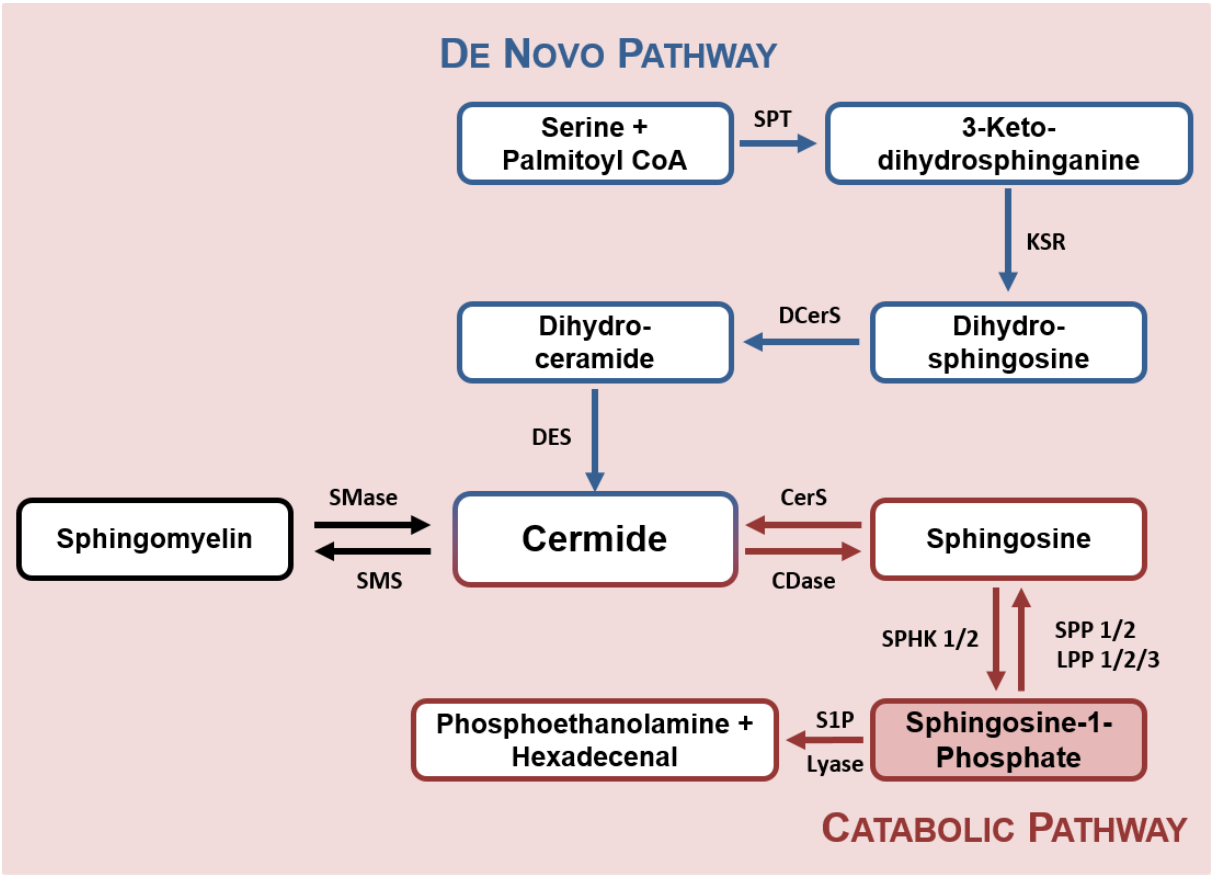

Figure 7: Schematic diagram of sphingolipid metabolism. The *de novo* pathway is marked in blue whereas the catabolic part of the pathway is marked in red. SPT, Serine palmitoyl transferase; KSR, Ketosphinganine reductase; DCerS, Dihydroceramide synthase; DES, Dihydroceramide desaturase; SMase, Sphingomyelinase; SMS, Sphingomyelin synthase, CerS, Ceramide synthase; CDase, Ceramidase; SPHK, Sphingosine-1-phosphate kinase; SPP, Sphingosine-1-phosphate phosphatase; LPP, Lipid phosphate phosphatase.

1.6.2 S1P signaling in endothelial cells

When first described, S1P was considered to be a second messenger until the discovery of five receptors specific for S1P which added new information about how S1P exerts its signaling effects [80]. These receptors were termed sphingosine-1-phosphate receptors 1-5 ($S1PR_{1-5}$). From these five different receptors only $S1PR_{1-3}$ are found on ECs with $S1PR_1$ being the most abundant receptor. $S1PR_4$ is mainly found in the lymphoid system and $S1PR_5$ expression is the highest in the central nervous system [81,82]. S1PRs are G protein coupled receptors but their coupling capacity to the different G protein alpha subunits varies [73]. $S1PR_1$ only couples with Gαi whereas $S1PR_2$ and $S1PR_3$ are less specific and couple with Gαi, Gαq and Gα12/13 although $S1PR_2$ prefers Gα12/13 and $S1PR_3$ prefers Gαq. $S1PR_4$ and $S1PR_5$ interact with Gαi and Gα12/13 [81].

The S1P/S1PR1/Gαi axis causes activation of the Ras/ERK pathway and the phosphatidylinositide 3-kinase (PI3K)/Akt/eNos pathway to promote vasorelaxation, proliferation and survival. Furthermore it leads to cell migration through cytoskeletal rearrangements and to enhanced barrier function of endothelial cells by activation of the PI3K/Rac pathway. $S1PR_2$ signaling through Gα12/13 leads to induction of Rho which in turn activates Rho kinase (RhoK) and phosphatase and tensin homologue. In that way, S1P signaling through $S1PR_2$ increases endothelial permeability and inhibits cell migration meaning that the actions exerted via $S1PR_2$ oppose the actions of the S1P/$S1PR_1$ axis [83,84]. In the context of inflammation it is suggested, that S1P signaling via $S1PR_1$ is anti-inflammatory whereas signaling through $S1PR_2$ leads to pro-inflammatory actions. The role of $S1PR_3$ on the other hand is more diverse. It was shown that $S1PR_3$ signaling is able to activate eNOS via Gαi just like $S1PR_1$ to perform anti-inflammatory and vasoprotective actions [85]. Furthermore $S1PR_3$ mediated signaling enhances adherens junction assembly and cell migration. But it was also reported that signaling via Gαq leads to increased calcium release through the PLC pathway which increases vascular permeability. $S1PR_3$ signaling also increases vascular permeability through stress fiber formation via the Rho/RhoK pathway [83,84] (Figure 8). Taken together this shows that the relative expression pattern of S1PRs and the availability of different G proteins under a specific condition seem to play an important role in how the endothelium responses to S1P.

S1PR signaling is transient and a sustained exposure to S1P leads to a desensitization process which causes the internalization of S1PR by endocytosis. Desensitization is initialized by the phosphorylation of the C-terminal tail of S1PR by G-protein coupled receptor kinase 2 or protein kinase C. This phosphorylation prevents the interaction of S1PR with G proteins thereby terminating S1PR signaling and enables the binding of β-arrestin to the S1PR. β -arrestin interacts with clathrin and adaptin-2 which triggers endocytosis of S1PR via clathrin

coated vesicles. However, internalization of S1PR does not inherently result in receptor degradation. S1PR can also be recycled back to the cell surface, thereby being ready for another signaling event within several hours. [86,87].

Apart from signaling through S1PRs, S1P triggers intracellular signaling processes which are less well investigated. S1P produced in the nucleus by SPHK2 is able to inhibit the function of histone deacetylase 1 and 2 thereby influencing histone acetylation dynamics and pushing the balance towards increased transcriptional activity [88]. Intracellular S1P also interacts with TRAF2 which is an adaptor protein involved in NF-κB signaling. TRAF2 ubiquitinates RIP1 which is necessary for NF-κB activation upon TNF-α stimulation and S1P was found to act as cofactor in activating the E3 ligase activity of TRAF2 [89]. It is worth mentioning that the involvement of S1P in NF-κB activation is still a matter of debate as there is another study which shows that NF-κB activation is independent of S1P [90]. Furthermore it was shown that S1P interacts with Prohibitin 2 (PHB2) which is a mitochondrial protein localized at the inner membrane and responsible for mitochondrial biogenesis and metabolism. The interaction

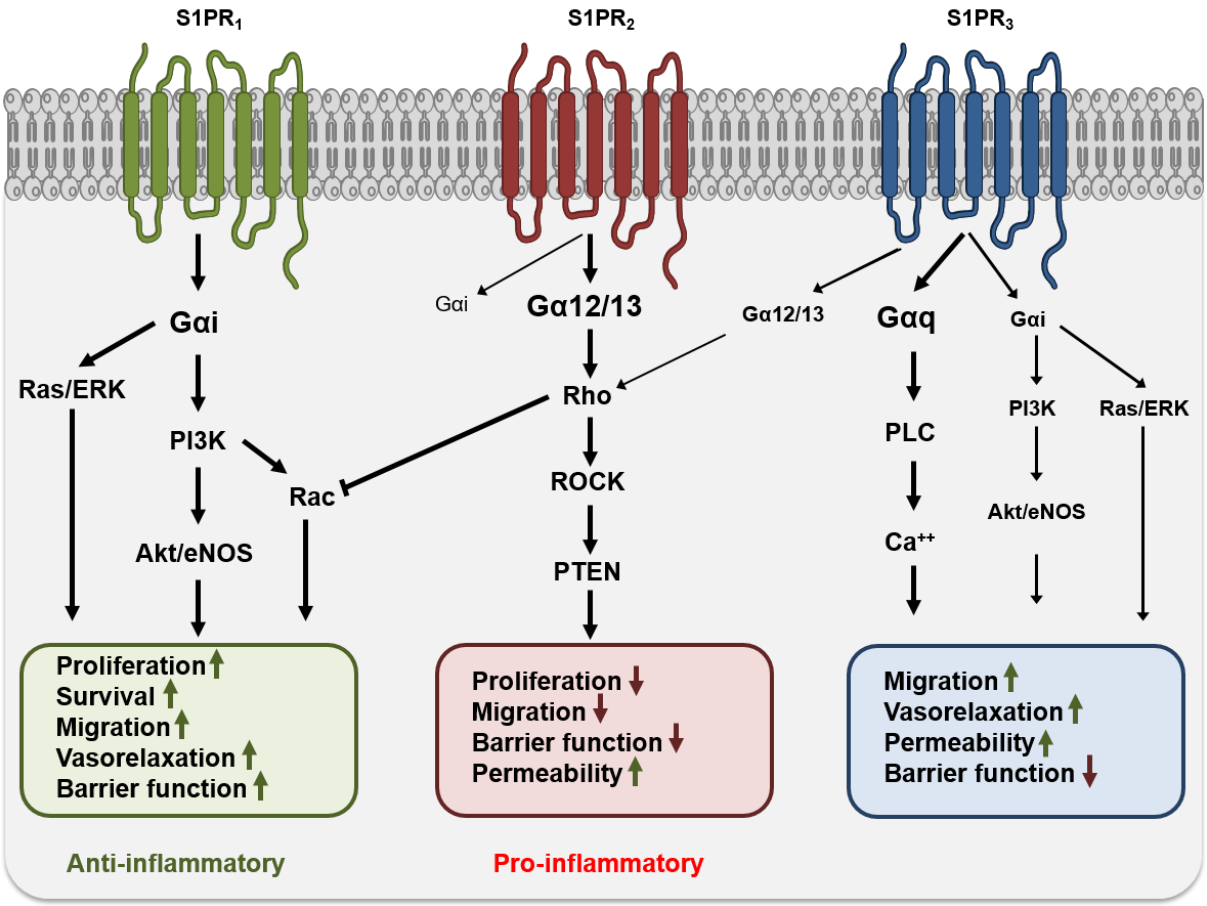

Figure 8: S1PR signalling in endothelial cells. S1P receptor subtypes can couple to different G proteins triggering different intracellular signalling mechanisms. $S1PR_1$ exclusively couples to Gαi thereby activating Ras/ERK and PI3K pathways promoting a pro-survival and anti-inflammatory outcome for endothelial cells. $S1PR_2$ most strongly couples to Gα12/13 which activates signalling through Rho thereby exerting contrary effects to $S1PR_1$, inhibiting proliferation and migration and causing a pro-inflammatory environment. $S1PR_3$ mainly signals via Gαq to trigger Ca^{++} release via PLC thereby increasing permeability. In endothelial cells signalling via $S1PR_3$ also leads to increased eNOS activity and improved vasorelaxation thereby protecting the vasculature.

between S1P and PHB2 is crucial for the assembly of cytochrome-c oxidase and thereby mitochondrial respiration [91]. Another study showed that S1P is involved in the production of amyloid-β peptide (Aβ) in neurons. Aβ is important in Alzheimer disease as it is a major constituent of the protein plaques found in the brains of diseased individuals. S1P directly regulates the activity of β-site amyloid precursor protein cleaving enzyme-1 (BACE1) which catalyzes the rate limiting reaction in the synthesis of Aβ. Therefore Aβ production could possibly be influenced by downregulation of SPHK or upregulation of SPP and/or S1P Lyase [92].

1.6.3 Secretion and transportation of S1P

To enable S1P signaling via S1PRs, intracellularly produced S1P needs to be transported out of synthesizing cells. Because of its hydrophilic head group S1P needs active transportation through the cell membrane. Therefore specific transporters are necessary. In ECs spinster homologue 2 (SPNS2) was identified as primary S1P transporter. SPNS2 seems to be a passive transporter as the amount of transported S1P increases with intracellular S1P concentrations. Although SPNS2 is the most important S1P transporter for ECs, downregulation or knock out of this transporter has only a minor effect on S1P plasma concentrations. This is because the main source for S1P in blood are erythrocytes and erythrocytes use different transporters to release S1P [93,94]. In the lymph system on the other hand, downregulation or knockout of SPNS2 has a major impact on lymph S1P concentration as lymphatic ECs are the main source of lymph S1P [95]. How S1P is exported from erythrocytes is still unclear. ABC transporters are under discussion for being responsible for S1P transport in erythrocytes but conflicting results are causing doubts concerning their involvement. Recently, MFSD2B which belongs like SPNS2 to the MFS superfamily of membrane transporters, was identified as a putative transporter for S1P in erythrocytes [96].

Once S1P is released into the bloodstream, S1P needs to bind to a protein carrier to provide aqueous solubility because of its amphiphilic character. The main carrier of S1P in blood is HDL as ~ 65% of blood S1P is bound to it. S1P is associated with HDL via ApoM. Crystal structure analysis of the ApoM-S1P complex revealed that S1P binds to a calyx shaped amphiphilic pocket in the lipocalin fold of ApoM. [97]. These findings were further confirmed in knockout mice experiments where S1P was only found in ApoM rich HDL but was absent in the HDL fraction of *Apom*$^{-/-}$ mice. Additionally ApoM deficient HDL failed to activate $S1PR_1$ signaling whereas ApoM containing HDL successfully initiated $S1PR_1$ signaling [97]. Apart from HDL, human serum albumin (HSA) is another carrier of S1P binding ~ 30 % of S1P in the bloodstream (Figure 9). A minor fraction of S1P is also bound to LDL and VLDL.

The type of carrier also influences the degradation of S1P. Experiments showed that HSA bound S1P has a half-life of 15 to 30 minutes depending on the experimental setting [72,98]. When S1P is associated with HDL, the half-life increases four fold compared to HSA-S1P and shows that HDL is superior to HSA to protect S1P from degradation by LPPs [98]. Apart from protection against degradation, the type of carrier also affects the interaction of S1P with its receptors. For example, HDL is recruited to the cell surface by SR-BI. Therefore binding of HDL to SR-BI may facilitate the transfer of HDL-S1P to its receptors by providing spatial proximity [99]. As mentioned before, S1P signaling via $S1PR_1$ enhances endothelial barrier function. Although this holds true whether S1P is bound to HDL or HSA, the barrier enhancing effect is considerably prolonged when S1P is associated with HDL compared to HSA [100]. Why the response of ECs to HDL-S1P is more sustained than the response to HSA-S1P is still unclear. One possible explanation is, that HDL-S1P influences $S1PR_1$ receptor recycling. By enhancing the recycling process of $S1PR_1$, HDL-S1P likely increases the levels of $S1PR_1$ on the cell surface which leads to prolonged S1P signaling compared to HSA-S1P [100]. How exactly HDL-S1P influences receptor recycling remains to be clarified. From current understanding of S1P transportation in the blood it becomes evident, that the protein carrier

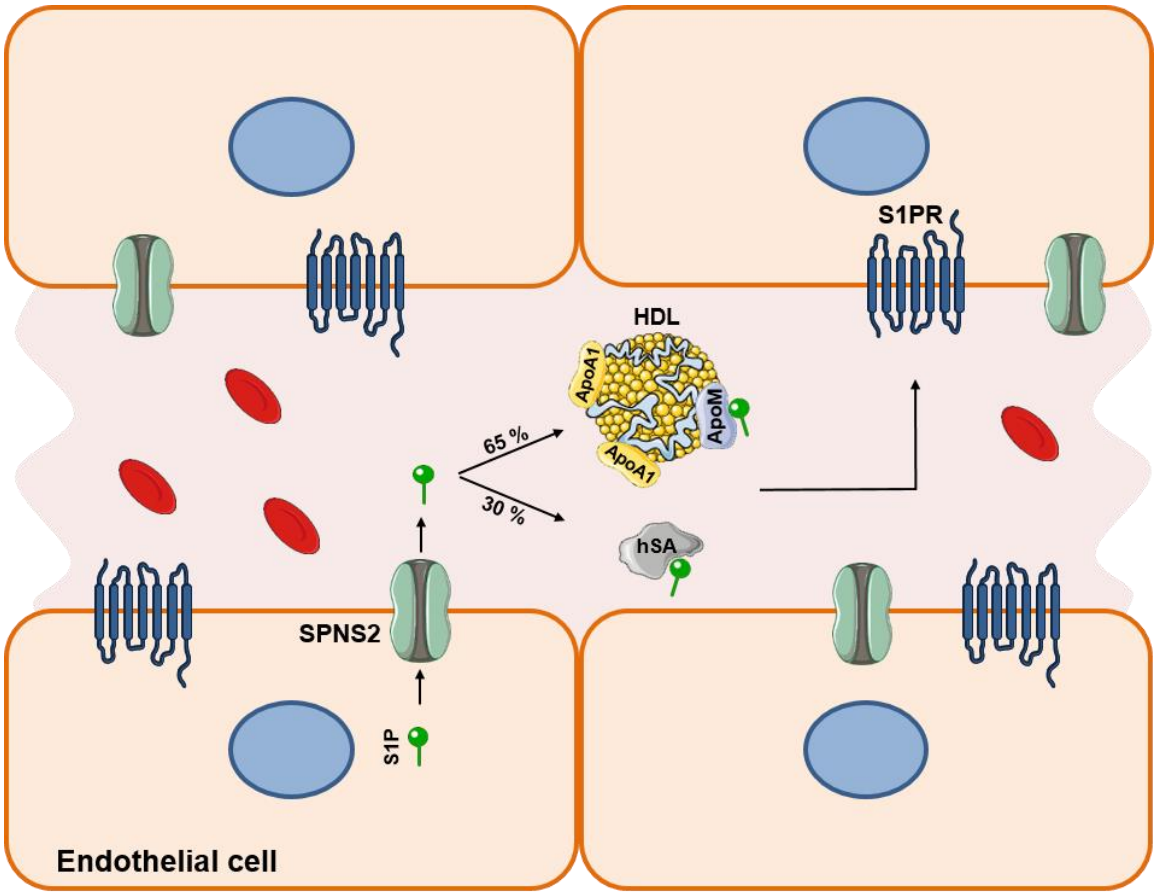

Figure 9: Secretion and transportation of S1P. Endothelial cells release S1P into the blood via SPNS2. Once released it binds via ApoM to HDL (~65 %) or to serum albumin (~30 %). Binding to carrier proteins increases the half-life of S1P, facilitates the interaction with S1PRs and allows S1P to act as a paracrine and endocrine signalling molecule. S1P: Sphingosine-1-phosphate; S1PR: Sphingosine-1-phosphate receptor; HSA: Human serum albumin; HDL: High density lipoprotein.

has an important impact on the functionality of S1P as a paracrine and endocrine signaling molecule.

1.6.4 Sphingosine-1-phosphate in the placenta

Research related to the role of sphingolipids in the placenta and even more in relation with PE are scarce and are just recently emerging. Nevertheless, S1P is well known for its pro-angiogenic [101] and vasculoprotective [83] properties therefore it is likely that S1P and enzymes related with S1P synthesis might play a considerable role in placentation, a processes that require extensive neovascularization and PE, a disease associated with impaired vascular functionality [7]. Furthermore, as mentioned above S1P is involved in inflammation and endothelial dysfunction two pathologic conditions prevalent in PE [7]. A study that investigated the relation of PE and S1P showed that the S1P axis is impaired in preeclampsia as the expression of SPHK1 as well as that of the angiogenic and anti-inflammatory receptors $S1PR_1$ and $S1PR_3$ is decreased whereas that of the anti-angiogenic and pro-inflammatory $S1PR_2$ is increased [102]. A few studies additionally investigated whether S1P concentrations are altered in the circulation of women suffering from PE. Results in this matter are controversial as one study reported decreased levels of S1P [103] whereas another study claimed increases serum S1P levels [104] compared to healthy pregnant women. But both studies revealed increased levels of ceramides which points towards disturbances in the ceramide/S1P rheostat that might lead to increased ceramide mediated apoptotic processes in PE [103,104].

Additionally recent in vitro studies report that the S1P axis also affects trophoblast. It was shown that the SPHK1/S1P pathway is involved in the differentiation of villous trophoblasts [105]. Furthermore, the influence of S1P on the invasiveness of extravillous trophoblast was investigated. Again results concerning the effect of S1P are conflicting as one study reported that S1P is able to boost invasion of extravillous trophoblasts via $S1PR_1$ [106] whereas another study claimed that S1P inhibits trophoblast invasion and that this process is mediated via $S1PR_2$ [107].

1.7 Hypothesis and objectives

Improper placentation and the resulting failure of the endothelium to show normal pregnancy adaption is associated with the manifestation of PE. Hallmark features of PE are vascular inflammation, endothelial dysfunction and hypertension highlighting the important role of the endothelium in PE. The sphingolipid S1P which is mainly associated with HDL in the circulation, has recently gained a lot of attention because of its role as a bioactive compound that extensively interacts with the endothelium. The complex signaling network of S1P plays an important role in endothelial barrier integrity and overall vascular functionality. We therefore hypothesize that functional neonatal HDL-S1P complexes may counteract the vascular inflammation and attenuate the endothelial dysfunction at the feto-placental endothelium, prevalent under preeclamptic conditions. Furthermore, we hypothesize that preeclamptic conditions alter S1P homeostasis contributing to the pathogenesis of the disease.

Therefore we aimed to:

I. Test the potential of preeclamptic maternal serum to act as a mimic for preeclamptic conditions in cell culture

II. Determine the anti-inflammatory potential of nHDL-S1P on HPAECs by measuring changes in expression levels of inflammatory markers as well as NF-κB activation

III. Evaluate the anti-oxidative capability of nHDL-S1P by measuring its influence on ROS levels in HPAECs.

IV. Asses the influence of preeclamptic conditions on expression levels and activity of enzymes involved in the S1P metabolism of HPAECs and placental tissue.

2 MATERIAL AND METHODS

2.1 Subjects

Maternal serum was collected from women with uncomplicated pregnancies (n = 5) and women diagnosed with preeclampsia (n = 5). Collection of maternal blood was approved by the ethnical committee of the Medical University of Graz (Vote no.: 29-319 ex 16/17) and all women gave written consent. In this study preeclampsia was defined by an elevated blood pressure (> 140 mmHg systolic; > 90mmHg diastolic) and a sFLT1/PIGF ratio > 85 (until gestational week 33+6) or a sFLT1/PIGF ratio > 110 (from gestational week 34+0). Clinical characteristics of the subjects are summarized in **Fehler! Verweisquelle konnte nicht gefunden werden.**. For the isolation of neonatal HDL (nHDL) women without pregnancy complications (n = 20) were recruited. Approval was granted by the local ethnics committee of the Medical University of Graz (Vote no.: 29-319 ex 16/17) and all women gave written consent.

Table 1: Clinical characteristics of healthy and preeclamptic women

Control						
Subject	**BMI**	**Age**	**gestational week**	**sFLT/PIGF ratio**	**blood pressure**	
					syst.	**diast.**
1	20.3	32	39	n. m.	136	95
2	23.8	32	39	n. m.	110	66
3	22.7	34	37	n. m.	130	83
4	26.2	29	38	n. m.	131	82
5	26.3	25	38	n. m.	118	70
mean ± SD	23.9 ± 2.3	30 ± 3	38 ± 1	-	125 ± 10	79 ± 10
Preeclampsia						
Subject	**BMI**	**Age**	**gestational week**	**sFLT/PIGF ratio**	**blood pressure**	
					syst.	**diast.**
6	21.8	41	27	267.9	163	100
7	19.6	25	24	925.9	149	88
8	20.1	29	35	352.1	168	106
9	27.3	37	34	106.6	151	92
10	20.8	30	28	503.1	146	88
mean ± SD	21.9 ± 2.8	32 ± 6	30 ± 4	431.1 ± 278.6	155 ± 9	95 ± 7

2.2 Isolation and characterisation of neonatal HDL

Mixed (arterial and venous) umbilical cord blood was collected from 10 male and 10 female offspring. EDTA-plasma was isolated by centrifuging the samples for 15 minutes at 200 x g and 4 °C. The density of the plasma was adjusted to 1.24 g/ml using potassium bromide (Merck KGaA, Darmstadt, Germany). Subsequently 1.7 ml of adjusted plasma was pipetted into quick seal polyallomer tubes (Beckman Coulter, CA, USA) and the plasma was overlaid with potassium bromide solution with a density of 1.006 g/ml. The plasma was centrifuged at 100,000 rpm for 3 hours in an ultracentrifuge (Optima XE-90; Beckman Coulter, CA, USA) using a 70 Ti rotor. After centrifugation the nHDL fraction was isolated from the plastic tubes using a syringe. In order to locate the nHDL fraction a reference tube was used where the nHDL fraction was stained with DiI-dye (1-1´dioctadecyl-3-3-3´-tetramethyl indocarbocyanine perchlorate). Afterwards nHDL was desalted by gel filtration using PD10 columns (GE healthcare, Little Chalfont, UK) filled with Sephadex G-25 Medium. First the column was equilibrated with PBS (Medicago, Uppsala, Sweden) and then the isolated nHDL was filtered through the column for desalting. The desalted, purified nHDL was pooled and stored at -20°C until usage. nHDL was characterized by measuring ApoA-1, cholesterol and S1P content. ApoA-1 and cholesterol concentrations were measured spectrophotometrically with an AU680 Chemistry Analyzer (Beckman Coulter, CA, USA) according to manufacturer's instructions. S1P concentrations were determined by HPLC according to a protocol described elsewhere [97]. Briefly, nHDL samples were spiked with 25ng of an internal standard (D-erythro-sphingosine-1-phosphate) and S1P was extracted by a two-step chloroform-methanol extraction. After derivatization with 2,3-naphthalene-dicarboxaldehyde samples were measured on a Synergi 4u Fusion-RP 80A column (30 x 2.0 mm) using an Agilent 1290 HPLC (Agilent Technologies, Santa Clara, USA).

2.3 Isolation of human placental aortic endothelial cells (HPAEC)

Term placentae were collected after delivery with informed consent and approval of the ethical committee of the Medical University of Graz (Vote no.: 29-319 ex 16/17). HPAECs were isolated from arterial chorionic blood vessels as firstly described by Lang et al [13]. First the amnion was removed and the chorionic plate was disinfected with Betaisodona solution (Mundipharma, Vienna, Austria). Next arterial chorionic vessels with a length of ~ 3 cm were resected and washed in Hank's balanced salt solution (HBSS; Gibco, Thermo Fisher Scientific, Carlsbad, USA). Then the artery was cannulated and flushed with HBSS containing 0.1 U/ml Collagenase (Roche, Basel, Switzerland), 0.8 U/ml Dispase (Roche, Basel, Switzerland) and 200µg/ml Penicillin/Streptomycin (GE Healthcare, Little Chalfont; UK) for 6 minutes (flow rate: 2.5 ml/min). Detached ECs were collected in 10 ml fetal calf serum (HyClone, GE Healthcare,

Little Chalfont; UK) and centrifuged at 900 rpm for 7 minutes. The cell pellet was resuspended in 1 ml endothelial microvascular basal medium (EBM; PAN Biotech, Aidenbach, Germany) containing EGM-MV Single Quots (Lonza, Basel, Switzerland) and 10 % pooled human serum from pregnant women. Cells were seeded into a well of a 12 well plate (Thermo Fisher Scientific, Carlsbad, USA) coated with 1 % gelatine (Thermo Fisher Scientific, Carlsbad, USA) for expansion. As soon as cells proliferated and reached a certain number, they were transferred into a 25 cm^2 flask (Nunc™; Thermo Fisher Scientific, Carlsbad, USA) and the pregnant serum was substituted by 5 % FBS for further cultivation. Once HPAECs reached confluency in a 75 cm^2 flask (Nunc™; Thermo Fisher Scientific, Carlsbad, USA) they were harvested and frozen in liquid nitrogen for long term storage. HPAECs were always cultured at 12 % O_2, 5 % CO_2, 90 % humidity and a temperature of 37 °C. To verify that the isolated cells are indeed ECs they were subjected to immunocytochemical characterization as described elsewhere [13].

2.4 Quantitative real-time PCR (qPCR)

2.4.1 RNA isolation from HPAECs

Cells were thawed, expanded and seeded in 12 well plates coated with 1 % gelatine at a density of 100,000 cells/well. After 2 days medium was changed to serum free EBM and cells were treated with 10 ng/ml TNF-α only or with 10 ng/ml TNF-α in the presence of 800 µg/ml nHDL or 1 µM HSA-S1P (Avanti Polar Lipids, Alabama, USA) for 6 hours. Treatment was performed in triplicates. After treatment cells were washed twice in prewarmed HBSS and harvested in 350 µl RLT Lysis buffer (Quiagen, Hilden, Germany) supplemented with 1 % β-mercaptoethanol (Sigma Aldrich, St. Louis, USA). Next total RNA content was isolated using the RNeasy® Mini Kit (Quiagen, Hilden, Germany) according to manufacturer's instructions. Therefore the cell lysates were homogenized by vortexing them for 1 minute. After completing the protocol, cells were eluted from the spin column membrane in 30 µl of DEPC treated water (Ambion®; Thermo Fisher Scientific, Carlsbad, USA) for 5 minutes. As RNA yields were low the eluate was again pipetted onto the spin column membrane and eluted a second time to increase RNA concentration. RNA concentration was determined by measuring absorbance at 260 nm using a microfluidic UV/VIS spectrophotometer (QIAxpert; Quiagen, Hilden, Germany).

2.4.2 RNA isolation from placental tissue

For isolation of RNA 20 mg snap frozen term placental tissue was used as starting material. The tissue samples were placed in a MagNA Lyser tube (Roche, Basel, Switzerland) and 600 µl of RLT Lysis buffer supplemented with 1 % β-mercaptoethanol was added to each tube. Tissue samples were homogenized using a MagNA Lyser Instrument (Roche, Basel, Switzerland) set to 6,500 rpm for 20 seconds, followed by a cooling step for 1 minute. This procedure was repeated three times. Afterwards the samples were centrifuged for 3 minutes at full speed. The supernatant was transferred into a new tube and used for further processing. After homogenization, RNA was isolated using the RNeasy® Mini Kit as described in 2.4.1 with the slight difference that the second elution step was skipped due to sufficient RNA yields.

2.4.3 cDNA synthesis

250 ng of total RNA of HPAECs were reverse transcribed by using random hexamer primers (200µg/reaction; Thermo Fisher Scientific, Carlsbad, USA) and Super Script™ II Reverese Transcriptase (200 units/reaction; Invitrogen™, Thermo Fisher Scientific, Carlsbad, USA) in 20 µl reaction volume. cDNA synthesis was carried out according to manufacturer's instruction for SuperScript™ II Reverse Transcriptase. RNAse inhibitor (40 units/reaction; RNaseOUT™, Thermo Fisher Scientific, Carlsbad, USA) was included during reverse transcription to prevent RNA degradation.

cDNA synthesis from placental tissue RNA was performed as described for RNA from HPAECs with the difference that 2 µg of total RNA was used and that the reaction volume was 40 µl. Therefore the amount of all reaction components was doubled.

2.4.4 Quantitative real-time PCR

Quantitative real-time PCR was performed on the CFX384 cycler (BioRad Technologies, Vienna, Austria) using TaqMan® Gene Expression assays (Applied Biosystems, Thermo Fisher Scientific, Carlsbad, USA) and TaqMan® Universal PCR Master Mix (Applied Biosystems, Thermo Fisher Scientific, Carlsbad, USA). Used TaqMan® Gene Expression assays are listed in Table 2. The efficiency of all gene expression assays was determined by a five point standard curve (Range: 12.5 ng/µl – 0.02 ng/µl cDNA). The cDNA used for the standard curve was extracted from HPAECs grown in 60 mm dishes as described in section 2.4.1 and 2.4.3. qPCR efficiency was calculated using the formula $E = 10^{1/-Slope}$. The slope was derived from a graph where the Cq values were plotted against the logarithmic cDNA concentrations. The slope of the standard curve should lie between -3.2 and -3.5 and the reproducibility of replicates (R^2) should be > 0.980. According to the manufacturer the efficiency of all TaqMan gene assays used should be in the range of 90 % – 110 %.

qPCR was performed in 10 µl reactions and master mix composition is depicted in Table 3. All samples were analysed in triplicates and cycling conditions are shown in Table 4. For each PCR-run a non-template control and a no reverse transcription control were included. The quantification cycle (Cq) was determined by using a multi-variable, non-linear regression model implemented in the CFX Manager 3.1 Software (BioRad Technologies, Vienna, Austria). Subsequently Cq values were used to calculate the relative gene expression by applying the ΔΔCq method [108].

Table 2: TaqMan® Gene Expression assays used for quantitative real-time PCR

Target	**TaqMan® Assay ID**	**Supplier**
Intercellular adhesion molecule 1 (ICAM1)	Hs00164932_m1	Thermo Fisher Scientific
Vascular cell adhesion molecule 1 (VCAM1)	Hs01003372_m1	Thermo Fisher Scientific
Interleukin 8 (IL-8)	Hs00174103_m1	Thermo Fisher Scientific
Monocyte chemoattractant protein 1 (MCP1)	Hs00234140_m1	Thermo Fisher Scientific
Serine palmitoyl transferase (SPTLC1)	Hs00272311_m1	Thermo Fisher Scientific
Sphingosine Kinase 1 (SPHK1)	Hs00184211_m1	Thermo Fisher Scientific
Sphingosine Phosphatase 1 (SPP1)	Hs04189357_m1	Thermo Fisher Scientific
Hypoxanthine phosphoribosyltransferase1 (HPRT1)	Hs02800695_m1	Thermo Fisher Scientific
TATA-box binding protein (TBP)	Hs00427620_m1	Thermo Fisher Scientific
Proteasome subunit beta 6 (PSMB6)	Hs00382586_m1	Thermo Fisher Scientific
Peptidylprolyl isomerase A (PPIA)	Hs04194521_s1	Thermo Fisher Scientific
Succinate dehydrogenase complex flavoprotein subunit A (SDHA)	Hs00188166_m1	Thermo Fisher Scientific

Table 3: Mastermix for detection of mRNA

PCR reaction mix	Volume/reaction [µl]	Final concentration
TaqMan® 2x Universal PCR Master Mix	5	1x
TaqMan® Gene Expression assays	0.5	1x
DEPC treated water	2.5	1x
Template cDNA HPAECs: 2.5 ng/µl; Tissue: 25 ng/µl	2	5 ng 50 ng
Total reaction Volume	10	

Table 4: Thermal cycling parameters for TaqMan ® Gene Expression assays

Step	Temperature [°C]	Time [mm:ss]
UNG Incubation [a]	50	02:00
Activation	95	10:00
Amplification (45 cycles)	95 60	00:15 00:30

a. Step activates uracil N-glycosylase to prevent reamplification of carryover PCR products

2.4.5 PrimePCR™ qPCR

RNA isolation from HPAECs and cDNA synthesis for PrimePCR assays was performed as described in section 2.4.1 and 2.4.3, respectively. The only difference here was that the concentration of the RNA was adjusted to 2 ng/µl. PrimePCR was performed on the CFX384 cycler. For gene expression analysis predesigned PrimePCR panels for pre-eclampsia (Pre-eclampsia Tier 1 H384; BioRad Technologies, Vienna, Austria) and apoptosis (Apoptotic TNF Family pathways H384; BioRad Technologies, Vienna, Austria) were used. PrimePCR assay was performed according to manufacturer's instructions. Samples were analysed in triplicates and mastermix composition as well as the PCR cycling protocol can be seen in Table 5 and Table 6, respectively. Analysis of qPCR data was done as described in section 2.4.4. HPRT1 and TBP served as reference genes.

Table 5: Master mix composition for PrimePCR gene expression analysis

PCR reaction mix	Volume/reaction [µl]	Final concentration
PrimePCR assay (20x)	lyophilized	1x
SsoAdvanced™ SYBR® Green Mix (2x)	5	1x
cDNA sample (2ng/µl)	2	4 ng
DEPC treated water	3	1x
Total reaction volume	10	

Table 6: Thermal cycling parameters for PrimePCR gene expression analysis

Step	Temperature [°C]	Time [mm:ss]
Activation	95	02:00
Amplification	95	00:05
(40 cycles)	60	00:30
Melt Curve	65-90 (0.5 increments)	00:05 / step

2.4.6 Evaluation of reference genes

In order to find the most reliable reference genes for quantifying qPCR results five potential reference genes were preselected based on literature search. The genes chosen are TBP, HPRT1, PSMB6, PPIA and SDAH (for details see Table 2). These genes were then evaluated using GeNorm [109], BestKeeper [110] and NormFinder [111] which are algorithms developed for reference gene analysis. For this purpose, HPAECs were treated as described in 2.4.1 and cDNA was generated as can be seen in section 2.4.3. Afterwards qPCR was performed and results were analysed using the algorithms mentioned above. First the genes were ranked by each algorithm separately. To rank putative reference genes, GeNorm calculates a gene stability parameter M which gives the pair-wise variation of a reference gene with all other reference genes. The M-value for all genes is calculated and the gene with the highest M-value is excluded. Then the calculation is repeated until only two reference genes remain. With this stepwise approach the genes with the lowest M-values and therefore the most stable expression are identified. BestKeeper determines the optimal reference gene based on descriptive statistics. The standard deviation of the Cq values gives a first impression of the expression stability. The lower the standard deviation the higher the expression stability of the gene. If the standard deviation exceeds 1 the gene should be excluded from the calculation. In a next step the algorithm calculates a so called BestKeeper index which is the geometric

mean of the Cq values of all genes. To rank the reference genes, a pair-wise correlation coefficient (r) between the BestKeeper index and each gene is calculated. The higher the correlation coefficient the more stable the expression of a gene is considered. NormFinder calculates a stability value for each possible reference gene. The lower this stability value is the more stable is the expression of a gene. In order to find the overall final ranking the geometric mean of the rankings established by the algorithms was calculated and the three best genes were chosen as reference genes.

2.5 Western Blot analysis

Cells were thawed, expanded and seeded at a density of 200,000 cells/well in 6 well plates (Thermo Fisher Scientific, Carlsbad, USA) coated with 1 % gelatine. After 2 days medium was changed to serum free EBM and cells were treated with 10 ng/ml TNF-α only (Sigma Aldrich, St. Louis, USA) or with 10 ng/ml TNF-α in the presence of 800 µg/ml nHDL or 1 µM HSA-S1P for 6 hours. To perform Western blotting, medium was removed and cells were washed twice in HBSS. Afterwards cells were scraped and collected in 50 µl RIPA lysis and extraction buffer (Sigma Aldrich, St. Louis, USA) containing protease inhibitors (Roche, Basel, Switzerland). Total protein concentration was determined by bicinchoninic acid assay (BCA; Thermo Fisher Scientific, Carlsbad, USA) according to manufacturer's guidelines. Protein lysates were mixed 1:1 with 2 x Laemmli buffer (Sigma Aldrich, St. Louis, USA) and denatured at 96°C for 5min. 10 µg of total protein were loaded onto 4 - 20% SDS-PAGE gradient gels (BioRad Technologies, Vienna, Austria) and resolved at 120 V for 1h 10 min. Proteins were transferred to a nitrocellulose membrane (BioRad Technologies, Vienna, Austria) using the TransBlot Turbo Transfer System (BioRad Technologies, Vienna, Austria). Nonspecific binding sites were blocked for 1h with 5 % non-fat dry milk (BioRad Technologies, Vienna, Austria) in Tris-buffered saline (TBS; Gatt-Koller, Absam, Austria) + 0.1% Tween 20 (Sigma Aldrich, St. Louis, USA). Thereafter, membranes were incubated with the appropriate primary antibody overnight at 4°C. Subsequently, the membranes were washed for 30 minutes in TBS Buffer + 0.1 % Tween 20 and incubated for 1 hour with the appropriate horseradish peroxidase conjugated secondary antibody. After another wash for 30 minutes the blots were developed for 5 minutes using SuperSignal® Chemiluminescent Substrate (Thermo Fisher Scientific, Carlsbad, USA).

Table 7: Antibodies used for Western blot analysis

Primary Antibody	**Supplier**	**Host**	**Dilution**	**Dilution 2nd AB**
VCAM1 (E1E8X);	Cell Signaling; #13622	Rabbit	1:1,000	1:2,000
ICAM1 (EPR4776);	Abcam; # ab109361	Rabbit	1:2,000	1:4,000
MCP1	Cell Signaling; #2027S	Rabbit	1:1,000	1:2,000
Phospho-NF-κB p65 (Ser536) (93H1);	Cell Signaling; #3033S	Rabbit	1:1,000	1:2,000
NF-κB p65 (D14E12)	Cell Signaling; #8242S	Rabbit	1:1,000	1:2,000
NOX1	Abcam; # ab55831	Rabbit	1:500	1:1000
SPTLC1	BD Bioscience # 611304	Mouse	1:1000	1:2000
Hsp90	BD Bioscience # 610418	Mouse	1:2000	1:4000
β-Actin (AC-15)	Abcam; # ab6276	Mouse	1:10,000	1:10,000
Secondary Antibody	**Supplier**	**Host**	**Conjugate**	
Anti-Rabbit IgG (H+L)	BioRad; #170-6515	Goat	Horseradish Peroxidase	
Anti-Mouse IgG (H+L)	BioRad; #170-6516	Goat	Horseradish Peroxidase	

Immunolabeling was visualized with the Fusion FX imaging system (Vilber Lourmat, Marne-la-Vallée, France) and band densiometry was performed using the Fusion© Software (Vilber Lourmat, Marne-la-Vallée, France). β-Actin or Hsp90 was used as reference protein. All antibodies were diluted in 5 % non-fat dry milk (BioRad Technologies, Vienna, Austria) and their characteristics are summarized in Table 7.

2.6 Fluorescence-activated cell sorting (FACS) analysis

2.6.1 Multiplex FACS analysis of maternal Serum

To evaluate whether sera obtained from preeclamptic or healthy pregnant women (n = 5 in each group) differ in cytokine composition, concentrations of the following cytokines were measured: IL-1β, IL-2, IL-5, IL-6, IL-9, IL-12 p70, TNF-α and INF γ. For this purpose a commercially available FACS based multiplex assay kit (Human TH1/TH1 11-Plex; AimPlex Biosciences, Pomona, USA) was purchased. The assay principle is based on bead populations with varying sizes and different levels of fluorescence intensity within each bead size. Cytokines are captured by specific antibodies bound to the beads. After capturing the protein of interest, a second, biotinylated antibody raised against another epitope binds the cytokines. Finally streptavidin conjugated R-phycoerythrin is added and samples are analysed on a flow cytometer. For quantification fluorescent intensities of the samples are compared to standards with known cytokine concentrations. The multiplex assay was performed according to manufacturer's instructions. Briefly, capture beads and 15 µl of SPB assay buffer were added to each well. Then 7.5 µl of sample or 22.5 µl of standard were pipetted into the wells. After 60 minutes of incubation at room temperature the plate was washed three times and 12.5 µl of biotinylated antibody solution was added. Another incubation period of 30 minutes at room temperature was followed by an additional wash step. Subsequently 12.5 µl streptavidin-PE solution were added for 20 minutes at room temperature. After one more wash step 150 µl of reading buffer was added to each well. Finally the samples were transferred to FACS tubes and read on a flow cytometer (LSR II; BD Biosciences, New Jersey, USA). Results were analysed in GraphPad Prism 7 by fitting the standard curves based on a five-parameter logistic function.

2.6.2 FACS analysis of HPAECs

Cells were thawed, expanded and seeded in 25 cm^2 cell culture flasks coated with 1 % gelatine at a density of 500,000 cells per flaks and treated as described in chapter 2.5. For flowcytometric analysis HPAECs were washed twice with prewarmed HBSS and harvested by using 1 ml of accutase (PAA, Pasching, Austria). Detached cells were collected in 10 ml HBSS, counted and centrifuged for 4 minutes at 800 rpm. Then the cell pellet was resuspended in PBS (Thermo Fisher Scientific, Carlsbad, USA) supplemented with 0.1 % bovine serum albumin (Sigma Aldrich, St. Louis, USA) and 20 mM EDTA (Thermo Fisher Scientific, Carlsbad, USA) (hereafter referred to as staining buffer) to a concentration of 1.25 x 10^6 cells/ml. Subsequently 1 x 10^5 cells were transferred to FACS tubes and FcRn receptor was blocked with heat inactivated human plasma for 10 minutes on ice. For surface protein staining cells

were incubated with fluorophore conjugated antibodies (Table 8) for 30 minutes at 4°C in the dark. Afterwards HPAECs were washed in 1 ml of staining buffer, centrifuged for 5 minutes at 1,200 rpm and resuspended in 250 µl of staining buffer. Measurement was performed on a CytoFLEX flow cytometer (Beckman Coulter, CA, USA) using the associated CytEXpert software (Beckman Coulter, CA, USA) for setting the gates and analysing the data. For each sample at least 10,000 cells were counted.

Table 8: Antibodies used for flowcytometric analysis.

Antibody	Label	Concentration [µg/ml]	Volume [µl]	Supplier
CD106	APC	100	5	BioLegend #305809
CD54	Pacific Blue	500	5	BioLegend #322715
CD 62E	PE	100	5	BioLegend #322605

2.7 Reactive oxygen species (ROS) Assay

A dark wall, clear bottom 96-well microplate (Costar®; Corning Inc., New York, USA) coated with 1 % gelatine was seeded with 20,000 cells/well. Cells were allowed to adhere overnight. The next day DCFDA (Abcam, Cambrige, UK) was diluted to a final concentration of 10 µM in HBSS. Afterwards cells were washed once in pre-warmed HBSS. Then 100 µl DCFDA solution was added to each well and cells were stained for 45 minutes at 37 °C in the dark. After staining cells were washed again with pre-warmed HBSS. Subsequently cells were treated with 0.5 and 1 µM AngII (Sigma Aldrich, St. Louis, USA) only or with 0.5 and 1 µM AngII in the presence of 800 µg/ml nHDL or 1 µM HSA-S1P for 4 hours. As a positive control, cells were treated with 200 µM tert-butyl hydrogen peroxide (TBHP; Abcam, Cambrige, UK) for 4 hours. All treatment compounds were diluted in phenol red free DMEM (Gibco, Thermo Fisher Scientific, Carlsbad, USA) without supplements. After treatment of the cells, fluorescent intensity of oxidized dichlorofluorescein (DCF) was measured immediately at a fluorescence plate reader (FLUOstar Optima; BMG Labtech, Offenburg, Germany) at Ex/Em = 485/535 in end point mode.

2.8 Serine Palmitoyl Transferase (SPT) activity assay

Cells were thawed, expanded and seeded in 60 mm dishes (Eppendorf AG, Hamburg, Germany) coated with 1 % gelatine at a density of 600,000 cells/dish. After 2 days medium was changed to serum free EBM and cells were treated either with 10 ng/ml TNF-α, 50 ng/ml TNF-α, 1 µM AngII or 5 µM AngII for 24 hours. Afterwards cells were washed once in pre-warmed HBSS. Then 200 µl of SPT reaction buffer were added to each dish. Subsequently cells were scraped and the lysates collected on ice. SPT reaction buffer is composed of 0.1 M Hepes pH 8.3 (Sigma Aldrich, St. Louis, USA), 5 mM dithiothreitol (Invitrogen™, Thermo Fisher Scientific, Carlsbad, USA), 2.5 mM EDTA pH 7.4 and 50 µM Pyridoxal 5' Phosphate (Sigma Aldrich, St. Louis, USA). Cell lysates were sonicated 2 x for 10 seconds (50 % amplitude, 50 % pulsation) using an ultrasonic processor (UP100H; Hielscher, Teltow, Germany). For normalization purposes, total protein content of the cell lysates was measured on an UV/VIS spectrophotometer (NanoDrop 2000; Thermo Fisher Scientific, Carlsbad, USA) according to manufacturer's instructions. Thereafter 100 µl of cell lysate were mixed with 1 µl palmitoyl coenzyme A (0.2 mM; Sigma Aldrich, St. Louis, USA) and 10 µl [^{3}H]Serine (33.3 mM, 1mCi/ml; Perkin Elmer, Boston, USA). SPT reaction was carried out in a heating block for 15 minutes at 37 °C. In order to stop the reaction 50 µl $NaBH_4$ (5 mg/ml; Sigma Aldrich, St. Louis, USA) were added to each tube for 5 minutes. Additionally $NaBH_4$ reduces the formed [^{3}H]3-ketosphinganine to [^{3}H]sphinganine. Next lipids were extracted by first adding 750 µl chloroform (Merck, Darmstadt, Germany) and methanol (Sigma Aldrich, St. Louis, USA) (ratio 1:2), followed by 250 µl chloroform and 250 µl NH_4OH (Merck, Darmstadt, Germany). After careful vortexing, tubes were spun down for 10 minutes at 12,000 rpm. Subsequently, the lower phase was transferred into a new tube. The tube was left open overnight under a fume hood to remove the organic solvent. The next day a thin layer chromatography (TLC) plate (Merck, Darmstadt, Germany) was dried for 10 minutes at 80 °C and a TLC tank (Camag, Mississippi, USA) was filled with TLC running buffer ($CHCl_3$: Methanol : NH_4OH in ration 65:25:2) at least 30 minutes before running the TLC plate. Afterwards the dried samples were resuspended in 40 µl $CHCl_3$ and loaded onto the TLC plate drop by drop (1µl) at a minimum distance of 1.5 cm. Sphinganine (Avanti Polar Lipids, Alabama, USA) and C18:0 ceramide (Avanti Polar Lipids, Alabama, USA) were included as standards. The TLC plate ran for 1 hour 30 minutes and dried for 1 hour under the fume hood. To visualize the separated lipids, the TLC plate was placed for 1 hour in a chamber which was saturated with iodine vapour. Spots containing the [^{3}H]Sphinganine fraction of the samples were identified with the help of the sphinganine standard and marked with a pencil. In order to allow the Iodine to evaporate from the TLC plate, it was placed under the fume hood overnight. The following day the marked sphinganine spots were cut out and placed in a scintillation vial containing 20 ml scintillation cocktail (Ultima Gold™, Perkin Elmer, Boston, USA). The scintillation vials were placed at 4

°C overnight to reduce unspecific signals and then [^{3}H]Sphinganine was detected using a β-Counter (Tri-Carb 2800TR, Perkin Elmer, Boston, USA). Each sample was counted for 5 minutes and resulting CPM values were quantified using a standard curve of [^{3}H]Serine. Finally, the calculated values were normalized to the total protein content of each sample.

2.9 Statistical analysis

All statistical analyses were performed using Graph Pad Prism 7 Software (GraphPad Software Inc., San Diego, USA). Values are presented as Mean ± SD unless stated otherwise in the figure legend. For PrimePCR data differences in experimental groups were evaluated by multiple Students' t-test using the Holm-Sidack method to correct for multiple comparison. The ROS assay and remaining qPCR data were analysed by two-way ANOVA including Tukey post-hoc analysis for multiple comparison. Western blot data were analysed by one-way ANOVA including Sidak's multiple comparison test. A p-value of < 0.05 was considered significant.

3 RESULTS

3.1 Implementation of TaqMan qPCR for HPAECs

The TaqMan gene assays used in this study are all validated by the manufacturer and should produce reliable results [112] [113]. Nevertheless it is important to check the performance of the gene assays under the specific experimental setup used. Therefore the efficiency of all assays was tested before proceeding with the experiments. Furthermore, when relative quantification methods are used in qPCR experiments, it is crucial to find stable expressed reference genes in order to create reliable results for the particular cells of interest. There is no universal reference gene which can be used under each experimental condition. That is why different reference gene evaluation algorithms were applied to find stable and reliable reference genes for working with HPAECs under inflammatory conditions.

3.1.1 Determination of TaqMan Gene Assay efficiency

All gene assays depicted in Table 9 showed efficiencies within the acceptable range of 90 % to 110 % with *SPP1* displaying the lowest efficiency (90.3 %) and *TBP* displaying the highest one (107.9 %). Furthermore the coefficient of correlation (R^2) has to be > 0.98 which indicates that the replicates are sufficiently reproducible. According to general convention [114] the slope of efficiency curves should range between -3.20 and -3.50 which is the case for all of the genes tested beside three. The slopes of *VCAM1* (-3.15) and *TBP* (-3.15) are slightly too high whereas the slope of *SPP1* (-3.58) is a bit too low. Nevertheless for reaching efficiencies between 90% and 110% (which is the cut-off set by the manufacturer [113]), slopes have to range between -3.10 and -3.58. As all of the tested assays range within the quality parameters set by the manufacturer and the coefficient of correlation is > 0.98 for all of them, none of the gene assays shown in Table 9 was excluded. Efficiency curves for all tested gene assays are shown in Appendix A. Furthermore the mean efficiency of the reference genes used for the experiments (*HPRT1*, *TBP* and *PSMB6*; see section 3.1.2) and the efficiency of the different target genes are within 10 % of each other which is important for generating reliable fold change values when using the ΔΔCq-method for quantification of qPCR results.

Off note, although efficiencies > 100 %, are not possible in PCR amplification theory, it is still possible to see such values when evaluating PCR assays. This is because often there are some polymerase inhibiting components (ethanol, humic acids, SDS, phenols, etc.) present in the cDNA samples which are difficult to completely remove. When preparing a dilution series for evaluating efficiencies this inhibitory effect is most pronounced in the higher concentrated

cDNA samples. This causes a deviation from linearity at higher concentrated cDNA samples resulting in calculated efficiencies exceeding 100 % [115].

Table 9: Efficiency of TaqMan gene expression assay tested in HPAECs

Target	Slope	Amplification factor	Efficiency	R^2
ICAM1	-3.44	1.95	95.4%	0.996
VCAM1	-3.15	2.08	107.8%	0.998
MCP1	-3.21	2.05	104.7%	0.997
IL-8	-3.34	1.99	99.1%	0.997
SPT	-3.37	1.98	98.0%	0.997
SPHK1	-3.46	1.95	94.6%	0.984
SPP1	-3.58	1.90	90.3%	0.986
HPRT1	-3.30	2.01	100.9%	0.998
TBP	-3.15	2.08	107.9%	0.996
PSMB6	-3.20	2.05	105.2%	0.998
PPIA	-3.34	1.99	99.2%	0.997

3.1.2 Evaluation of putative reference genes with different algorithms

When qPCR results are normalised to reference genes it is crucial to find genes which are stably expressed under the individual conditions of the qPCR experiments. Additionally, it is recommended to normalise qPCR data to three different reference genes to increase reliability of the results. To get a first idea of possible reference genes which are suitable for placental endothelial cells under inflammatory conditions, a literature search was conducted. Based on the literature *HPRT1, PSMB6, TBP, PPIA* and *SDAH* were chosen as putative reference genes. These genes were further analysed by three different reference gene evaluation algorithms: GeNorm [109], NormFinder [111] and BestKeeper [110]. Based on the results from this evaluation, the three most suitable reference genes were chosen for the analysis of qPCR data in this study. As shown in Table 10, part A GeNorm ranks genes according to their stability value M (for detailed information about the M-value see section 2.4.6). *HPRT1* and *PSMB6* are the genes with the lowest M-value and therefore the most stably expressed ones followed by *TBP, PPIA* and *SDHA*. Because of the pairwise-correlation approach of this algorithm the best two reference genes cannot be ranked any further. Like GeNorm, NormFinder calculates a stability value for each putative reference gene but uses another mathematical approach. According to NormFinder the most stable reference gene, which displays the lowest stability value, is as well *HPRT1*. *TBP* is considered the second most stable reference gene followed

by *PPIA* on the third rank. Unlike GeNorm and BestKeeper, NormFinder does not rank *PSMB6* under the top three reference genes (Table 10, part B). BestKeeper uses descriptive statistics to find the most suitable reference gene. As depicted in Table 10, part C all genes included in the analysis showed SD values below one which means none of the genes under investigation needed to be excluded from the calculations. BestKeeper ranks the reference genes based on coefficient of correlation values (R) which are calculated by comparing the reference genes with the BestKeeper index. *HPRT1* was again ranked the most suitable reference gene with the best correlation to the Index and thereby the highest R-value. Second best correlation was scored by *PSMB6*. Surprisingly, *SDHA* was placed on rank three by BestKeeper whereas all other algorithms considered this gene the least stable one. To unite the results of the three algorithms used, the geometric mean of the weights from all rankings was calculated (Table 10, part D). In the final ranking *HPRT1* is on the first position followed by *PSMB6* and *TBP*. Based on this ranking, these three genes were then chosen as reference genes for the analysis of qPCR data using the ΔΔCq method. Furthermore, these three genes are involved in very distinct biological processes and therefore it is unlikely that they are co-regulated. This biological independency is another important aspect to consider when choosing reference genes.

Table 10: Evaluation of putative reference genes using GeNorm. Normfinder and BestKeeper.

A GeNorm

Gene	M-Value	Rank
HPRT1	0.362	1
PSMB6	0.362	1
TPB	0.415	3
PPIA	0.461	4
SDAH	0.555	5

B NormFinder

Gene	Stability value	Rank
HPRT1	0.097	1
TBP	0.101	2
PPIA	0.109	3
PSMB6	0.118	4
SDAH	0.139	5

C BestKeeper

Gene	SD	R	Rank
HPRT1	0.43	0.827	1
PSMB6	0.37	0.693	2
SDHA	0.63	0.647	3
TBP	0.34	0.631	4
PPIA	0.37	0.628	5

D Final Ranking

Gene	Geometric Mean	Rank
HPRT1	1.00	1
PSMB6	2.00	2
TBP	2.88	3
PPIA	3.91	4
SDAH	4.22	5

3.2 Characterisation of neonatal HDL

In order to elucidate the composition of nHDL used for the experiments ApoA-1, total cholesterol and S1P content was determined and results are shown in Table 11. The protein ApoA-1 is one of the major constituents of HDL particles and was found at concentrations of 1.5 mg/ml on both, nHDL particles isolated form male and female offspring. Cholesterol which is one of the main lipid species transported by nHDL was present at concentrations of 0.8 mg/ml and 0.7 mg/ml in nHDL samples from male and female offspring respectively. As this study focuses particularly on the effects of S1P under inflammatory condition and its role in endothelial dysfunction, the concentration of S1P on nHDL was determined. The concentration of S1P was 0.4 (male offspring) and 0.5 (female offspring) nmol per mg of total nHDL protein content measured by HPLC. For all of the characteristics examined, there was no statistically significant difference detectable between nHDL collected from male or female offspring (ApoA-1: $p = 0.94$; Cholesterol: $p = 0.46$; S1P: $p = 0.58$)

Table 11: Characteristics of neonatal HDL used in the study.

Characteristic	Male	Female
Sample number	10	10
ApoA-1 [mg/ml]	1.5 ± 0.4	1.5 ± 0.4
total cholesterol [mg/ml]	0.8 ± 0.3	0.7 ± 0.2
Sphingosine 1 Phosphate [nmol/mg nHDL Protein]	0.4 ± 0.1	0.5 ± 0.1

3.3 Determination of inflammatory markers in sera of preeclamptic patients

As a first approach to mimic inflammation and to test endothelial dysfunction, both hallmarks of preeclampsia, HPAECs were treated with serum from preeclamptic women. For this purpose serum samples were collected and characterised. Clinical characteristics of the subjects are shown in Table 1. There were no statistical significant differences in age ($p = 0.56$) and BMI ($p = 0.31$) of preeclamptic and healthy pregnant women. Women suffering from preeclampsia delivered ~ 8 weeks earlier than healthy pregnant women which is not surprising as an early delivery is currently the only option to cure this disease. As typical for preeclamptic women they show higher blood pressure (155 ± 9 syst.; 95 ± 7 diast.) than women without pregnancy complications (125 ± 10 syst.; 79 ± 10 diast.). Additionally the serum concentrations of IL-1β, IL-2, IL-5, IL-6, IL-9, IL-12 p70, TNF-α and INF γ were measured in order to check if the serum

of preeclamptic women contains higher levels of pro-inflammatory cytokines than the serum of healthy women. The only difference that was found was that levels of IL-6 were 110.8 ± 95.8 pg/ml in preeclamptic women whereas IL-6 concentrations were below the detection limit in healthy subjects. However, concentrations of IL-6 in sera of preeclamptic women ranged between 16.1 pg/ml and 228.3 pg/ml indicating a large biological variation between subjects. For all other cytokines concentrations were below the detection limit. This finding and the fact that treatment with preeclamptic serum failed to induce a pronounced expression of inflammatory adhesion molecules VCAM1 and ICAM1, in HPAECs (data not shown) lead to the conclusion that available preeclamptic sera are not eligible for stimulating inflammation and endothelial dysfunction in HPAECs. Therefore, for all further experiments recombinant TNF-α (10 ng/ml) or AngII (0.5 µM and 1 µM) was used to mimic inflammation and endothelial dysfunction in HPAECs.

3.4 Effect of S1P and nHDL on expression of genes associated with inflammation and preeclampsia

We firstly investigated the effect of TNF-α stimulation on gene expression of HPAECs. Therefore, a panel of genes known to be associated with signaling pathways in inflammation and preeclampsia was examined. Furthermore, we wanted to know whether nHDL and S1P are capable of counteracting effects of TNF-α on the endothelium.

As depicted in Figure 10 stimulation with TNF-α induces the expression of genes belonging to the TNF superfamily like *TNFSF10* and *TNFSF18* and the TNF receptor superfamily including *TNFRSF1A* and *TNFRSF10* whereas the expression of *TNFRSF25* was downregulated. *TNFSF10* and *TNFRSF10B* are members of the TRAIL pathway which induces TNF-α mediated apoptosis [116]. Apart from these two genes *CASP3, CASP7*, *FAS*, *MYC* and *BID,* which are also associated with apoptosis, were slightly upregulated. As TNF-α exerts its pro-inflammatory effects through the NF-κB signaling pathway it is not surprising that genes like *TRADD*, *TRAF2, TRAF3, BRIC2, NFKB1* and *NFKBIA* are upregulated upon TNF-α stimulation. Although NFKBIA is a negative regulator of NF-κB signalling upregulation of this gene is part of a negative feedback regulatory mechanism for terminating TNF-α induced NF-κB response [117]. The most pronounced increase in gene expression upon TNF-α treatment could be observed for the pro-inflammatory cytokines IL-1β, IL-8 and TNF-α itself which was to be expected as TNF-α is potent inducer of inflammation. Notably there was a marked downregulation of *NOS3* which encodes eNOS.

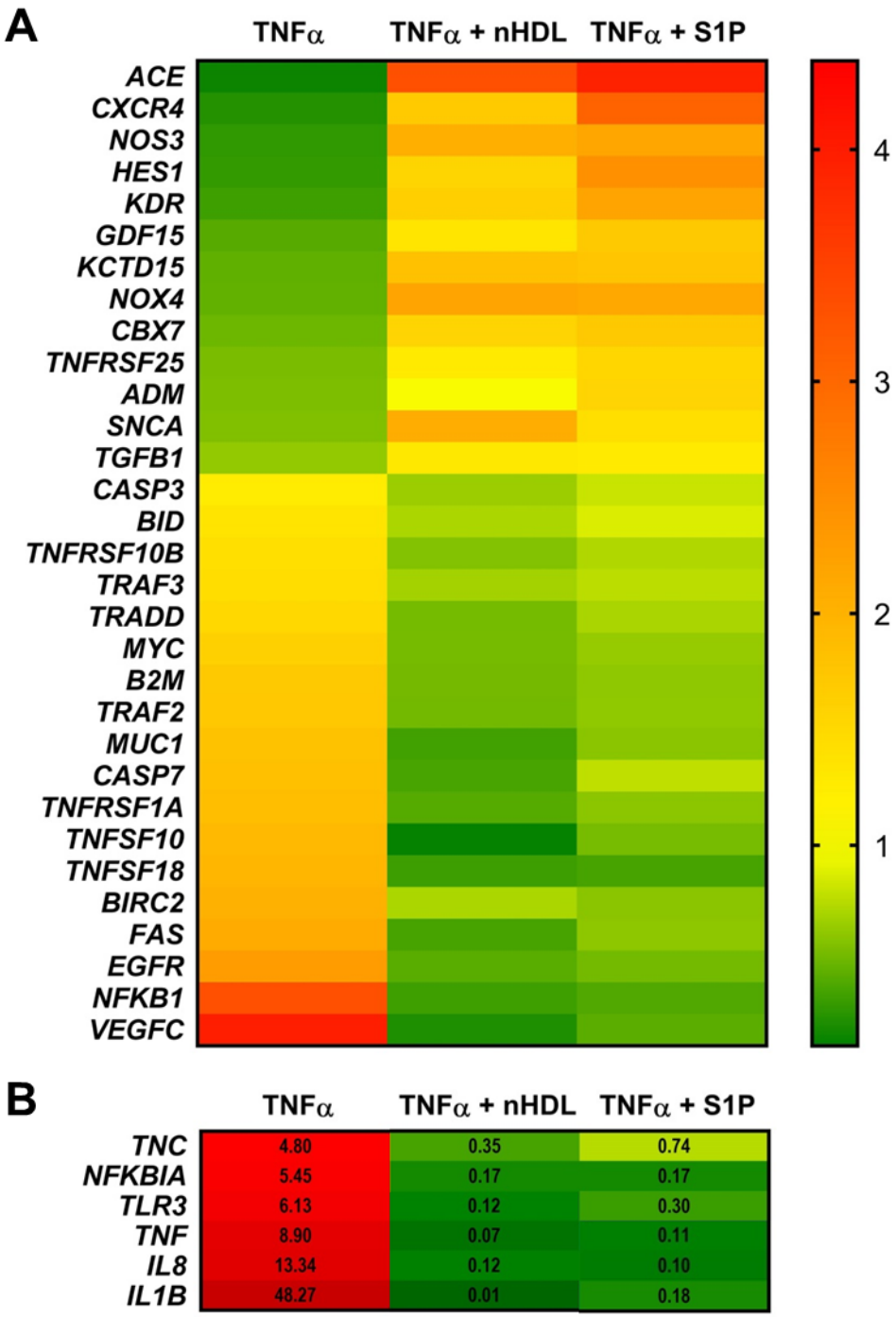

Figure 10: S1P and nHDL counteract TNF-α induced regulation of genes associated with inflammation and preeclampsia. HPAECs were seeded at a density of 100,000 cells/well in 12 well plates and treated with 10 ng/ml TNF-α only or with TNF-α in the presence of 800 µg/ml nHDL or 1 µM HSA-S1P for 6 h. After total RNA isolation and reverse transcription, expression of 128 genes related to preeclampsia and TNF-induced apoptosis was examined. **(A)** Genes which are significantly regulated as determined by multiple t-testing are depicted in the heatmap. The heatmap shows the fold change mRNA expression (Mean of n = 3). **(B)** Genes where the fold change values exceed the scale shown in **A** are depicted here. The numbers represent the respective fold change values.

Figure 10 shows that TNF-α is a very versatile cytokine capable of influencing the expression of many different genes which are involved in different biological processes for example inflammation, apoptosis and endothelial dysfunction but also cell proliferation and cell survival. As shown in Figure 10, nHDL as well as S1P successfully counteracted the effects of TNF-α on mRNA expression of all inflammation related genes shown, indicating that nHDL and S1P inhibit TNF-α signalling before it can affect its transcription.

3.5 S1P and nHDL suppress mRNA expression of inflammatory markers in HPAECs

To further clarify the role of nHDL and S1P in TNF-α induced inflammation, the influence on mRNA expression of the inflammatory mediators ICAM1, VCAM1, IL-8 and MCP1 in HPAECs was elucidated. ICAM1 and VCAM1 are intracellular adhesion molecules which control the firm adhesion of leukocytes to the endothelium and therefore are important mediators of inflammation in ECs [118]. IL-8 and MCP1 act as chemotactic cytokines during inflammation for neutrophils [119] and monocytes [120] respectively. mRNA expression of all these genes was increased upon TNF-α stimulation in HPAECs (Figure 11). The most pronounced effect could be observed for VCAM1 with a nearly 30 fold increase of mRNA followed by ICAM1 (28 fold), IL-8 (21 fold) and MCP1 (12 fold). When HPAECs were treated with TNF-α in the

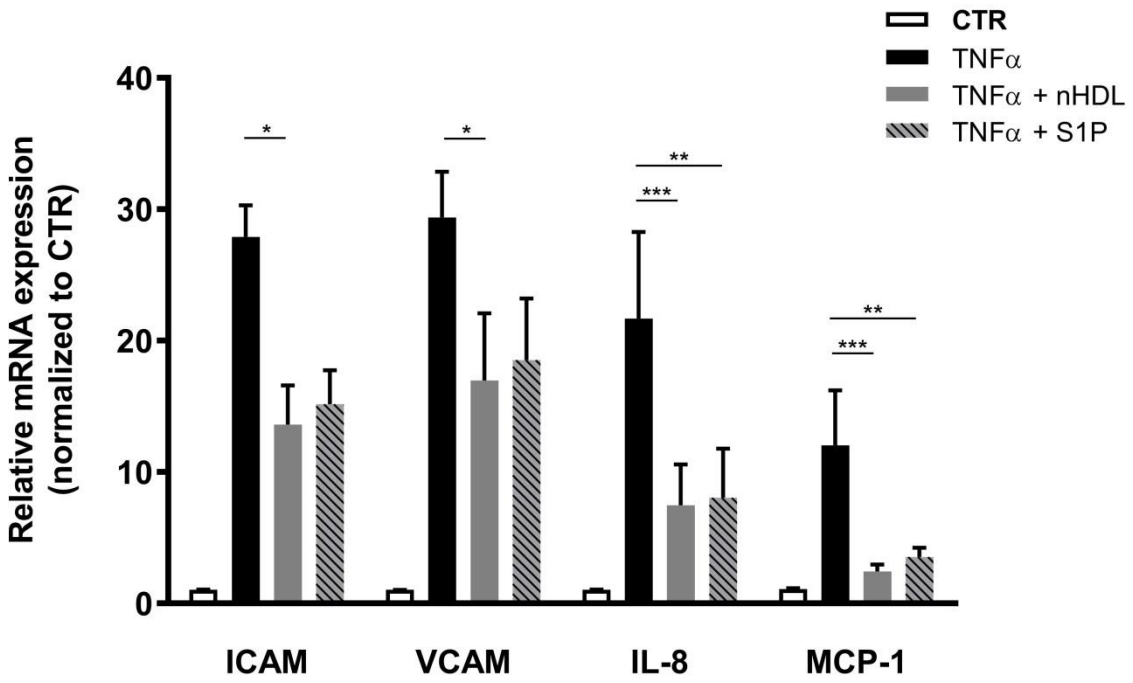

Figure 11: S1P-nHDL reduces mRNA expression of inflammatory markers at the feto-placental endothelium. HPAECs were seeded at a density of 100,000 cells/well in 12 well plates and treated with 10 ng/ml TNF-α only or with TNF-α in the presence of 800 µg/ml nHDL or 1 µM HSA-S1P for 6 h. Total RNA was reverse transcribed and analysed by RT-PCR using TaqMan probes. Differences in mRNA expression are calculated using the ΔΔ-Cq method. Data are presented as fold change (mean ± SD; n = 4) compared to control condition. * = $p<0.05$; ** = $p<0.01$; *** = $p < 0.001$

presence of 800µg/ml nHDL this inflammatory response was significantly attenuated. Expression of MCP1 dropped by 80 % followed by IL-8 by ~ 65 % compared to controls. The expression of the adhesion molecules ICAM1 and VCAM1 was also reduced by ~50 % and ~ 40 % respectively. Co-incubation of HPAECs with TNF-α and S1P dampens the inflammatory response although the effects were less pronounced suggesting that beside S1P additional proteins may account for the pronounced effect of nHDL. Upon S1P treatment mRNA levels of MCP1 declined the most by a reduction of around 70 %, followed again by IL-8 (~ 60 %). Although the effects of S1P on the expression of ICAM1 ($p = 0.14$) and VCAM1 ($p = 0.25$) are not statistically significant, there is a clear downward trend visible. There was still a decrease of mRNA levels of ~45 % for ICAM1 and of ~35 % for VCAM1. These results show that nHDL and S1P are able to counteract the inflammatory response of HPAECs induced by TNF-α on transcriptional levels by reducing the expression of adhesion molecules and pro-inflammatory cytokines.

3.6 S1P and nHDL attenuate the inflammatory response by inhibiting NF-κB signalling

It is well known that TNF-α signals by the NF-κB pathway to promote the inflammatory response. NF-κB controls the general pro-inflammatory response on ECs by controlling the expression of adhesions molecules and cytokine production e.g., IL-8 and MCP1 [121–124]. To check whether nHDL and S1P are able to influence this signaling pathway, the phosphorylation of NF-κB subunit p65 at Ser536 was examined. This phosphorylation leads to enhanced transactivation of NF-κB corroborated by increased expression of regulated genes [125]. TNF-α induces the phosphorylation of p65 at Ser536. In the presence of nHDL the phosphorylation of p65 at Ser536 dropped by 50% to basal levels as seen under control conditions (Figure 12A). Similar suppression of p-NF-κB was obtained upon TNF-α and S1P treatment of HPAECs. The alleviative effect of nHDL and S1P on the transactivation of the NF-κB pathway was already observed after 2 hours (data not shown) and persisted at least for 6 hours after induction of inflammation with TNF-α. These findings implicate that nHDL and S1P exert their anti-inflammatory actions in HPAECs by inhibiting NF-κB signaling and correlate with observed reduction of mRNA expression for selected inflammatory markers mentioned in section 3.5. Furthermore, 15 of the 24 genes in Figure 10 that were found to be upregulated upon TNF-α stimulation are also regulated by NF-κB possibly explaining how nHDL and S1P affect their transcription .

3.7 nHDL and S1P do not affect protein expression of inflammatory mediators

To investigate whether the observed decrease in NF-κB signalling and the reduction of mRNA expression of inflammatory mediators caused by nHDL and S1P translate to protein levels, protein expression of VCAM1, ICAM1 and MCP1 was tested. As clearly shown in Figure 12B, the expression of all three proteins was markedly increased when inflammation was stimulated in HPAECs by adding TNF-α. Surprisingly, neither treatment with nHDL or with S1P reduced the protein levels of VCAM1, ICAM1 or MCP1. To rule out the possibility that the influence of nHDL and S1P on protein expression is a matter of protein stability, the levels were also checked after 2, 4, and 24 hours. Independent of the time-dependent kinetics, TNF-α was always able to induce the expression of VCAM1, ICAM1 and MCP1 but S1P and nHDL failed to reduce protein expression of these inflammatory markers (data not shown but similar to Figure 12B).

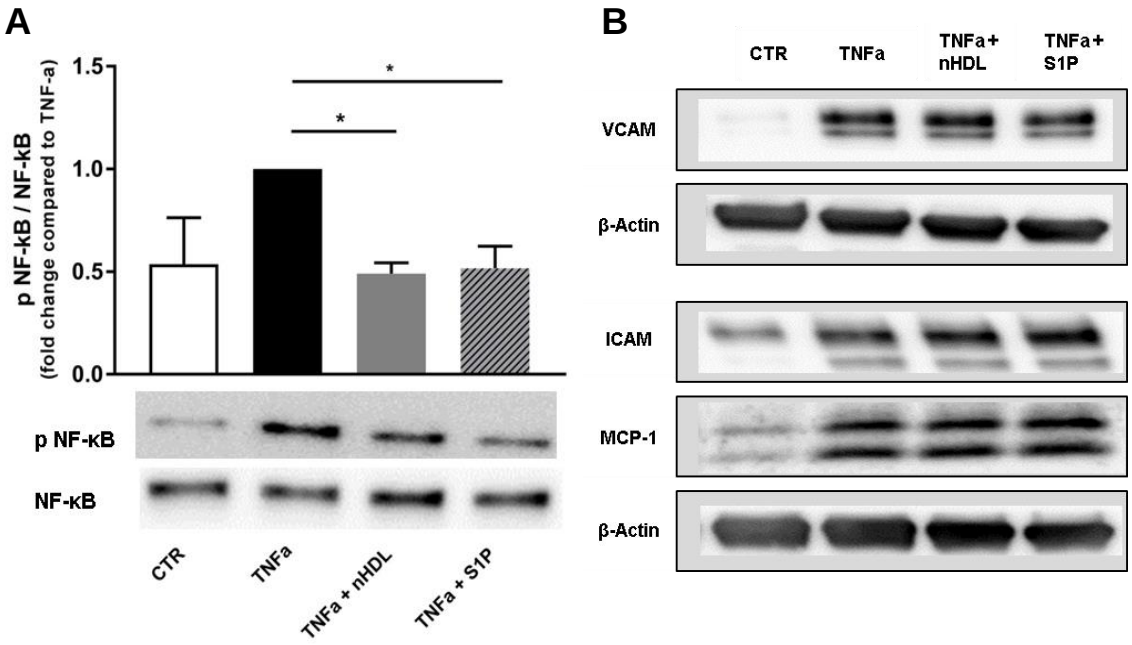

Figure 12: S1P-nHDL inhibits the phosphorylation of NF-κB subunit p65 at Ser536 but not the protein expression of inflammatory markers at the feto-placental endothelium. HPAECs were seeded at a density of 200,000 cells/well in 6 well plates and treated with 10 ng/ml TNF-α only or with TNF-α in the presence of 800 µg/ml nHDL or 1 µM HSA-S1P for 6 h. **(A)** The phosphorylation state of NF-kB at Ser536 was examined by Western blot analysis in whole cell lysates. After protein separation and blotting, membranes were incubated overnight at 4 °C with the primary antibody. Data were normalised to TNF-α and are shown as fold change (mean ± SD; n = 3). * $p < 0.05$. **(B)** Protein expression analysis of inflammatory markers by Western blot analysis in whole cell lysates after 6 h. After protein separation and blotting, membranes were incubated overnight at 4 °C with the primary antibody. β-Actin served as internal loading control.

3.8 Cell surface expression of adhesion molecules is affected neither by nHDL nor by S1P

Because of the lack of detected total protein levels, we further tested if nHDL and S1P could influence the expression of adhesion molecules on the cell surface of HPAECs. Upon inflammatory stimuli adhesion molecules are presented on the surface of ECs and interact with leukocytes in order to navigate the adhesion of them to the endothelium [126]. Additionally to VCAM1 and ICAM1 the cell surface expression of E-Selectin was investigated. E-Selectin is an important mediator of leucocyte rolling, which is the first mechanistically step in leukocyte adhesion, and is also inducible by TNF-α [127]. As depicted in Figure 13, unstimulated HPAECs do not express adhesion molecules on their cell surface. However upon stimulation with TNF-α, cell surface expression of VCAM1, ICAM1 and E-Selectin is strongly induced. The most pronounced stimulation could be observed for ICAM1 with around 80 % of positively stained cells (Figure 13A) followed by VCAM1 with ~ 60 % (Figure 13B), whereas expression of E-Selectin was less prominent with ~ 40 % of positively stained cells (Figure 13C). As already observed for total protein expression, the presence of nHDL did not decrease the cell surface expression of VCAM1, ICAM1 or E-Selectin. Like nHDL, S1P could also not dampen the cell surface expression of these adhesion molecules upon stimulation of inflammation.

Taken together these results indicate that nHDL and S1P possesses anti-inflammatory properties by reducing NF-kB mediated mRNA expression of genes linked to inflammation. Surprisingly, this anti-inflammatory capability of nHDL or the bioactive S1P could not be observed on protein levels.

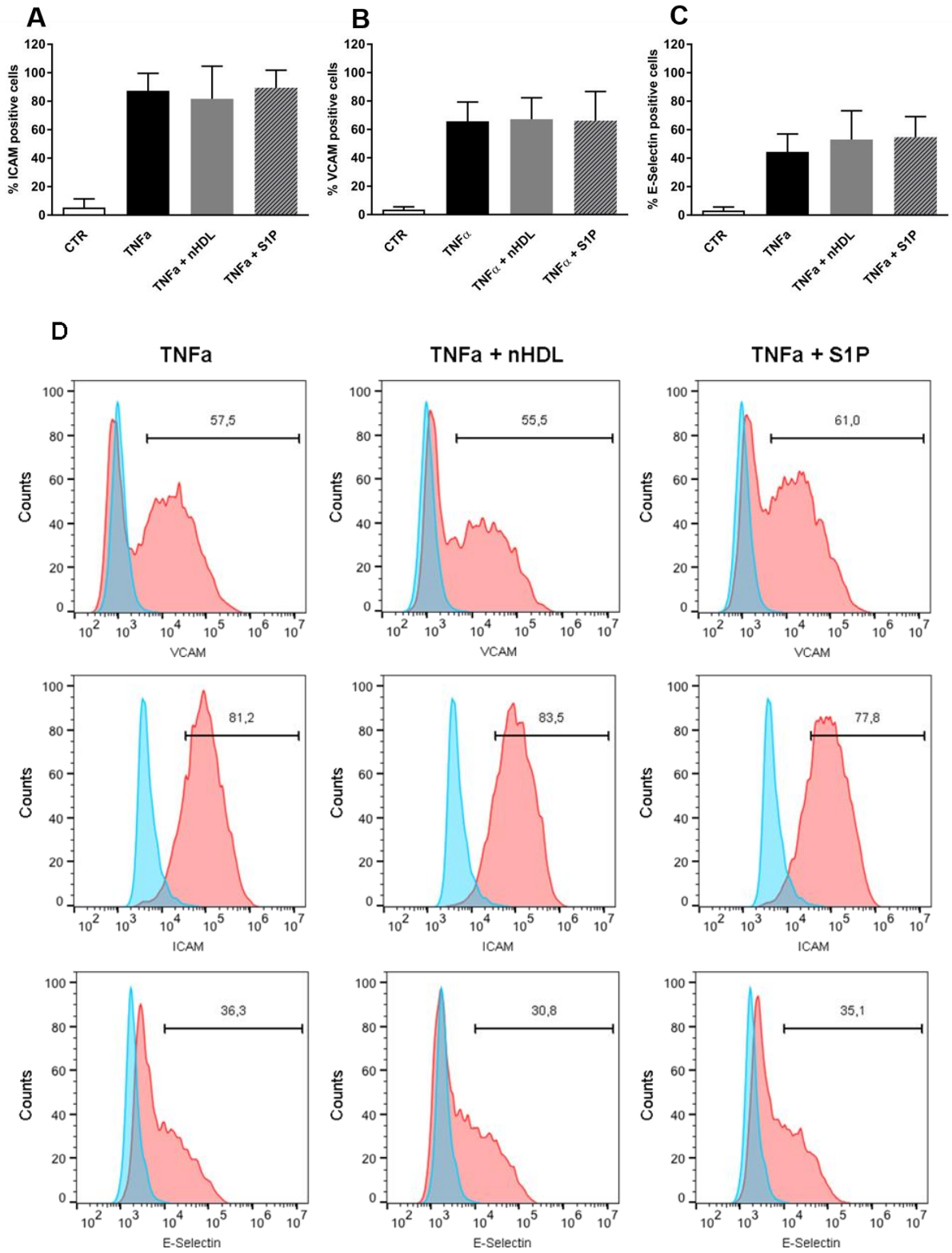

Figure 13: S1P or nHDL does not impact cell surface expression of adhesion molecules on HPAECs. HPAECs were seeded at a density of 500.000 cells/well in 25 cm^2 Flask and 10 ng/ml TNF-α only or with TNF-α in the presence of 800 µg/ml nHDL or 1 µM HSA-S1P for 6 h. After Fc receptor blocking for 10 minutes cells were incubated for 30 minutes with fluorophore labelled antibodies against **(A)** VCAM, **(B)** ICAM and **(C)** E-Selectin. Bar charts show the percentage of positive stained cells (mean ± SD; n = 3). **(D)** One representative of three surface marker analyses. Blue histograms show control cells without treatment whereas red histograms show cells treated as indicated. Black bars show the gate which was chosen to define positively stained cells. The values given in each histogram represent the percentage of positively stained cells.

3.9 nHDL and S1P protect endothelial cells from AngII induced ROS production

Increases production of ROS plays a crucial role in the progression of endothelial dysfunction and hypertension [36]. A major source of ROS in endothelial cells is the NADPH oxidase complex whose activity is stimulated by AngII [128]. In this set of experiments we investigated whether nHDL and S1P are capable to influence AngII induced ROS formation in HPAECs. Treatment of HPAECs with AngII increased intracellular ROS production by ~ 60 % (0.5 µM AngII) and ~ 85 % (1 µM AngII) compared to control conditions (Figure 14A). To increase the concentration of AngII from 0.5 µM to 1 µM did not lead to a significant increase in ROS levels. In the presence of nHDL ROS production dropped by 75 % (0.5 µM AngII) and 80 % (1 µM AngII) when compared to ROS levels caused by AngII. nHDL works as effective inhibitor of oxidative stress because ROS production was reduced to even lower levels than observed under control conditions. S1P is less effective in preventing ROS production in HPAECs under hypertensive conditions. Although the protective effect of S1P is not statistically significant (0.5 µM AngII: p = 0.88; 1 µM AngII: p = 0.60), a downward trend in ROS levels is evident. ROS levels were reduced by 20 % (0.5 µM AngII) and 25 % (1 µM AngII) when comparing them with

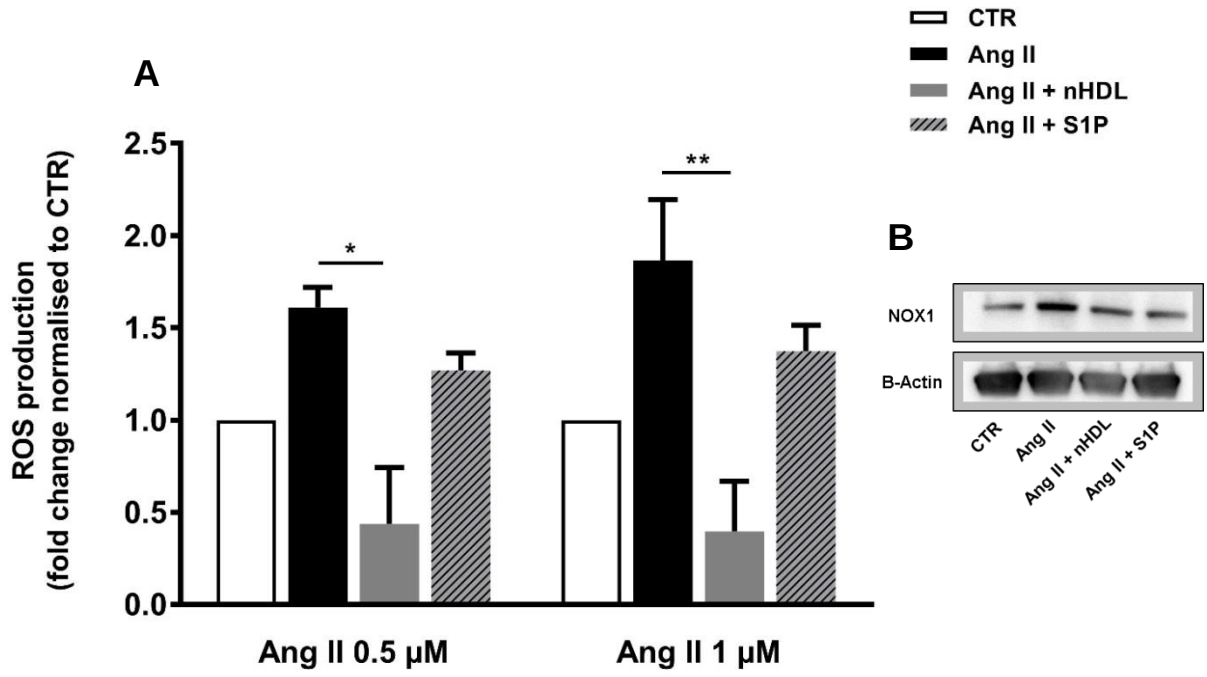

Figure 14: S1P-nHDL lowers the AngII induced oxidative stress in human placental endothelial cells. (A) HPAECs were seeded at a density of 20,000 cells in a 96 well plate and incubated with Dichlorofluorescin diacetate (DCFDA) for 45 minutes. After one washing step HPAECs were treated with 0.5 and 1 µM Angiotensin II only or with 0.5 and 1 µM AngII in the presence of 800 µg/ml nHDL or 1 µM HSA-S1P for 4 hours. Intracellular oxidation of DCFDA into dichlorofluorescein was detected by fluorescence spectroscopy (Ex/Em: 295/529). Tert-butyl hydrogen peroxide (200µM) was used as a positive control. The bar chart shows the generation of ROS as fold change (mean ± SD; n = 3) compared to control. * $p < 0.05$; ** $p < 0.01$ **(B)** HPAECs were seeded at a density of 200,000 cells/well in 6 well plates and treated with 1 µM AngII only or with AngII in the presence of 800 µg/ml nHDL or 1 µM S1P for 6 h. Protein expression of NOX1 was analysed by Western blot in whole cell lysates. After protein separation and blotting, membranes were incubated overnight at 4 °C with the primary antibody. β-Actin served as internal loading control.

ROS amounts induced by AngII (Figure 14A). Preliminary data also suggest an impact of nHDL and S1P on the protein expression of NADPH oxidase 1 (NOX1) in HPAECs. As shown in Figure 14B AngII treatment markedly increased NOX1 levels whereas nHDL and S1P reduced the induction of NOX1 expression upon AngII treatment

3.10 Impairment of S1P metabolism in preeclampsia

To test if the metabolic intracellular pathway by which S1P is produced is altered during inflammation and is corroborated by endothelial dysfunction, HPAECs were challenged with TNF-α and AngII. Figure 15A shows the effects of TNF-α on key enzymes involved in the intracellular sphingolipd metabolism. Expression of SPT, SPHK1 and SPP1 was examined on transcritpional levels. No change was detectable in the expression of SPTLC1 under inflammatory conditions. Stimulation of HPAECs with TNF-α caused a markedly 3.8-fold increase of SPHK1 mRNA whereas the expression of SPP1 was unaffected by TNF-α indicating a shift towards increased S1P synthesis when HPAECS are confronted with an inflammatory environment. Preeclampsia also appears to impact the sphingolipid metabolism on transcriptional level. As already observed in HPAECs mRNA levels of SPTLC1 were not significantly changed in preeclamptic placental tissue. When comparing the mRNA expression of SPHK1 in healthy and preeclamptic placentae the outcome was different to the results obtained with HPAECs under inflammatory conditions (Figure 15B). Although not statistically significant (p = 0.29) there was a downregulation of ~ 30 % of SPHK1 mRNA in preeclamptic placental tissue detectable. More distinct conclusions could be drawn when examining mRNA

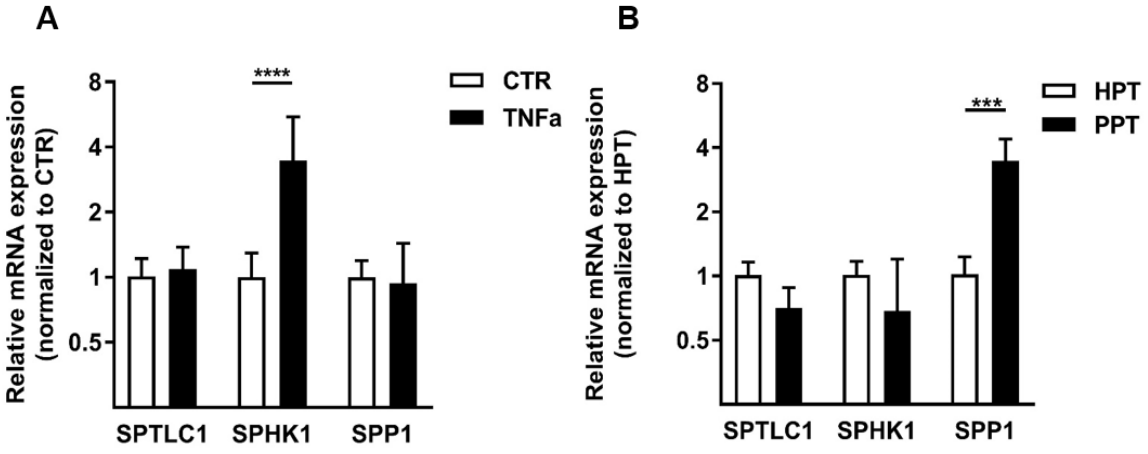

Figure 15: **Sphingolipid metabolism is impaired under TNF-α induced inflammation and in preeclampsia. (A)** HPAECs were seeded at a density of 100,000 cells/well in 12 well plates and treated with 10 ng/ml TNF-α for 6 h. Total RNA was reverse transcribed and analysed by RT-PCR using TaqMan probes. Data are presented as fold change (mean ± SD; n = 3) compared to control condition **(B)** Healthy placental tissue (HPT) and preeclamptic placental tissue (PPT) were collected immediately after delivery and snap frozen until RNA isolation. Tissue was homogenized with a MagNA Lyser device and total RNA was isolated using an RNeasy Mini Kit. After reverse transcription gene expression was analysed by qPCR using TaqMan probes. Data are expressed as fold change and were normalised to healthy placental tissue. Bar chart shows the mean ± SD; n = 4. Y-axis is $\log_2$ transformed. *** $p < 0.001$; **** $p<0.0001$

levels of SPP1. There was a significant (p = 0.0008), 3.5-fold increase of SPP1 mRNA in preeclamptic placental tissue in comparison to healthy placental tissue.

3.10.1 Enzymatic activity of SPT is upregulated by TNF-α but not by AngII.

SPT is the rate limiting enzyme in the *de novo* synthesis of sphingolipids. To further clarify the impact of inflammatory stimuli on this key enzyme, the protein expression of SPTLC1 was determined. As shown in Figure 16A and B, SPTLC1 protein did not change after 6 and 24 hours of TNF-α treatment. As there was no change observable, neither on mRNA nor on protein level, next the enzymatic activity of SPT was measured. Stimulation of HPAECs with TNF-α led to a roughly 2-fold increase in [^{3}H]Sphinganine amounts as compared to control treatment (Figure 16C). Increasing the concentration of TNF-α from 10 ng/ml to 50 ng/ml did not lead to a further increase in SPT activity indicating that 10 ng/ml are sufficient to reach maximal induction of SPT by TNF-α. Contrary to TNF-α, stimulation of HPAECs with AngII did not cause any change in the activity of SPT. Increasing the AngII concentration from 1 µM to 5 µM had no further impact on SPT activity. This experiment shows that under inflammatory conditions induced by TNF-α, the *de novo* synthesis of sphingolipids is enhanced by increased activity of the rate limiting enzyme SPT.

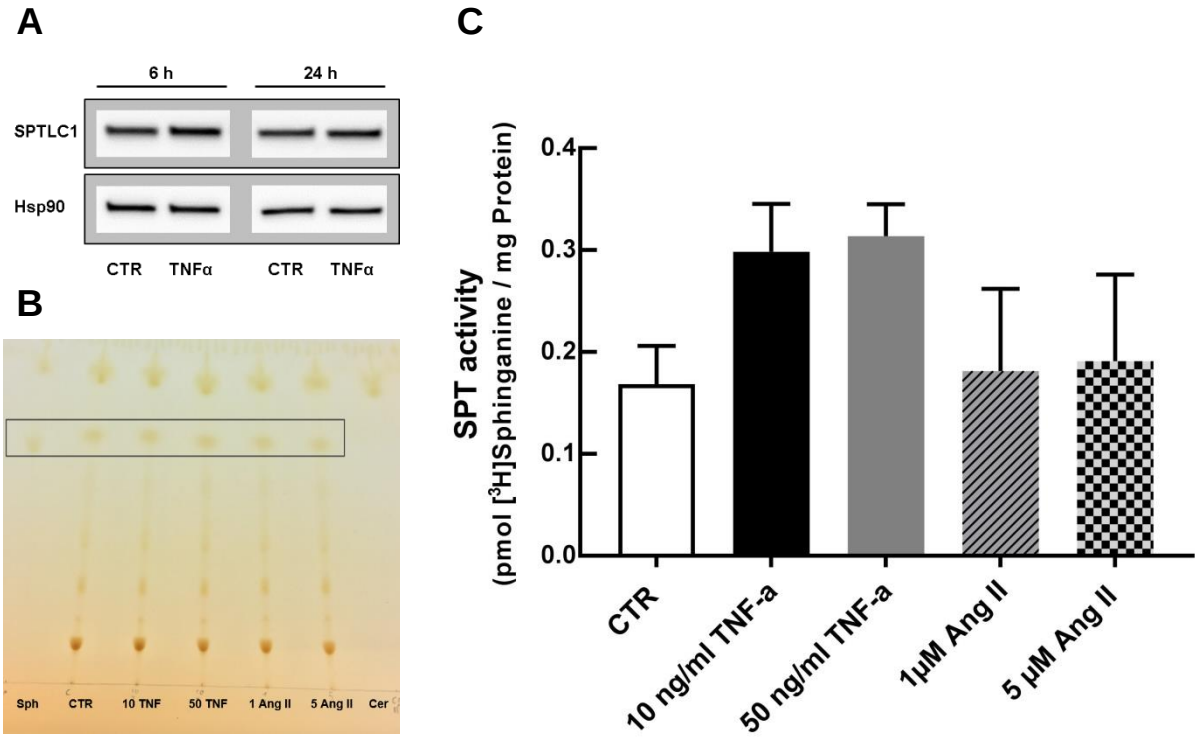

Figure 16: SPT enzyme activity is increased under inflammatory conditions. (A) HPAECs were seeded at a density of 200,000 cells/well in 6 well plates and treated with 10 ng/ml TNF-α for the time indicated. Protein expression of SPT was examined by Western blot. Hsp90 served as internal loading control. One representative of three independent experiments is shown here. **(B)** HPAECs were seeded at a density of 600,000 cells in 60 mm dishes and treated with 10 ng/ml TNF-α, 50 ng/ml TNF-α, 1 µM AngII or 5 µM AngII for 24 hours. [^{3}H]Serine was added to HPAECs lysates as a traceable substrate for SPT. After performing the SPT reaction, lipids were extracted and separated using TLC. For visualisation and identification of lipid species, lipids were stained with iodine vapour. The band in the black rectangle represents the [^{3}H]Sphinganine fraction as verified by the external sphinganine standard (Sph). **(C)** SPT activity was evaluated by measuring [^{3}H]Sphinganine radioactivity. For this purpose, sphinganine band was cut out and analysed by a β-counter. Reading values were quantified using a standard curve of [^{3}H]Serine. Bar chart shows the results of 2 independent experiments as mean values ± SD.

4 DISCUSSION

Pregnancies complicated by PE are characterized by maternal hypertension, proteinuria, systemic inflammation and endothelial dysfunction. As all these cardinal features are in connection with the endothelium it is clear that the endothelium plays a pivotal role in the pathogenesis of PE. The bioactive sphingolipid S1P is known to have a major impact on the endothelium. Therefore understanding the effects of S1P on the endothelium impaired by preeclamptic conditions may ad valuable information to understand the incompletely elucidated etiology of PE.

In this study we could show that nHDL and S1P show anti-inflammatory properties by reducing the mRNA expression of inflammatory markers although these effects seem not to translate to the protein level within the investigated timeframes. Additionally, we could show that nHDL and S1P dampen NF-κB signaling induced by TNF-α. Increased ROS production, a major hallmark feature of endothelial dysfunction, is also markedly reduced by nHDL and to some extent by S1P. This observation implicates that nHDL and S1P show endothelium protective properties that could weaken the adverse outcomes for endothelial cells during preeclamptic conditions like inflammation and endothelial dysfunction. To better understand the link between S1P and preeclampsia we also investigated the influence of preeclamptic conditions on S1P metabolism. We found that in an inflamed state, the enzymatic activity of SPT, the rate limiting enzyme in sphingolipid synthesis, is increased around 2-fold in HPAECs. This goes along with a 3.8-fold increase in SPHK1 expression whereas SPP expression is unaffected under this condition in HPAECs. Interestingly, in preeclamptic tissue samples we could observe the opposite as the expression of SPP is increased up to 3.5-fold along with a slight but not statistically significant decrease in SPHK1 expression.

In a first attempt to find the best fitting mimetic for preeclamptic conditions in cell culture we aimed to use serum of preeclamptic women. One important aspect for our serum samples to serve as a mimetic for preeclampsia were the levels of inflammatory cytokines as it is well known that levels are increased in women suffering from preeclampsia [129–132]. Unfortunately, characterization of our samples revealed that all cytokine levels except for IL-6 were too low to be detected. A possible reason for that may be because sample acquisition was hampered by the unexpectedly small number of preeclamptic women available as test subjects. Therefore we additionally used samples which were not freshly sampled but already in storage. Unfortunately, sample storage was not optimized for conserving cytokines in these samples and due to storage and age of the samples it is likely that most of the cytokines were already degraded. Most cytokines are stable up to 2 years if stored at -80 °C [133], but used samples were already stored for 2 to 3 years old which exceeds the mentioned time-limit for

storage. Furthermore, it was not possible to obtain information about the number of freezing - thawing cycles of the samples as most cytokines are only stable for up to three of these cycles [134]. To overcome this problem, we switched to an *in vitro* approach by using TNF-α and AngII to mimic preeclamptic conditions in our cell culture system. TNF-α was used as it is well known that levels of this cytokine are elevated in placentas of preeclamptic women [135,136] as well as in their systemic circulations [137]. Furthermore, TNF-α plays a key role in the exaggerated inflammatory response prevalent in PE [138], it is involved in the abnormal apoptotic and necrotic processes in trophoblasts during PE [139] and promotes endothelial dysfunction [140]. We choose to use TNF-α at a concentration of 10 ng/ml as was shown that this concentration is sufficient to induce a pronounced inflammatory response as NF-κB activation peaks at this concentration [141]. AngII was used because it is a known vasoconstrictor that induces hypertension, a cardinal feature of PE. Additionally, in PE formation of autoantibodies against the angiotensin receptor 1 was reported which leads to increased AngII sensitivity [142,143]. Furthermore, endothelial AngII significantly contributes to the production of ROS via NOX thereby causing endothelial dysfunction [35]. Previous studies showed a dose dependent activation of NOX in the range of 0.01 to 1 µM AngII [144,145]. Based on these findings we chose to use 0.5 and 1 µM AngII to ensure sufficient induction of NOX. Although, neither TNF-α nor AngII do fully represent the complex pathology of PE, both represent key molecules especially if one is investigating endothelial inflammation and dysfunction in the context of PE like we aimed to do.

S1P is involved in the regulation of endothelial inflammation which has been shown in several studies [146–149]. However, there is still some controversy whether S1P acts pro- or anti-inflammatory [150,151]. In this study we used TNF-α to induce the expression of the adhesion molecules VCAM1 and ICAM1 and the cytokines MCP1 and IL-8 in HPAECs as these cells do not express these inflammation related proteins under basal conditions. We could show that nHDL and S1P present anti-inflammatory properties by reducing TNF-α induced mRNA expression of VCAM1 and ICAM1 as well as of IL-8 and MCP1. Furthermore, we provided evidence that the downregulation is achieved by antagonizing the TNF-α induced activation of NF-κB which has been shown by others [147]. Surprisingly we could not see any changes on protein levels or in the cell surface expression of adhesion molecules. Ruiz et al [146] reported similar observations although in this study the discrepancy between transcription and translation was solely attributed to ICAM1. Furthermore, although IL-8 and MCP1 mRNA levels were not measured, this study also failed to show that S1P reduces IL-8 and MCP1 protein levels under inflammatory conditions [146]. The question why the observed reduction of mRNA does not translate to the protein level is difficult to answer without extensive additional research which - to our best of knowledge – has not been done yet. One possibility why the observed reduction in mRNA levels does not translate to the protein level might be that remaining amount

of mRNA present is still sufficient to induce a pronounced inflammatory response. Furthermore, inflammation is a dynamic process that evolves over time and one limitation of our study is that it only shows a snapshot of a distinct time point. Therefore extensive kinetic studies with multiple time points would likely draw a more complete picture of the consequences of nHDL and S1P administration in inflammation. In a physiological context it is not surprising that nHDL and S1P alone is not sufficient to completely abolish the inflammatory response of ECs as this process is a complex, dynamic and redundantly regulated one [19].

As outlined above, depending on which receptor is activated by S1P the response of ECs is different. Although the anti-inflammatory $S1PR_1$ is the most abundantly expressed, the pro-inflammatory $S1PR_2$ is also present on ECs [83]. To investigate whether pathological conditions alter the relative expression of S1PRs would help to improve the understanding of the effects of S1P in HPAECs. Studies in HUVECs already showed that TNF-α administration increases expression of $S1PR_1$ and even more pronounced that of $S1PR_2$ [152]. Based on this studies it would be interesting to investigate whether nHDL and S1P administration could also influence the expression of these receptors thereby inhibiting the stimulating effect of TNF-α on $S1PR_2$ expression and/or further increase $S1PR_1$ expression.

The role of S1P in inflammation is undoubtedly a complex one and it becomes more and more evident that the function of S1P in inflammation is not a straight forward mechanism but depends on many interconnected factors like the relative expression of the S1PRs, the local concentration of S1P in relation with the sphingolipid rheostat and the activity of SPHK and SPP in certain (patho)physiological conditions to name some. To sum up it seems very likely that S1P has beneficial properties on the placental endothelium in inflammation but the exact underlying mechanism and regulatory influences remain to be elucidated in more detail.

We could show that nHDL is very efficient in reducing ROS formation in HPAECs thereby protecting cells from oxidative stress which is in line with observations by other groups [153–155]. The exact mechanism how nHDL is affecting the regulation of intracellular ROS metabolism in non-phagocytosing cells are still poorly understood. As already mentioned one of the main contributor for ROS in ECs is NOX [32]. One possible explanation for this might be, that HDL disrupts the formation of lipid rafts on cell membranes which are important for the assembly and functionality of NOX thereby preventing the production of ROS [154,156]. Molecular mechanisms by which HDL interferes with intracellular ROS production are also incompletely understood. NOX is stimulated by AngII via the angiotensin receptor type 1 (ATR_1) [32] and it has been shown that this process involves protein kinase C (PKC) [157]. PKC phosphorylates the NOX subunit $p47^{phox}$, which causes translocation of $p47^{phox}$ to the cell membrane to participate in the formation of active NOX complexes [156,157]. Furthermore, the assembly of the NOX complex requires the small GTPase Rac1 [158]. Others have shown

that in presence of HDL PKC phosphorylation [155], translocation of $p47^{phox}$ [153] as well as Rac1 activation [153] is attenuated giving some insight on how HDL decreases intracellular ROS levels. Tölle et al [153] could also show that S1P alone is able to prevent NADPH oxidase induced ROS production in the same way as HDL. We could also show a downward trend in ROS levels in the presence of S1P but the effect was less pronounced than with nHDL. As S1P is associated with HDL it is likely that the effect of HDL on ROS production is partially mediated by S1P which was shown in experiments where removal of S1P from HDL particles decreased the capacity of HDL to prevent ROS production [153]. But still it seems like HDL additionally prevents ROS formation by S1P independent mechanisms (like the disruption of lipid rafts mentioned above) explaining why it is more effective than S1P alone. Furthermore, it is known that HDL improves S1P signaling by retaining S1PR on the cell surface and by boosting S1PR recycling [100]. Additionally, interactions of HDL and SR-BI facilitate the transfer of HDL bound S1P to its receptors by providing spatial proximity [99].

In a preliminary experiment we found evidence that nHDL and S1P rescue the AngII induced upregulation of NOX1 in HPAECs which possibly provides another way how nHDL and S1P protect the endothelium from oxidative stress. Although our data need further validation, it is known that NOX1 expression is regulated via NF-κB [159]. Our results indicate that nHDL and S1P inhibit NF-κB signaling which supports the idea that nHDL and S1P modulate NOX1 also on expressional level. Furthermore, on mRNA level we could show that nHDL and S1P reverse the TNF-α induced downregulation of NOX4 which additionally points towards their endothelium protective effects as NOX4 (contrary to all other NOX isoforms) is known for its endothelium protective properties by increasing NO bioavailability and suppressing cell death pathways [160].

Especially in the context of ROS it is worth mentioning that apart from ECs other adjacent cell types like SMCs, fibroblasts and especially several types of leucocytes also express NOX isoforms [160], therefore considerably contributing to ROS levels present in the vasculature, especially under pathological conditions. This means although it is important to understand the role of ROS in ECs it is also important to highlight that our study only shows one pathway of a more complex biological system.

As our findings implicate beneficial effects of HDL and S1P in inflammation and endothelial dysfunction we were interested whether these conditions interfere with the intracellular synthesis pathway in a way that reduce S1P concentrations thereby diminishing this protective influences. Our results revealed that SPT activity is elevated under inflammatory conditions pointing towards increased *de novo* sphingolipid synthesis. Additionally, our study showed that SPHK1 is slightly downregulated whereas SPP1 expression is significantly increased in PPT which leads to a shift towards the reversible dephosphorylation of S1P. Increased *de novo*

synthesis of sphingolipids in combination with higher levels of S1P dephosphorylation indicate a net increase in intracellular ceramide levels in PPT which was also reported by Melland-Smith et al [103]. Additionally, this study could also demonstrate lower levels of circulating S1P in women suffering from preeclampsia compared to normotensive women and reported increased SPT activity in PPT which supports our own findings [103]. This in turn leads to a disruption of the so called sphingolipid rheostat which describes the balance of intracellular levels of ceramide and S1P [161]. Ceramide is known for its pro-apoptotic properties [162,163] whereas S1P suppresses apoptosis and promotes cell proliferation [62,164] by regulating opposing signaling pathways. Therefore increased ceramide levels in combination with decreased S1P levels lead to more apoptotic processes which may account for observed adverse outcomes in preeclampsia [165]. However, obtained results cannot rule out that the observed alterations in the sphingolipid metabolism lead to an accumulation of other sphingolipids especially that of sphingomyelin instead of ceramide, which is known to serve as a reservoir for the synthesis of ceramide and also S1P [76,77]. But it is interesting to mention that others have shown decreased expression and activity of ASAH1, the enzyme that converts ceramide to sphingosine, under preeclamptic conditions which further argues for increased ceramide levels [103]. Interestingly, we could also see increased levels of ceramide under inflammatory conditions in our SPT activity assay (data not shown). As the used assay was not validated to measure ceramides obtained results should be interpreted with caution, but still this is an additional proof for increased ceramide levels under preeclamptic conditions. In order to increase our understanding of alterations in the sphingolipid rheostat, direct measurement of ceramides, sphingomyelin and S1P concentrations would add further valuable information.

Additionally, to placental tissue we also measured expression of SPT, SPHK1 and SPP1 in primary HPAECs. In line with the placental tissue we could not find any changes in SPT mRNA in HPAECs which further confirms our findings that SPT is regulated solely on the level of enzymatic activity under pathological conditions related to preeclampsia. Interestingly and contrary to our findings in PPT, expression of SPHK1 was significantly upregulated in HPAECs upon treatment with TNF-α. This could mean that HPAECs, when confronted with an inflammatory stimulus, increase the intracellular synthesis of S1P by upregulating SPHK1. In that manner this might protect the endothelium by establishing a positive feedback loop that promotes the anti-inflammatory response by increased inside-out signaling of S1P. Ruiz et al., reported similar findings supporting our concept and additionally showed that addition of TNF-α in combination with ApoM bound S1P further increases the expression of SPHK1 [146]. The differences of our findings in HAPECs and PPT might be explained by two ways: a) other adverse influences of preeclampsia which are not reflected in our cell culture system block this compensatory mechanism in the endothelium or b) as placental tissue is composed of more

than just endothelial cells what happens in the endothelium must not hold true for the whole placental tissue.

In conclusion we could show that nHDL associated S1P shows anti-inflammatory properties that protect the feto-placental endothelium. Furthermore we provided evidence that nHDL is very effective in preventing ROS formation thereby protecting the endothelium from oxidative stress prevalent in endothelial dysfunction. Although S1P alone is not as potent as nHDL in preventing ROS formation it is likely that nHDL associated S1P is partially responsible for the observed effects. Taken together this shows that nHDL and S1P protect the endothelium in pathological conditions that are prevalent in preeclampsia indicating a beneficial role in this pregnancy complication. Additionally this study revealed that S1P metabolism is impaired under preeclamptic conditions in a way that interferes with the protective properties of S1P possibly contributing to adverse outcomes in preeclampsia.

5 REFERENCES

[1] Desoye, G., Gauster, M. and Wadsack, C. (2011) Placental transport in pregnancy pathologies. *The American Journal of Clinical Nutrition*, **94**, 1896S-1902S. https://doi.org/10.3945/ajcn.110.000851

[2] Gude, N.M., Roberts, C.T., Kalionis, B. and King, R.G. (2004) Growth and function of the normal human placenta. *Thrombosis Research*, **114**, 397–407. https://doi.org/10.1016/j.thromres.2004.06.038

[3] Gaccioli, F. and Lager, S. (2016) Placental Nutrient Transport and Intrauterine Growth Restriction. *Frontiers in Physiology*, **7**. https://doi.org/10.3389/fphys.2016.00040

[4] Benirschke, K., Burton, G.J. and Baergen, R.N. (2013) Pathology of the Human Placenta. 6., th ed. Springer Berlin, Berlin.

[5] Griffiths, S.K. and Campbell, J.P. (2015) Placental structure, function and drug transfer. *Continuing Education in Anaesthesia Critical Care & Pain*, **15**, 84–9. https://doi.org/10.1093/bjaceaccp/mku013

[6] Steegers, E.A.P., von Dadelszen, P., Duvekot, J.J. and Pijnenborg, R. (2010) Pre-eclampsia. *Lancet (London, England)*, **376**, 631–44. https://doi.org/10.1016/S0140-6736(10)60279-6

[7] Goulopoulou, S. and Davidge, S.T. (2015) Molecular mechanisms of maternal vascular dysfunction in preeclampsia. *Trends in Molecular Medicine*, **21**, 88–97. https://doi.org/10.1016/j.molmed.2014.11.009

[8] Wadsack, C., Desoye, G. and Hiden, U. (2012) The feto-placental endothelium in pregnancy pathologies. *Wiener Medizinische Wochenschrift*, **162**, 220–4. https://doi.org/10.1007/s10354-012-0075-2

[9] Lockwood, C.J., Yen, C.-F., Basar, M., Kayisli, U.A., Martel, M., Buhimschi, I. et al. (2008) Preeclampsia-Related Inflammatory Cytokines Regulate Interleukin-6 Expression in Human Decidual Cells. *The American Journal of Pathology*, **172**, 1571–9. https://doi.org/10.2353/ajpath.2008.070629

[10] Félétou, M. (2011) The Endothelium: Part 1: Multiple Functions of the Endothelial Cells—Focus on Endothelium-Derived Vasoactive Mediators [Internet]. Morgan & Claypool Life Sciences, San Rafael (CA).

[11] Galley, H.F. and Webster, N.R. (2004) Physiology of the endothelium. *British Journal of Anaesthesia*, **93**, 105–13. https://doi.org/10.1093/bja/aeh163

[12] Dye, J.F., Jablenska, R., Donnelly, J.L., Lawrence, L., Leach, L., Clark, P. et al. (2001) Phenotype of the endothelium in the human term placenta. *Placenta*, **22**, 32–43. https://doi.org/10.1053/plac.2000.0579

[13] Lang, I., Schweizer, A., Hiden, U., Ghaffari-Tabrizi, N., Hagendorfer, G., Bilban, M. et al. (2008) Human fetal placental endothelial cells have a mature arterial and a juvenile venous phenotype with adipogenic and osteogenic differentiation potential. *Differentiation*, **76**, 1031–43. https://doi.org/10.1111/j.1432-0436.2008.00302.x

[14] Michiels, C. (2003) Endothelial cell functions. *Journal of Cellular Physiology*, **196**, 430–43. https://doi.org/10.1002/jcp.10333

[15] Yuan, S.Y. and Rigor, R.R. (2010) The Endothelial Barrier [Internet]. Morgan & Claypool Life Sciences.

[16] Komarova, Y. and Malik, A.B. (2010) Regulation of Endothelial Permeability via Paracellular and Transcellular Transport Pathways. *Annual Review of Physiology*, **72**, 463–93. https://doi.org/10.1146/annurev-physiol-021909-135833

[17] Rajendran, P., Rengarajan, T., Thangavel, J., Nishigaki, Y., Sakthisekaran, D., Sethi, G. et al. (2013) The Vascular Endothelium and Human Diseases. *International Journal of Biological Sciences*, **9**, 1057–69. https://doi.org/10.7150/ijbs.7502

[18] Sandoo, A., van Zanten, J.J.C.. V., Metsios, G.S., Carroll, D. and Kitas, G.D. (2010) The Endothelium and Its Role in Regulating Vascular Tone. *The Open Cardiovascular Medicine Journal*, **4**, 302–12. https://doi.org/10.2174/1874192401004010302

[19] Pober, J.S. and Sessa, W.C. (2007) Evolving functions of endothelial cells in inflammation. *Nature Reviews Immunology*, **7**, 803–15. https://doi.org/10.1038/nri2171

[20] Saba, H.I. and Saba, S.R. (2014) Vascular Endothelium, Influence on Hemostasis: Past and Present. *Hemostasis and Thrombosis*, Wiley-Blackwell. p. 14–29. https://doi.org/10.1002/9781118833391.ch2

[21] Chapin, J.C. and Hajjar, K.A. (2015) Fibrinolysis and the control of blood coagulation. *Blood Reviews*, **29**, 17–24. https://doi.org/10.1016/j.blre.2014.09.003

[22] Breuss, J.M. and Uhrin, P. (2012) VEGF-initiated angiogenesis and the uPA/uPAR system. *Cell Adhesion & Migration*, **6**, 535–40. https://doi.org/10.4161/cam.22243

[23] Fraisl, P. (2013) Crosstalk between oxygen- and nitric oxide-dependent signaling pathways in angiogenesis. *Experimental Cell Research*, **319**, 1331–9. https://doi.org/10.1016/j.yexcr.2013.02.010

[24] Carmeliet, P. and Jain, R.K. (2011) Molecular mechanisms and clinical applications of angiogenesis. *Nature*, **473**, 298–307. https://doi.org/10.1038/nature10144

[25] Engelse, M.A., Hanemaaijer, R., Koolwijk, P. and van Hinsbergh, V.W. (2004) The fibrinolytic system and matrix metalloproteinases in angiogenesis and tumor progression. *Seminars in Thrombosis and Hemostasis*, **30**, 71–82. https://doi.org/10.1055/s-2004-822972

[26] Elad, D., Levkovitz, R., Jaffa, A.J., Desoye, G. and Hod, M. (2014) Have We Neglected the Role of Fetal Endothelium in Transplacental Transport? *Traffic*, **15**, 122–6. https://doi.org/10.1111/tra.12130

[27] SU, E.J. (2015) Role of the Fetoplacental Endothelium in Fetal Growth Restriction with Abnormal Umbilical Artery Doppler Velocimetry. *American Journal of Obstetrics and Gynecology*, **213**, S123–30. https://doi.org/10.1016/j.ajog.2015.06.038

[28] Pober, J.S. and Cotran, R.S. (1990) THE ROLE OF ENDOTHELIAL CELLS IN INFLAMMATION. *Transplantation*, **50**, 537.

[29] Mitchell, J.A., Ali, F., Bailey, L., Moreno, L. and Harrington, L.S. (2008) Role of nitric oxide and prostacyclin as vasoactive hormones released by the endothelium. *Experimental Physiology*, **93**, 141–7. https://doi.org/10.1113/expphysiol.2007.038588

[30] Yuan, S.Y. and Rigor, R.R. (2010) Signaling Mechanisms in the Regulation of Endothelial Permeability [Internet]. Morgan & Claypool Life Sciences.

[31] Muller, W.A. (2013) Getting Leukocytes to the Site of Inflammation. *Veterinary Pathology*, **50**, 7–22. https://doi.org/10.1177/0300985812469883

[32] Konukoglu, D. and Uzun, H. (2017) Endothelial Dysfunction and Hypertension. *Advances in Experimental Medicine and Biology*, **956**, 511–40. https://doi.org/10.1007/5584_2016_90

[33] Endemann, D.H. and Schiffrin, E.L. (2004) Endothelial Dysfunction. *Journal of the American Society of Nephrology*, **15**, 1983–92. https://doi.org/10.1097/01.ASN.0000132474.50966.DA

[34] Aouache, R., Biquard, L., Vaiman, D. and Miralles, F. (2018) Oxidative Stress in Preeclampsia and Placental Diseases., Oxidative Stress in Preeclampsia and Placental Diseases. *International Journal of Molecular Sciences, International Journal of Molecular Sciences*, **19**, **19**. https://doi.org/10.3390/ijms19051496, 10.3390/ijms19051496

[35] Rajagopalan, S., Kurz, S., Münzel, T., Tarpey, M., Freeman, B.A., Griendling, K.K. et al. (1996) Angiotensin II-mediated hypertension in the rat increases vascular superoxide production via membrane NADH/NADPH oxidase activation. Contribution to alterations of vasomotor tone. *Journal of Clinical Investigation*, **97**, 1916–23. https://doi.org/10.1172/JCI118623

[36] Schulz, E., Gori, T. and Münzel, T. (2011) Oxidative stress and endothelial dysfunction in hypertension. *Hypertension Research*, **34**, 665–73. https://doi.org/10.1038/hr.2011.39

[37] Forstermann, U. (2006) Endothelial Nitric Oxide Synthase in Vascular Disease: From Marvel to Menace. *Circulation*, **113**, 1708–14. https://doi.org/10.1161/CIRCULATIONAHA.105.602532

[38] Laursen, J.B., Somers, M., Kurz, S., McCann, L., Warnholtz, A., Freeman, B.A. et al. (2001) Endothelial Regulation of Vasomotion in ApoE-Deficient Mice : Implications for Interactions Between Peroxynitrite and Tetrahydrobiopterin. *Circulation*, **103**, 1282–8. https://doi.org/10.1161/01.CIR.103.9.1282

[39] Holden, D.P., Fickling, S.A., Whitley, G.S. and Nussey, S.S. (1998) Plasma concentrations of asymmetric dimethylarginine, a natural inhibitor of nitric oxide synthase, in normal pregnancy and preeclampsia. *American Journal of Obstetrics and Gynecology*, **178**, 551–6.

[40] Crowley, S.D. (2014) The Cooperative Roles of Inflammation and Oxidative Stress in the Pathogenesis of Hypertension. *Antioxidants & Redox Signaling*, **20**, 102–20. https://doi.org/10.1089/ars.2013.5258

[41] Hossain, M., Qadri, S.M. and Liu, L. (2012) Inhibition of nitric oxide synthesis enhances leukocyte rolling and adhesion in human microvasculature. *Journal of Inflammation (London, England)*, **9**, 28. https://doi.org/10.1186/1476-9255-9-28

[42] Verma, S., Wang, C.-H., Li, S.-H., Dumont, A.S., Fedak, P.W.M., Badiwala, M.V. et al. (2002) A Self-Fulfilling Prophecy: C-Reactive Protein Attenuates Nitric Oxide Production

and Inhibits Angiogenesis. *Circulation*, **106**, 913–9. https://doi.org/10.1161/01.CIR.0000029802.88087.5E

[43] Yan, G., You, B., Chen, S.-P., Liao, J.K. and Sun, J. (2008) TNF-alpha Downregulates Endothelial Nitric Oxide Synthase mRNA Stability via Translation Elongation Factor 1-alpha 1. *Circulation Research*, **103**, 591–7. https://doi.org/10.1161/CIRCRESAHA.108.173963

[44] Lund-Katz, S. and Phillips, M.C. (2010) High Density Lipoprotein Structure–Function and Role in Reverse Cholesterol Transport. *Sub-Cellular Biochemistry*, **51**, 183–227. https://doi.org/10.1007/978-90-481-8622-8_7

[45] Feingold, K.R. and Grunfeld, C. (2000) Introduction to Lipids and Lipoproteins. In: De Groot LJ, Chrousos G, Dungan K, Feingold KR, Grossman A, Hershman JM, et al., editors. *Endotext*, MDText.com, Inc., South Dartmouth (MA).

[46] Zhang, L., Yan, F., Zhang, S., Lei, D., Charles, M.A., Cavigiolio, G. et al. (2012) Structural basis of transfer between lipoproteins by cholesteryl ester transfer protein. *Nature Chemical Biology*, **8**, 342–9. https://doi.org/10.1038/nchembio.796

[47] Soran, H., Hama, S., Yadav, R. and Durrington, P.N. (2012) HDL functionality. *Current Opinion in Lipidology*, **23**, 353–66. https://doi.org/10.1097/MOL.0b013e328355ca25

[48] Shah, A.S., Tan, L., Long, J.L. and Davidson, W.S. (2013) Proteomic diversity of high density lipoproteins: our emerging understanding of its importance in lipid transport and beyond1. *Journal of Lipid Research*, **54**, 2575–85. https://doi.org/10.1194/jlr.R035725

[49] Woollett, L. and Heubi, J.E. (2000) Fetal and Neonatal Cholesterol Metabolism. In: De Groot LJ, Chrousos G, Dungan K, Feingold KR, Grossman A, Hershman JM, et al., editors. *Endotext*, MDText.com, Inc., South Dartmouth (MA).

[50] Wiesner, P., Leidl, K., Boettcher, A., Schmitz, G. and Liebisch, G. (2009) Lipid profiling of FPLC-separated lipoprotein fractions by electrospray ionization tandem mass spectrometry. *Journal of Lipid Research*, **50**, 574–85. https://doi.org/10.1194/jlr.D800028-JLR200

[51] Sattler, K. and Levkau, B. (2009) Sphingosine-1-phosphate as a mediator of high-density lipoprotein effects in cardiovascular protection. *Cardiovascular Research*, **82**, 201–11. https://doi.org/10.1093/cvr/cvp070

[52] Vickers, K.C., Palmisano, B.T., Shoucri, B.M., Shamburek, R.D. and Remaley, A.T. (2011) MicroRNAs are Transported in Plasma and Delivered to Recipient Cells by High-Density Lipoproteins. *Nature Cell Biology*, **13**, 423–33. https://doi.org/10.1038/ncb2210

[53] Nagasaka, H., Chiba, H., Kikuta, H., Akita, H., Takahashi, Y., Yanai, H. et al. (2002) Unique character and metabolism of high density lipoprotein (HDL) in fetus. *Atherosclerosis*, **161**, 215–23. https://doi.org/10.1016/S0021-9150(01)00663-3

[54] Averna, M.R., Barbagallo, C.M., Di Paola, G., Labisi, M., Pinna, G., Marino, G. et al. (1991) Lipids, lipoproteins and apolipoproteins AI, AII, B, CII, CIII and E in newborns. *Biology of the Neonate*, **60**, 187–92. https://doi.org/10.1159/000243407

[55] Sreckovic, I., Birner-Gruenberger, R., Obrist, B., Stojakovic, T., Scharnagl, H., Holzer, M. et al. (2013) Distinct composition of human fetal HDL attenuates its anti-oxidative capacity. *Biochimica Et Biophysica Acta*, **1831**, 737–46. https://doi.org/10.1016/j.bbalip.2012.12.015

[56] Rosen, H., Stevens, R.C., Hanson, M., Roberts, E. and Oldstone, M.B.A. (2013) Sphingosine-1-Phosphate and Its Receptors: Structure, Signaling, and Influence. *Annual Review of Biochemistry*, **82**, 637–62. https://doi.org/10.1146/annurev-biochem-062411-130916

[57] Hannun, Y.A. and Obeid, L.M. (2008) Principles of bioactive lipid signalling: lessons from sphingolipids. *Nature Reviews Molecular Cell Biology*, **9**, 139–50. https://doi.org/10.1038/nrm2329

[58] Stoffel, W. and Assmann, G. (1970) Metabolism of sphingosine bases. XV. Enzymatic degradation of 4t-sphingenine 1-phosphate (sphingosine 1-phosphate) to 2t-hexadecen-1-al and ethanolamine phosphate. *Hoppe-Seyler's Zeitschrift Fur Physiologische Chemie*, **351**, 1041–9. https://doi.org/10.1515/bchm2.1970.351.2.1041

[59] Olivera, A. and Spiegel, S. (1993) Sphingosine-1-phosphate as second messenger in cell proliferation induced by PDGF and FCS mitogens. *Nature*, **365**, 557–60. https://doi.org/10.1038/365557a0

[60] Cuvillier, O., Pirianov, G., Kleuser, B., Vanek, P.G., Coso, O.A., Gutkind, S. et al. (1996) Suppression of ceramide-mediated programmed cell death by sphingosine-1-phosphate. *Nature*, **381**, 800–3. https://doi.org/10.1038/381800a0

[61] Mattie, M., Brooker, G. and Spiegel, S. (1994) Sphingosine-1-phosphate, a putative second messenger, mobilizes calcium from internal stores via an inositol trisphosphate-independent pathway. *Journal of Biological Chemistry*, **269**, 3181–8.

[62] Paik, J.H., Chae, S., Lee, M.-J., Thangada, S. and Hla, T. (2001) Sphingosine 1-Phosphate-induced Endothelial Cell Migration Requires the Expression of EDG-1 and EDG-3 Receptors and Rho-dependent Activation of αvβ3- and β1-containing Integrins. *Journal of Biological Chemistry*, **276**, 11830–7. https://doi.org/10.1074/jbc.M009422200

[63] Spiegel, S. (1999) Sphingosine 1-phosphate: a prototype of a new class of second messengers. *Journal of Leukocyte Biology*, **65**, 341–4. https://doi.org/10.1002/jlb.65.3.341

[64] Donati, C. and Bruni, P. (2006) Sphingosine 1-phosphate regulates cytoskeleton dynamics: Implications in its biological response. *Biochimica et Biophysica Acta (BBA) - Biomembranes*, **1758**, 2037–48. https://doi.org/10.1016/j.bbamem.2006.06.015

[65] Chi, H. (2011) Sphingosine 1-phosphate and immune regulation: trafficking and beyond. *Trends in Pharmacological Sciences*, **32**, 16–24. https://doi.org/10.1016/j.tips.2010.11.002

[66] Sato, K. and Okajima, F. (2010) Role of sphingosine 1-phosphate in anti-atherogenic actions of high-density lipoprotein. *World Journal of Biological Chemistry*, **1**, 327–37. https://doi.org/10.4331/wjbc.v1.i11.327

[67] Lai, W.-Q., Wong, W.S.F. and Leung, B.P. (2011) Sphingosine kinase and sphingosine 1-phosphate in asthma. *Bioscience Reports*, **31**, 145–50. https://doi.org/10.1042/BSR20100087

[68] Wang, J., Badeanlou, L., Bielawski, J., Ciaraldi, T.P. and Samad, F. (2014) Sphingosine kinase 1 regulates adipose proinflammatory responses and insulin resistance. *American Journal of Physiology - Endocrinology and Metabolism*, **306**, E756–68. https://doi.org/10.1152/ajpendo.00549.2013

[69] Chiba, K. and Adachi, K. (2012) Sphingosine 1-Phosphate Receptor 1 as a Useful Target for Treatment of Multiple Sclerosis. *Pharmaceuticals*, **5**, 514–28. https://doi.org/10.3390/ph5050514

[70] Pyne, N.J. and Pyne, S. (2010) Sphingosine 1-phosphate and cancer. *Nature Reviews Cancer*, **10**, 489–503. https://doi.org/10.1038/nrc2875

[71] Hänel, P., Andréani, P. and Gräler, M.H. (2007) Erythrocytes store and release sphingosine 1-phosphate in blood. *FASEB Journal: Official Publication of the Federation of American Societies for Experimental Biology*, **21**, 1202–9. https://doi.org/10.1096/fj.06-7433com

[72] Venkataraman, K., Lee, Y.-M., Michaud, J., Thangada, S., Ai, Y., Bonkovsky, H.L. et al. (2008) Vascular Endothelium As a Contributor of Plasma Sphingosine 1-Phosphate. *Circulation Research*, **102**, 669–76. https://doi.org/10.1161/CIRCRESAHA.107.165845

[73] Hla, T., Venkataraman, K. and Michaud, J. (2008) The vascular S1P gradient—Cellular sources and biological significance. *Biochimica et Biophysica Acta*, **1781**, 477–82. https://doi.org/10.1016/j.bbalip.2008.07.003

[74] Pralhada Rao, R., Vaidyanathan, N., Rengasamy, M., Mammen Oommen, A., Somaiya, N. and Jagannath, M.R. (2013) Sphingolipid Metabolic Pathway: An Overview of Major Roles Played in Human Diseases. *Journal of Lipids*, **2013**. https://doi.org/10.1155/2013/178910

[75] Lowther, J., Naismith, J.H., Dunn, T.M. and Campopiano, D.J. (2012) Structural, mechanistic and regulatory studies of serine palmitoyltransferase. *Biochemical Society Transactions*, **40**, 547–54. https://doi.org/10.1042/BST20110769

[76] Pyne, S. and Pyne, N.J. (2000) Sphingosine 1-phosphate signalling in mammalian cells. *The Biochemical Journal*, **349**, 385–402. https://doi.org/10.1042/bj3490385

[77] Książek, M., Chacińska, M., Chabowski, A. and Baranowski, M. (2015) Sources, metabolism, and regulation of circulating sphingosine-1-phosphate. *Journal of Lipid Research*, **56**, 1271–81. https://doi.org/10.1194/jlr.R059543

[78] Mandala, S.M. (2001) Sphingosine-1-Phosphate Phosphatases. *Prostaglandins & Other Lipid Mediators*, **64**, 143–56. https://doi.org/10.1016/S0090-6980(01)00111-3

[79] Pyne, S., Kong, K.-C. and Darroch, P.I. (2004) Lysophosphatidic acid and sphingosine 1-phosphate biology: the role of lipid phosphate phosphatases. *Seminars in Cell & Developmental Biology*, **15**, 491–501. https://doi.org/10.1016/j.semcdb.2004.05.007

[80] Lee, M.-J., Brocklyn, J.R.V., Thangada, S., Liu, C.H., Hand, A.R., Menzeleev, R. et al. (1998) Sphingosine-1-Phosphate as a Ligand for the G Protein-Coupled Receptor EDG-1. *Science*, **279**, 1552–5. https://doi.org/10.1126/science.279.5356.1552

[81] Chun, J., Hla, T., Lynch, K.R., Spiegel, S. and Moolenaar, W.H. (2010) International Union of Basic and Clinical Pharmacology. LXXVIII. Lysophospholipid Receptor Nomenclature. *Pharmacological Reviews*, **62**, 579–87. https://doi.org/10.1124/pr.110.003111

[82] Obinata, H. and Hla, T. (2012) Sphingosine 1-phosphate in coagulation and inflammation. *Seminars in Immunopathology*, **34**, 73–91. https://doi.org/10.1007/s00281-011-0287-3

[83] Sanchez, T. (2016) Sphingosine-1-Phosphate Signaling in Endothelial Disorders. *Current Atherosclerosis Reports*, **18**, 31. https://doi.org/10.1007/s11883-016-0586-1

[84] Sammani, S., Moreno-Vinasco, L., Mirzapoiazova, T., Singleton, P.A., Chiang, E.T., Evenoski, C.L. et al. (2010) Differential Effects of Sphingosine 1–Phosphate Receptors on Airway and Vascular Barrier Function in the Murine Lung. *American Journal of Respiratory Cell and Molecular Biology*, **43**, 394–402. https://doi.org/10.1165/rcmb.2009-0223OC

[85] Theilmeier, G., Schmidt, C., Herrmann, J., Keul, P., Schäfers, M., Herrgott, I. et al. (2006) High-Density Lipoproteins and Their Constituent, Sphingosine-1-Phosphate, Directly Protect the Heart Against Ischemia/Reperfusion Injury In Vivo via the S1P3 Lysophospholipid Receptor. *Circulation*, **114**, 1403–9. https://doi.org/10.1161/CIRCULATIONAHA.105.607135

[86] Watterson, K.R., Johnston, E., Chalmers, C., Pronin, A., Cook, S.J., Benovic, J.L. et al. (2002) Dual Regulation of EDG1/S1P1 Receptor Phosphorylation and Internalization by Protein Kinase C and G-protein-coupled Receptor Kinase 2. *Journal of Biological Chemistry*, **277**, 5767–77. https://doi.org/10.1074/jbc.M110647200

[87] Pyne, N. and Pyne, S. (2017) Sphingosine 1-Phosphate Receptor 1 Signaling in Mammalian Cells. *Molecules*, **22**, 344. https://doi.org/10.3390/molecules22030344

[88] Hait, N.C., Allegood, J., Maceyka, M., Strub, G.M., Harikumar, K.B., Singh, S.K. et al. (2009) Regulation of Histone Acetylation in the Nucleus by Sphingosine-1-Phosphate. *Science (New York, NY)*, **325**, 1254–7. https://doi.org/10.1126/science.1176709

[89] Alvarez, S.E., Harikumar, K.B., Hait, N.C., Allegood, J., Strub, G.M., Kim, E. et al. (2010) SPHINGOSINE-1-PHOSPHATE: A MISSING COFACTOR FOR THE E3 UBIQUITIN LIGASE TRAF2. *Nature*, **465**, 1084–8. https://doi.org/10.1038/nature09128

[90] Adada, M.M., Orr-Gandy, K.A., Snider, A.J., Canals, D., Hannun, Y.A., Obeid, L.M. et al. (2013) Sphingosine Kinase 1 Regulates Tumor Necrosis Factor-mediated RANTES Induction through p38 Mitogen-activated Protein Kinase but Independently of Nuclear Factor κB Activation. *The Journal of Biological Chemistry*, **288**, 27667–79. https://doi.org/10.1074/jbc.M113.489443

[91] Strub, G.M., Paillard, M., Liang, J., Gomez, L., Allegood, J.C., Hait, N.C. et al. (2011) Sphingosine-1-phosphate produced by sphingosine kinase 2 in mitochondria interacts with prohibitin 2 to regulate complex IV assembly and respiration. *The FASEB Journal*, **25**, 600–12. https://doi.org/10.1096/fj.10-167502

[92] Takasugi, N., Sasaki, T., Suzuki, K., Osawa, S., Isshiki, H., Hori, Y. et al. (2011) BACE1 activity is modulated by cell-associated sphingosine-1-phosphate. *The Journal of Neuroscience : The Official Journal of the Society for Neuroscience*, **31**, 6850–7. https://doi.org/10.1523/JNEUROSCI.6467-10.2011

[93] Hisano, Y., Kobayashi, N., Yamaguchi, A. and Nishi, T. (2012) Mouse SPNS2 Functions as a Sphingosine-1-Phosphate Transporter in Vascular Endothelial Cells. *PLoS ONE*, **7**. https://doi.org/10.1371/journal.pone.0038941

[94] Takabe, K. and Spiegel, S. (2014) Export of sphingosine-1-phosphate and cancer progression. *Journal of Lipid Research*, **55**, 1839–46. https://doi.org/10.1194/jlr.R046656

[95] Mendoza, A., Bréart, B., Ramos-Perez, W.D., Pitt, L.A., Gobert, M., Sunkara, M. et al. (2012) The Transporter Spns2 Is Required for Secretion of Lymph but Not Plasma Sphingosine-1-Phosphate. *Cell Reports*, **2**, 1104–10. https://doi.org/10.1016/j.celrep.2012.09.021

[96] Kobayashi, N., Kawasaki-Nishi, S., Otsuka, M., Hisano, Y., Yamaguchi, A. and Nishi, T. (2018) MFSD2B is a sphingosine 1-phosphate transporter in erythroid cells. *Scientific Reports*, **8**. https://doi.org/10.1038/s41598-018-23300-x

[97] Christoffersen, C., Obinata, H., Kumaraswamy, S.B., Galvani, S., Ahnström, J., Sevvana, M. et al. (2011) Endothelium-protective sphingosine-1-phosphate provided by HDL-associated apolipoprotein M. *Proceedings of the National Academy of Sciences*, **108**, 9613–8. https://doi.org/10.1073/pnas.1103187108

[98] Kimura, T., Sato, K., Kuwabara, A., Tomura, H., Ishiwara, M., Kobayashi, I. et al. (2001) Sphingosine 1-Phosphate May Be a Major Component of Plasma Lipoproteins Responsible for the Cytoprotective Actions in Human Umbilical Vein Endothelial Cells. *Journal of Biological Chemistry*, **276**, 31780–5. https://doi.org/10.1074/jbc.M104353200

[99] Poti, F., Simoni, M. and Nofer, J.-R. (2014) Atheroprotective role of high-density lipoprotein (HDL)-associated sphingosine-1-phosphate (S1P). *Cardiovascular Research*, **103**, 395–404. https://doi.org/10.1093/cvr/cvu136

[100] Wilkerson, B.A., Grass, G.D., Wing, S.B., Argraves, W.S. and Argraves, K.M. (2012) Sphingosine 1-Phosphate (S1P) Carrier-dependent Regulation of Endothelial Barrier. *The Journal of Biological Chemistry*, **287**, 44645–53. https://doi.org/10.1074/jbc.M112.423426

[101] Takuwa, Y., Du, W., Qi, X., Okamoto, Y., Takuwa, N. and Yoshioka, K. (2010) Roles of sphingosine-1-phosphate signaling in angiogenesis. *World Journal of Biological Chemistry*, **1**, 298–306. https://doi.org/10.4331/wjbc.v1.i10.298

[102] Dobierzewska, A., Palominos, M., Sanchez, M., Dyhr, M., Helgert, K., Venegas-Araneda, P. et al. (2016) Impairment of Angiogenic Sphingosine Kinase-1/Sphingosine-1-Phosphate Receptors Pathway in Preeclampsia. *PLOS ONE*, **11**, e0157221. https://doi.org/10.1371/journal.pone.0157221

[103] Melland-Smith, M., Ermini, L., Chauvin, S., Craig-Barnes, H., Tagliaferro, A., Todros, T. et al. (2015) Disruption of sphingolipid metabolism augments ceramide-induced autophagy in preeclampsia. *Autophagy*, **11**, 653–69. https://doi.org/10.1080/15548627.2015.1034414

[104] Charkiewicz, K., Goscik, J., Blachnio-Zabielska, A., Raba, G., Sakowicz, A., Kalinka, J. et al. (2017) Sphingolipids as a new factor in the pathomechanism of preeclampsia – Mass spectrometry analysis. *PLOS ONE*, **12**, e0177601. https://doi.org/10.1371/journal.pone.0177601

[105] Singh, A.T., Dharmarajan, A., Aye, I.L.M.H. and Keelan, J.A. (2012) Sphingosine–sphingosine-1-phosphate pathway regulates trophoblast differentiation and syncytialization. *Reproductive BioMedicine Online*, **24**, 224–34. https://doi.org/10.1016/j.rbmo.2011.10.012

[106] Yang, W., Li, Q. and Pan, Z. (2014) Sphingosine-1-Phosphate Promotes Extravillous Trophoblast Cell Invasion by Activating MEK/ERK/MMP-2 Signaling Pathways via S1P/S1PR1 Axis Activation. *PLoS ONE*, **9**. https://doi.org/10.1371/journal.pone.0106725

[107] Westwood, M., Al-Saghir, K., Finn-Sell, S., Tan, C., Cowley, E., Berneau, S. et al. (2017) Vitamin D attenuates sphingosine-1-phosphate (S1P)-mediated inhibition of extravillous trophoblast migration. *Placenta*, **60**, 1–8. https://doi.org/10.1016/j.placenta.2017.09.009

[108] Pfaffl, M.W. (2001) A new mathematical model for relative quantification in real-time RT–PCR. *Nucleic Acids Research*, **29**, e45.

[109] Vandesompele, J., De Preter, K., Pattyn, F., Poppe, B., Van Roy, N., De Paepe, A. et al. (2002) Accurate normalization of real-time quantitative RT-PCR data by geometric averaging of multiple internal control genes. *Genome Biology*, **3**, research0034.1-research0034.11.

[110] Pfaffl, M.W., Tichopad, A., Prgomet, C. and Neuvians, T.P. (2004) Determination of stable housekeeping genes, differentially regulated target genes and sample integrity: BestKeeper – Excel-based tool using pair-wise correlations. *Biotechnology Letters*, **26**, 509–15. https://doi.org/10.1023/B:BILE.0000019559.84305.47

[111] Andersen, C.L., Jensen, J.L. and Ørntoft, T.F. (2004) Normalization of Real-Time Quantitative Reverse Transcription-PCR Data: A Model-Based Variance Estimation Approach to Identify Genes Suited for Normalization, Applied to Bladder and Colon Cancer Data Sets. *Cancer Research*, **64**, 5245–50. https://doi.org/10.1158/0008-5472.CAN-04-0496

[112] Katherine Lazaruk, Yu Wang, Jennifer Zhong, Sergei Maltchenko, Steven Rabkin, Kathryn Hunkapiller et al. (2014) The design process of quantitative TaqMan® gene expression analysis tools [Internet].

[113] Life Technologies Corporation. (2010) Gene Expression Assay Performance Guaranteed With the TaqMan® Assays QPCR Guarantee Program [Internet].

[114] Nolan, T., Hands, R.E. and Bustin, S.A. (2006) Quantification of mRNA using real-time RT-PCR. *Nature Protocols*, **1**, 1559–82. https://doi.org/10.1038/nprot.2006.236

[115] Svec, D., Tichopad, A., Novosadova, V., Pfaffl, M.W. and Kubista, M. (2015) How good is a PCR efficiency estimate: Recommendations for precise and robust qPCR efficiency assessments. *Biomolecular Detection and Quantification*, **3**, 9–16. https://doi.org/10.1016/j.bdq.2015.01.005

[116] Thorburn, A. (2007) Tumor Necrosis Factor-Related Apoptosis-Inducing Ligand (TRAIL) Pathway Signaling. *Journal of Thoracic Oncology*, **2**, 461–5. https://doi.org/10.1097/JTO.0b013e31805fea64

[117] Klement, J.F., Rice, N.R., Car, B.D., Abbondanzo, S.J., Powers, G.D., Bhatt, P.H. et al. (1996) IkappaBalpha deficiency results in a sustained NF-kappaB response and severe widespread dermatitis in mice. *Molecular and Cellular Biology*, **16**, 2341–9.

[118] Yusuf-Makagiansar, H., Anderson, M.E., Yakovleva, T.V., Murray, J.S. and Siahaan, T.J. (2002) Inhibition of LFA-1/ICAM-1 and VLA-4/VCAM-1 as a therapeutic approach to inflammation and autoimmune diseases. *Medicinal Research Reviews*, **22**, 146–67.

[119] Harada Akihisa, Sekido Nobuaki, Akahoshi Tohru, Wada Takashi, Mukaida Naofumi and Matsushima Kouji. (1994) Essential involvement of interleukin-8 (IL-8) in acute inflammation. *Journal of Leukocyte Biology*, **56**, 559–64. https://doi.org/10.1002/jlb.56.5.559

[120] Deshmane, S.L., Kremlev, S., Amini, S. and Sawaya, B.E. (2009) Monocyte Chemoattractant Protein-1 (MCP-1): An Overview. *Journal of Interferon & Cytokine Research*, **29**, 313–26. https://doi.org/10.1089/jir.2008.0027

[121] Ping, D., Jones, P.L. and Boss, J.M. (1996) TNF Regulates the In Vivo Occupancy of Both Distal and Proximal Regulatory Regions of the MCP-1/JE Gene. *Immunity*, **4**, 455–69. https://doi.org/10.1016/S1074-7613(00)80412-4

[122] Kunsch, C. and Rosen, C.A. (1993) NF-kappa B subunit-specific regulation of the interleukin-8 promoter. *Molecular and Cellular Biology*, **13**, 6137–46. https://doi.org/10.1128/MCB.13.10.6137

[123] Neish, A.S. (1992) Functional analysis of the human vascular cell adhesion molecule 1 promoter. *Journal of Experimental Medicine*, **176**, 1583–93. https://doi.org/10.1084/jem.176.6.1583

[124] Ledebur, H.C. and Parks, T.P. (1995) Transcriptional Regulation of the Intercellular Adhesion Molecule-1 Gene by Inflammatory Cytokines in Human Endothelial Cells ESSENTIAL ROLES OF A VARIANT NF-κB SITE AND p65 HOMODIMERS. *Journal of Biological Chemistry*, **270**, 933–43. https://doi.org/10.1074/jbc.270.2.933

[125] Christian, F., Smith, E.L. and Carmody, R.J. (2016) The Regulation of NF-κB Subunits by Phosphorylation. *Cells*, **5**. https://doi.org/10.3390/cells5010012

[126] Granger, D.N. and Senchenkova, E. (2010) Inflammation and the Microcirculation [Internet]. Morgan & Claypool Life Sciences.

[127] Kunkel, E.J. and Ley, K. (1996) Distinct Phenotype of E-Selectin–Deficient Mice: E-Selectin Is Required for Slow Leukocyte Rolling In Vivo. *Circulation Research*, **79**, 1196–204. https://doi.org/10.1161/01.RES.79.6.1196

[128] Li, J.-M. and Shah, A.M. (2003) Mechanism of Endothelial Cell NADPH Oxidase Activation by Angiotensin II. *Journal of Biological Chemistry*, **278**, 12094–100. https://doi.org/10.1074/jbc.M209793200

[129] Vince, G.S., Starkey, P.M., Austgulen, R., Kwiatkowski, D. and Redman, C.W. (1995) Interleukin-6, tumour necrosis factor and soluble tumour necrosis factor receptors in women with pre-eclampsia. *British Journal of Obstetrics and Gynaecology*, **102**, 20–5.

[130] Jonsson, Y., Rubèr, M., Matthiesen, L., Berg, G., Nieminen, K., Sharma, S. et al. (2006) Cytokine mapping of sera from women with preeclampsia and normal pregnancies. *Journal of Reproductive Immunology*, **70**, 83–91. https://doi.org/10.1016/j.jri.2005.10.007

[131] Huang, X., Huang, H., Dong, M., Yao, Q. and Wang, H. (2005) Serum and placental interleukin-18 are elevated in preeclampsia. *Journal of Reproductive Immunology*, **65**, 77–87. https://doi.org/10.1016/j.jri.2004.09.003

[132] Szarka, A., Rigó, J., Lázár, L., Bekő, G. and Molvarec, A. (2010) Circulating cytokines, chemokines and adhesion molecules in normal pregnancy and preeclampsia determined by multiplex suspension array. *BMC Immunology*, **11**, 59. https://doi.org/10.1186/1471-2172-11-59

[133] de Jager, W., Bourcier, K., Rijkers, G.T., Prakken, B.J. and Seyfert-Margolis, V. (2009) Prerequisites for cytokine measurements in clinical trials with multiplex immunoassays. *BMC Immunology*, **10**, 52. https://doi.org/10.1186/1471-2172-10-52

[134] Thavasu, P.W., Longhurst, S., Joel, S.P., Slevin, M.L. and Balkwill, F.R. (1992) Measuring cytokine levels in blood. Importance of anticoagulants, processing, and storage conditions. *Journal of Immunological Methods*, **153**, 115–24.

[135] Pang, Z.-J. and Xing, F.-Q. (2003) Comparative study on the expression of cytokine--receptor genes in normal and preeclamptic human placentas using DNA microarrays. *Journal of Perinatal Medicine*, **31**, 153–62. https://doi.org/10.1515/JPM.2003.021

[136] Wang, Y. and Walsh, S.W. (1996) TNF alpha concentrations and mRNA expression are increased in preeclamptic placentas. *Journal of Reproductive Immunology*, **32**, 157–69.

[137] Koçyigit, Y., Atamer, Y., Atamer, A., Tuzcu, A. and Akkus, Z. (2004) Changes in serum levels of leptin, cytokines and lipoprotein in pre-eclamptic and normotensive pregnant women. *Gynecological Endocrinology: The Official Journal of the International Society of Gynecological Endocrinology*, **19**, 267–73.

[138] Redman, C.W.G., Sacks, G.P. and Sargent, I.L. (1999) Preeclampsia: An excessive maternal inflammatory response to pregnancy. *Am J Obstet Gynecol*, **180**, 8.

[139] Chen, L.M., Liu, B., Zhao, H.B., Stone, P., Chen, Q. and Chamley, L. (2010) IL-6, TNFα and TGFβ Promote Nonapoptotic Trophoblast Deportation and Subsequently Causes Endothelial Cell Activation. *Placenta*, **31**, 75–80. https://doi.org/10.1016/j.placenta.2009.11.005

[140] Zhang, H., Park, Y., Wu, J., Chen, X. ping, Lee, S., Yang, J. et al. (2009) Role of TNF-α in vascular dysfunction. *Clinical Science (London, England : 1979)*, **116**, 219–30. https://doi.org/10.1042/CS20080196

[141] Turner, D.A., Paszek, P., Woodcock, D.J., Nelson, D.E., Horton, C.A., Wang, Y. et al. (2010) Physiological levels of TNFα stimulation induce stochastic dynamics of NF-κB responses in single living cells. *J Cell Sci*, **123**, 2834–43. https://doi.org/10.1242/jcs.069641

[142] Wenzel, K., Rajakumar, A., Haase, H., Geusens, N., Hubner, N., Schulz, H. et al. (2011) Angiotensin II Type 1 Receptor Antibodies and Increased Angiotensin II Sensitivity in Pregnant Rats. *Hypertension*, **58**, 77–84. https://doi.org/10.1161/HYPERTENSIONAHA.111.171348

[143] Wallukat, G., Homuth, V., Fischer, T., Lindschau, C., Horstkamp, B., Jüpner, A. et al. (1999) Patients with preeclampsia develop agonistic autoantibodies against the angiotensin AT1 receptor. *Journal of Clinical Investigation*, **103**, 945–52.

[144] Griendling, K.K., Minieri, C.A., Ollerenshaw, J.D. and Alexander, R.W. (1994) Angiotensin II stimulates NADH and NADPH oxidase activity in cultured vascular smooth muscle cells. *Circulation Research*, **74**, 1141–8.

[145] Rodríguez-Puyol, M., Griera-Merino, M., Pérez-Rivero, G., Díez-Marqués, M.L., Ruiz-Torres, M.P. and Rodríguez-Puyol, D. (2002) Angiotensin II induces a rapid and transient increase of reactive oxygen species. *Antioxidants & Redox Signaling*, **4**, 869–75. https://doi.org/10.1089/152308602762197407

[146] Ruiz, M., Frej, C., Holmér, A., Guo, L.J., Tran, S. and Dahlbäck, B. (2017) High-Density Lipoprotein-Associated Apolipoprotein M Limits Endothelial Inflammation by Delivering Sphingosine-1-Phosphate to the Sphingosine-1-Phosphate Receptor 1. *Arteriosclerosis, Thrombosis, and Vascular Biology*, **37**, 118–29. https://doi.org/10.1161/ATVBAHA.116.308435

[147] Galvani, S., Sanson, M., Blaho, V.A., Swendeman, S.L., Obinata, H., Conger, H. et al. (2015) HDL-bound sphingosine 1-phosphate acts as a biased agonist for the endothelial

cell receptor S1P1 to limit vascular inflammation. *Science Signaling*, **8**, ra79. https://doi.org/10.1126/scisignal.aaa2581

[148] Kimura, T., Tomura, H., Mogi, C., Kuwabara, A., Damirin, A., Ishizuka, T. et al. (2006) Role of Scavenger Receptor Class B Type I and Sphingosine 1-Phosphate Receptors in High Density Lipoprotein-induced Inhibition of Adhesion Molecule Expression in Endothelial Cells. *Journal of Biological Chemistry*, **281**, 37457–67. https://doi.org/10.1074/jbc.M605823200

[149] Clay, M.A., Pyle, D.H., Rye, K.A., Vadas, M.A., Gamble, J.R. and Barter, P.J. (2001) Time sequence of the inhibition of endothelial adhesion molecule expression by reconstituted high density lipoproteins. *Atherosclerosis*, **157**, 23–9.

[150] Kimura, T., Tomura, H., Mogi, C., Kuwabara, A., Ishiwara, M., Shibasawa, K. et al. (2006) Sphingosine 1-phosphate receptors mediate stimulatory and inhibitory signalings for expression of adhesion molecules in endothelial cells. *Cellular Signalling*, **18**, 841–50. https://doi.org/10.1016/j.cellsig.2005.07.011

[151] Alewijnse, A.E. and Peters, S.L.M. (2008) Sphingolipid signalling in the cardiovascular system: good, bad or both? *European Journal of Pharmacology*, **585**, 292–302. https://doi.org/10.1016/j.ejphar.2008.02.089

[152] Zhang, G., Yang, L., Kim, G.S., Ryan, K., Lu, S., O'Donnell, R.K. et al. (2013) Critical role of sphingosine-1-phosphate receptor 2 (S1PR2) in acute vascular inflammation. *Blood*, **122**, 443–55. https://doi.org/10.1182/blood-2012-11-467191

[153] Tölle, M., Pawlak, A., Schuchardt, M., Kawamura, A., Tietge, U.J., Lorkowski, S. et al. (2008) HDL-associated lysosphingolipids inhibit NAD(P)H oxidase- dependent monocyte chemoattractant protein-1 production. *Arteriosclerosis, Thrombosis, and Vascular Biology*, **28**, 1542–8. https://doi.org/10.1161/ATVBAHA.107.161042

[154] Peshavariya, H., Dusting, G.J., Di Bartolo, B., Rye, K.-A., Barter, P.J. and Jiang, F. (2009) Reconstituted high-density lipoprotein suppresses leukocyte NADPH oxidase activation by disrupting lipid rafts. *Free Radical Research*, **43**, 772–82. https://doi.org/10.1080/10715760903045304

[155] Wen, S.-Y., Tamilselvi, S., Shen, C.-Y., Day, C.H., Chun, L.-C., Cheng, L.-Y. et al. (2017) Protective effect of HDL on NADPH oxidase-derived super oxide anion mediates hypoxia-induced cardiomyocyte apoptosis. *PLOS ONE*, **12**, e0179492. https://doi.org/10.1371/journal.pone.0179492

[156] Jin, S. and Zhou, F. (2009) Lipid raft redox signaling platforms in vascular dysfunction: features and mechanisms. *Current Atherosclerosis Reports*, **11**, 220–6.

[157] Seshiah, P.N., Weber, D.S., Rocic, P., Valppu, L., Taniyama, Y. and Griendling, K.K. (2002) Angiotensin II Stimulation of NAD(P)H Oxidase Activity. *Circulation Research*,.

[158] Pendyala, S., Usatyuk, P.V., Gorshkova, I.A., Garcia, J.G.N. and Natarajan, V. (2009) Regulation of NADPH Oxidase in Vascular Endothelium: The Role of Phospholipases, Protein Kinases, and Cytoskeletal Proteins. *Antioxidants & Redox Signaling*, **11**, 841–60. https://doi.org/10.1089/ars.2008.2231

[159] Manea, A., Tanase, L.I., Raicu, M. and Simionescu, M. (2010) Transcriptional regulation of NADPH oxidase isoforms, Nox1 and Nox4, by nuclear factor-kappaB in human aortic smooth muscle cells. *Biochemical and Biophysical Research Communications*, **396**, 901–7. https://doi.org/10.1016/j.bbrc.2010.05.019

[160] Drummond, G.R. and Sobey, C.G. (2014) Endothelial NADPH oxidases: which NOX to target in vascular disease? *Trends in Endocrinology & Metabolism*, **25**, 452–63. https://doi.org/10.1016/j.tem.2014.06.012

[161] Newton, J., Lima, S., Maceyka, M. and Spiegel, S. (2015) Revisiting the sphingolipid rheostat: evolving concepts in cancer therapy. *Experimental Cell Research*, **333**, 195–200. https://doi.org/10.1016/j.yexcr.2015.02.025

[162] Thon, L., Möhlig, H., Mathieu, S., Lange, A., Bulanova, E., Winoto-Morbach, S. et al. (2005) Ceramide mediates caspase-independent programmed cell death. *FASEB Journal: Official Publication of the Federation of American Societies for Experimental Biology*, **19**, 1945–56. https://doi.org/10.1096/fj.05-3726com

[163] Kolesnick, R.N. and Krönke, M. (1998) Regulation of ceramide production and apoptosis. *Annual Review of Physiology*, **60**, 643–65. https://doi.org/10.1146/annurev.physiol.60.1.643

[164] Spiegel, S., Cuvillier, O., Edsall, L.C., Kohama, T., Menzeleev, R., Olah, Z. et al. (1998) Sphingosine-1-Phosphate in Cell Growth and Cell Death. *Annals of the New York Academy of Sciences*, **845**, 11–8. https://doi.org/10.1111/j.1749-6632.1998.tb09658.x

[165] DiFederico, E., Genbacev, O. and Fisher, S.J. (1999) Preeclampsia Is Associated with Widespread Apoptosis of Placental Cytotrophoblasts within the Uterine Wall. *The American Journal of Pathology*, **155**, 293–301.

6 APPENDIX A

Efficiency curves qPCR analysis

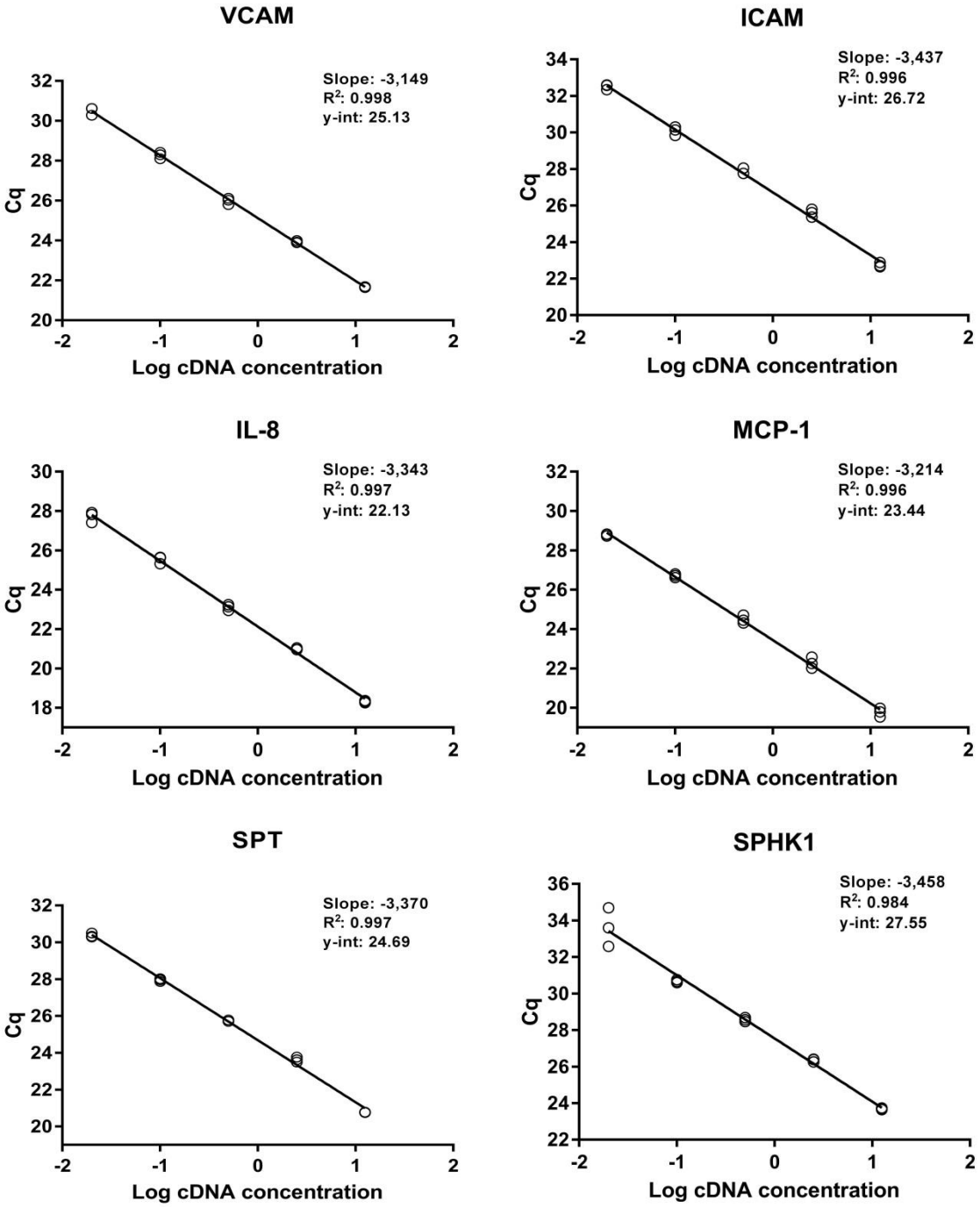

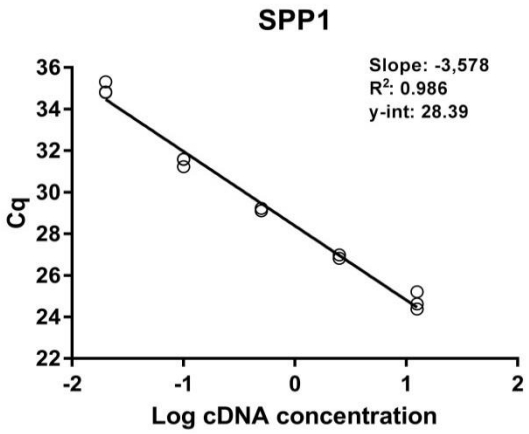
SPP1
Slope: -3,578
R2: 0.986
y-int: 28.39
Cq
Log cDNA concentration

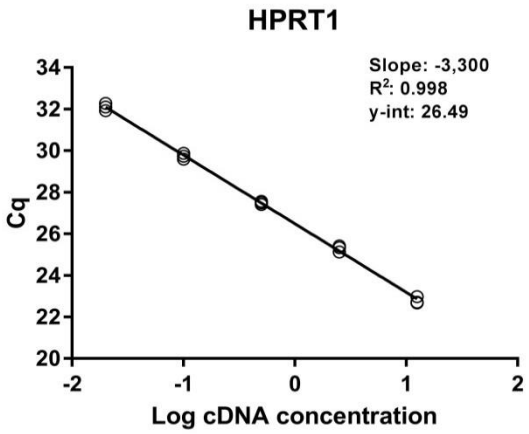
HPRT1
Slope: -3,300
R2: 0.998
y-int: 26.49
Cq
Log cDNA concentration

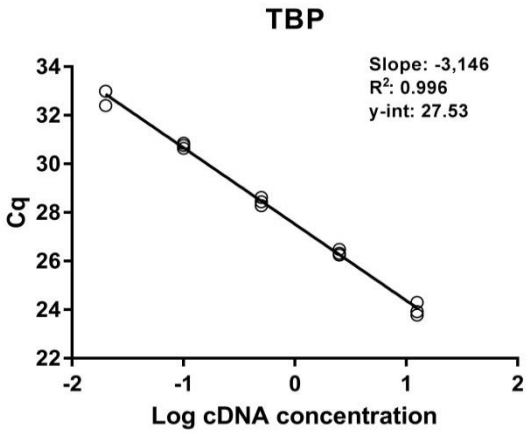
TBP
Slope: -3,146
R2: 0.996
y-int: 27.53
Cq
Log cDNA concentration

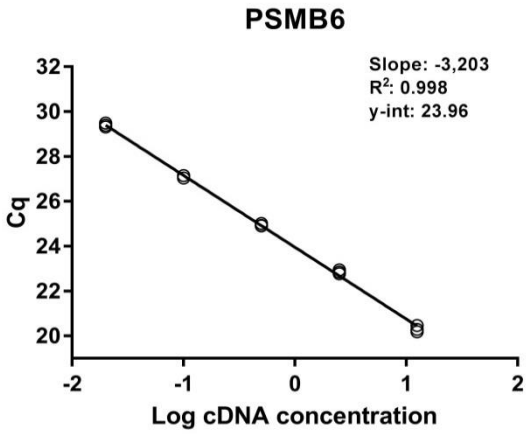
PSMB6
Slope: -3,203
R2: 0.998
y-int: 23.96
Cq
Log cDNA concentration

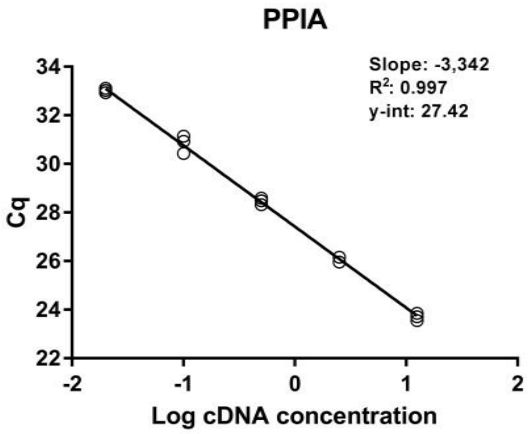
PPIA
Slope: -3,342
R2: 0.997
y-int: 27.42
Cq
Log cDNA concentration